1. Report No.	2. Government Accession No.	3. Recipient's Catalog No.
FHWA/TX-07/0-4519-2		

4. Title and Subtitle	5. Report Date
CONSIDERATION OF REGIONAL VARIATIONS IN CLIMATIC AND SOIL CONDITIONS IN THE MODIFIED TRIAXIAL DESIGN METHOD	March 2007 Published: November 2008
	6. Performing Organization Code

7. Author(s)	8. Performing Organization Report No.
Emmanuel G. Fernando, Jeongho Oh, Duchwan Ryu, and Soheil Nazarian	Report 0-4519-2

9. Performing Organization Name and Address	10. Work Unit No. (TRAIS)
Texas Transportation Institute The Texas A&M University System College Station, Texas 77843-3135	11. Contract or Grant No. Project 0-4519

12. Sponsoring Agency Name and Address	13. Type of Report and Period Covered
Texas Department of Transportation Research and Technology Implementation Office P. O. Box 5080 Austin, Texas 78763-5080	Technical Report: Sept. 2002 – Dec. 2005
	14. Sponsoring Agency Code

15. Supplementary Notes

Project performed in cooperation with the Texas Department of Transportation and the Federal Highway Administration.
Project Title: Verification of the Modified Triaxial Design Procedure
URL: http://tti.tamu.edu/documents/0-4519-2.pdf

16. Abstract

The Texas Department of Transportation (TxDOT) uses the modified triaxial design procedure to check pavement designs from the flexible pavement system program. Since its original development more than 50 years ago, little modification has been made to the original triaxial design method. There is a need to verify the existing load-thickness design chart to assess its applicability for the range in pavement materials used by the districts and the range in service conditions encountered in practice. Additionally, there is a conservatism in the current method, which assumes the worst condition in characterizing the strength properties of the subgrade. While this approach may apply to certain areas of the state such as east Texas, it can lead to unduly conservative assessments of pavement load bearing capacity in districts where the climate is drier, or where the soils are not as moisture susceptible. Clearly, there is a need to consider regional differences to come up with a more realistic assessment of pavement thickness requirements for the given local conditions. To address this need, researchers characterized the variation of climatic and soil conditions across Texas to develop a procedure that accounts for moisture effects and differences in moisture susceptibilities among different soils. Researchers incorporated this procedure in a computer program for triaxial design analysis that offers greater versatility in modeling pavement systems compared to the limited range of approximate layered elastic solutions represented in the existing modified triaxial design curves. This program permits engineers to correct soil strength parameters to values considered representative of expected in-service conditions when such corrections are deemed appropriate for the given local climatic and soil conditions.

17. Key Words	18. Distribution Statement
Pavement Design, Modified Triaxial Design Method, Environmental Effects, Texas Climatic-Soil Regions, Integrated Climatic Effects Model, Mohr-Coulomb Failure Criterion, Plate Bearing Test, Load Bearing Capacity, Small-Scale Pavement Models	No restrictions. This document is available to the public through NTIS: National Technical Information Service Springfield, VA 22161 http://www.ntis.gov

19. Security Classif.(of this report)	20. Security Classif.(of this page)	21. No. of Pages	22. Price
Unclassified	Unclassified	100	

CONSIDERATION OF REGIONAL VARIATIONS IN CLIMATIC AND SOIL CONDITIONS IN THE MODIFIED TRIAXIAL DESIGN METHOD

by

Emmanuel G. Fernando
Research Engineer
Texas Transportation Institute

Jeongho Oh
Associate Transportation Researcher
Texas Transportation Institute

Duchwan Ryu
Former Graduate Research Assistant
Texas Transportation Institute

and

Soheil Nazarian
Professor of Civil Engineering
The University of Texas at El Paso

Report 0-4519-2
Project 0-4519
Project Title: Verification of the Modified Triaxial Design Procedure

Performed in cooperation with the
Texas Department of Transportation
and the
Federal Highway Administration

March 2007
Published: November 2008

TEXAS TRANSPORTATION INSTITUTE
The Texas A&M University System
College Station, Texas 77843-3135

DISCLAIMER

The contents of this report reflect the views of the authors, who are responsible for the facts and the accuracy of the data presented. The contents do not necessarily reflect the official views or policies of the Texas Department of Transportation or the Federal Highway Administration (FHWA). This report does not constitute a standard, specification, or regulation, nor is it intended for construction, bidding, or permit purposes. The United States Government and the State of Texas do not endorse products or manufacturers. Trade or manufacturers' names appear herein solely because they are considered essential to the object of this report. The engineer in charge of the project was Dr. Emmanuel G. Fernando, P.E. # 69614.

ACKNOWLEDGMENTS

The work reported herein was conducted as part of a research project sponsored by the Texas Department of Transportation and the Federal Highway Administration. The authors gratefully acknowledge the support and guidance of the project director, Mr. Mark McDaniel, of the Materials and Pavements Section of TxDOT. Mr. McDaniel provided a compilation of Texas triaxial classifications for soils found across the state that researchers incorporated into the soils database of the *LoadGage* program developed from this project. In addition, the authors give thanks to members of the Project Monitoring Committee for their support of this project. In particular, Ms. Darlene Goehl and Mr. Billy Pigg provided assistance in identifying and testing materials used in field sections to verify TxDOT's modified triaxial design method. Mr. Miguel Arellano of the Austin District also compiled information on the statewide use of various base materials that was helpful in developing the field test plan for this project. In addition, Mr. Joe Leidy provided information on typical pavement designs researchers used in evaluating expected soil moisture conditions across the state. The authors also acknowledge the significant contributions of their colleagues:

- Ms. Cindy Estakhri developed the construction plans for the full-scale pavement sections used in verifying the existing triaxial design method and was responsible for getting the sections built according to plans.
- Mr. Gerry Harrison and Mr. Lee Gustavus provided technical expertise in setting up and conducting the plate bearing tests on full-scale field sections. In addition, Mr. Gustavus assisted in monitoring the construction of test sections and conducting construction quality control and quality assurance tests.
- Ms. Stacy Hilbrich characterized the soil-water characteristic curves of the base and subgrade materials used in constructing the test sections in this project.
- Dr. Wenting Liu wrote the data acquisition program for the plate bearing test and assisted in collecting the data from these tests.

Finally, the authors extend a special note of thanks to Dr. Robert Lytton for providing expert advice in the characterization of regional moisture conditions across Texas, particularly in the application of the integrated climatic effects model he developed in a project sponsored by the FHWA.

TABLE OF CONTENTS

Page

LIST OF FIGURES

Figure Page

LIST OF TABLES

CHAPTER I. INTRODUCTION

The Texas Department of Transportation (TxDOT) uses the Texas modified triaxial design procedure as a design check on the Flexible Pavement System (FPS) program. The current version of this design program, FPS-19, uses the backcalculated layer moduli from falling weight deflectometer (FWD) measurements and the expected number of 18-kip equivalent single axle loads (ESALs) to determine design thicknesses for the specified pavement materials. On many Farm-to-Market (FM) roads where the expected number of cumulative 18-kip ESALs is low, it is not uncommon to find trucks with wheel loads that exceed the structural capacity of the pavement. These occasional overloads could give rise to subgrade shear failure, particularly under conditions where the base or subgrade is wet. Thus, pavement engineers check the results from FPS against the Texas modified triaxial design procedure to ensure that the design thickness provides adequate cover to protect the subgrade against occasional overstressing. In cases where the thickness requirement from the triaxial method is greater than the pavement thickness determined from FPS, current practice recommends using the pavement thickness based on the modified triaxial design method unless the engineer can justify using the FPS results.

Since its original development more than 50 years ago, the original triaxial design method has had little modification. There is a need to verify the existing load-thickness curves to assess their applicability for the range in pavement materials used by the districts, and the range in service conditions that pavements are subjected to. Additionally, there is conservatism in the existing design method that is manifested in the way the subgrade is characterized. Specifically, the subgrade material is moisture conditioned prior to testing to define the Texas triaxial class. While this approach may represent climatic and soil conditions in certain areas of the state such as east Texas, it can be notably conservative in districts where the climate is drier, or where the soils are not as moisture susceptible. Clearly, engineers need to consider regional differences in climatic and soil conditions in the existing triaxial design method to come up with a more realistic assessment of pavement thickness requirements for the given climatic and soil moisture conditions, pavement materials, and design load.

RESEARCH OBJECTIVES

The primary objectives of this project are to:

- verify the load-thickness design curves in TxDOT's Test Method Tex-117E that are used in the current modified triaxial design method, and
- account for regional variations in climatic and soil conditions across Texas in the pavement design check of FPS-generated flexible pavement designs.

Researchers accomplished these objectives by carrying out a comprehensive work plan that covered the following tasks:

- a literature review of the development of the load-thickness design curves that enabled researchers to re-create the curves based on the review findings,
- development of a plan to verify the load-thickness design curves based on testing full-scale field sections and small-scale pavement models,
- construction of test sections and fabrication of small-scale pavement models,
- field and laboratory testing to characterize pavement materials and evaluate load carrying capacity of test sections built to verify the thickness design curves,
- investigation of the correspondence between small-scale and full-scale pavement test results,
- analysis of test data to verify the current load-thickness design curves,
- compilation of climatic and soils data on the different Texas counties,
- evaluation of expected moisture contents using a comprehensive model of climatic effects originally developed by Lytton et al. (1990) in a project conducted for the Federal Highway Administration,
- investigation of the relationships between soil moisture and soil strength properties, and
- development of a stress-based analysis program for checking FPS-generated pavement designs based on the Mohr-Coulomb strength criterion.

This report documents the research conducted to develop a methodology to account for variations in climatic and soil conditions in checking the adequacy of pavement designs from the FPS program. A companion report by Fernando, Oh, Estakhri, and Nazarian (2007) documents the research conducted to verify the existing load-thickness design curves in the modified Texas triaxial design method.

BACKGROUND

Chester McDowell, former Soils Engineer of what was then the Texas Highway Department, spearheaded the development of the Texas triaxial design method in the mid-1940s to the early 1960s. To verify the load-thickness design curves in this project, researchers initially reviewed published information to establish how the existing design method was developed and identify underlying principles and assumptions made to generate the design charts. Fernando, Oh, Estakhri, and Nazarian (2007) present at length the findings from this literature review in the companion report (0-4519-1) to this project. From this task, researchers verified the method used by McDowell to develop the existing triaxial design curves, which are based on determining the depth of cover required such that the load induced stresses do not exceed the soil shear strength. The computation of wheel load stresses for deriving the thickness design curves was done using layered elastic theory along with assumptions McDowell made regarding the variation of modular ratios with depth. Researchers demonstrated the methodology by re-creating the existing load-thickness design curves as documented in research report 0-4519-1.

Based on the findings from the literature review, researchers established a field and laboratory test program to verify the load-thickness design curves in the modified Texas triaxial design method. Considering that the design curves in Tex-117E were determined using layered elastic theory, researchers conducted plate bearing tests on full-scale field sections. The load configuration for this test most closely approximates the assumptions used in developing the existing design curves. A total of 30 full-scale pavement sections were constructed within the Riverside Campus of Texas A&M University for the purpose of conducting plate bearing tests. In addition, researchers at the University of Texas at El Paso (UTEP) conducted laboratory plate bearing tests on small-scale pavement models fabricated with the same base and subgrade materials used on the full-scale field sections. The analyses of data from these tests verified the conservatism in the existing design method that TxDOT engineers have previously recognized. In addition, observed differences in load bearing capacities at various moisture conditions from tests done on small-scale pavement specimens suggested the need to properly account for moisture effects and differences in moisture susceptibilities between different soils.

This report follows up on the verification work documented in research report 0-4519-1. The report details the efforts to improve the existing triaxial design method in Tex-117E. These efforts covered the following areas:

- Provide a more refined method of computing wheel load stresses for estimating pavement load bearing capacity that offers greater versatility in modeling pavement systems and load configurations.
- Characterize the variation of climatic and soil conditions across Texas, and develop a procedure that accounts for moisture effects and differences in moisture susceptibilities among different soils.
- Incorporate a procedure in the triaxial design check that gives engineers the option to adjust soil strength parameters determined from Tex-117E tests on moisture conditioned specimens to values representative of expected in-service moisture conditions. The engineer can then perform the design check based on soil strength parameters he/she considers to be more representative of in-service conditions.

From these efforts, researchers developed a revised procedure for triaxial design analysis that is implemented in a computer program called *LoadGage*, which features the following enhancements to the current modified triaxial design method:

- a stress-based analysis procedure that provides users with greater versatility in modeling flexible pavement systems compared to the limited range of approximate layered elastic solutions represented in the Tex-117E design curves;
- more realistic modeling of pavement wheel loads, in lieu of the current practice of using a correction factor of 1.3;
- an extensive database of soil properties covering each of the 254 Texas counties for evaluating the effects of moisture changes on soil strength properties; and
- a moisture correction procedure (to account for differences between wet and dry regions of the state) that provides users the option of adjusting strength properties determined from laboratory triaxial tests on soil specimens prepared at a given moisture content to the expected in-service moisture conditions.

Instructions on the operation of the *LoadGage* computer program are given in the user's manual prepared by Fernando, Oh, and Liu (2007).

SCOPE OF RESEARCH REPORT

This report documents the development of a revised procedure for conducting the triaxial design check of FPS pavement designs. The revised procedure uses a multi-layered elastic analysis program for computing wheel load stresses and incorporates an option for correcting failure envelope parameters to account for moisture effects. The report is organized into the following chapters:

- Chapter I (this chapter) provides the background for this project and states its objectives.
- Chapter II presents the characterization of climatic and soil variations across Texas, which resulted in a database of climatic and soil variables that researchers used to evaluate expected in-service moisture conditions as part of developing the method for correcting soil strength parameters to consider moisture effects in the triaxial design check.
- Chapter III presents the procedure for moisture correction developed from this project, which researchers evaluated using the data from plate bearing tests conducted on full-scale pavement sections and on small-scale pavement models. The moisture correction procedure is included as an option in the *LoadGage* program for cases where engineers may deem it appropriate to correct strength properties to values they consider representative of expected in-service soil moisture conditions.
- Chapter IV describes the work done by researchers to estimate expected in-service soil moisture contents for the purpose of developing a database to support the application of the moisture correction procedure developed in this project.
- Finally, Chapter V summarizes the findings from the research reported herein and recommends modifications to the Tex-117E design method.

CHAPTER II. CHARACTERIZATION OF CLIMATIC AND SOIL VARIATIONS IN TEXAS

INTRODUCTION

Climatic factors and the properties of soils on which pavements are built affect pavement design because of the influence of these variables on pavement performance. For the purpose of evaluating the load bearing capacity of roads to check thickness designs based on the modified Texas class, or for routing super heavy loads, or establishing load zoning requirements, it is necessary (in the researchers' opinion) to consider the variation of climatic and soil conditions to conduct a proper analysis. Thus, researchers characterized the variation of climatic and soil conditions throughout Texas to establish climatic-soil regions for pavement design and pavement evaluation applications.

This task was accomplished by reviewing and collecting available data from weather stations in Texas and from county soil survey reports published by the Natural Resources Conservation Service of the U.S. Department of Agriculture (USDA). Climatic data collected in this project included air temperatures, precipitation, relative humidity, and Thornthwaite Moisture Index. From published county soil surveys, researchers likewise identified the predominant soil types by volume in each Texas county, and established representative soil-water characteristic curves that define the relationship between soil suction and soil moisture content. Researchers used these curves to group counties into several soil regions through cluster analysis.

Groups that resulted from the cluster analyses of climatic and soil variables were superimposed to establish climatic-soil regions for implementing a moisture correction procedure in the modified triaxial design check developed from this project. This correction is based on the shear strength equation for unsaturated soils that is presented in Chapter III of this report. According to this equation, the shear strength of unsaturated soils is a function of the effective normal stress and soil suction. Since the soil-water characteristic curve defines the relationship between soil suction and soil moisture content, it provides the linkage between soil moisture content and shear strength. Thus, researchers compiled a data base of soil-water characteristic curves to implement the moisture correction procedure developed from this project. These curves covered the range of soils found across Texas as established from the characterization of climatic and soil variations documented in this chapter.

CLIMATIC REGIONS

Researchers used the following factors to characterize the climatic conditions for each county:

- mean air temperature,
- mean precipitation,
- daily temperature drop,
- maximum and minimum relative humidities, and
- Thornthwaite Moisture Index.

Thirty-year averages for these variables were determined for each county. It is noted that some counties did not have weather station data to compute these averages. For these counties, researchers estimated the missing values by interpolating data from neighboring counties. The cluster analysis was then performed based on the thirty-year averages of the climatic variables. Figures A1 to A6 in Appendix A show these averages for each of the six climatic variables considered. The numbers on each map identify the different counties following the numbering scheme used by TxDOT that is given in Table A1. In addition, Table A2 summarizes the averages determined for each county.

Two counties with similar values of the six climatic variables can be classified into the same climatic region or, alternatively, into two distinct regions if the counties are dissimilar. The cluster analysis performed by researchers may be explained by defining the dissimilarity between two counties as:

$$D_{ij} = \sum_{k=1}^{6} \left(X_{ik} - X_{jk} \right)^2, \quad i \neq j \tag{2.1}$$

where X_{ik} and X_{jk} are values of the climatic variable k for counties i and j, respectively. The clustering may be performed beginning with one cluster (representing the entire state of Texas) and progressing to n clusters, which in the limit will equal the number of Texas counties (note that researchers characterized the climatic conditions by county, thus establishing the county as the basic unit for the cluster analysis). This approach is called the top-down method. Alternatively, the clustering may begin with n clusters that are systematically reduced to fewer clusters by grouping similar counties (bottom-up method). To establish Texas climatic regions, researchers implemented this latter method. Hence, at the first step, two closest counties that have the smallest dissimilarity among all possible pairs of counties are assigned in the same group. At the next step, the dissimilarity between a

group and other counties is defined by the average of dissimilarities between each county of the group and the other county. The next group will then consist of the two closest counties, or one county and one group. After some steps, the dissimilarity between groups is calculated by the average of dissimilarities of all possible pairs of counties that are from different groups. Hence, two counties, one county and one group, or two groups are classified in a group. Figure 2.1 displays a diagram explaining the procedure. This procedure is called the average method of clustering. The average method tends to minimize the variance of climatic variables in each group.

To decide on the appropriate number of climatic regions for characterizing climatic conditions, researchers examined the change in the mean square error statistic (given by equation 2.2) with increase in the number of clusters. For this analysis, let X_{ijk} be the i^{th} climatic variable for the k^{th} county classified in the j^{th} cluster. Then, for the given number of clusters J_c, the mean square error indicating the variability of climatic conditions for J_c clusters is determined as follows:

$$MSE = \sum_{i=1}^{6} \sum_{j=1}^{J_c} \sum_{k=1}^{K_j} \left(X_{ijk} - \bar{X}_{ij.} \right)^2 \Big/ 6\left(254 - J_c\right) \qquad (2.2)$$

where K_j is the number of counties in the j^{th} cluster. Obviously, the sum of the number of counties for all clusters equals 254, the total number of counties in the state.

Researchers examined the MSE as the number of clusters is increased. Starting with one cluster (J_c =1), statistical hypothesis testing (partial F-tests) was found to be too sensitive to determine the proper number of clusters. Hence, researchers used an alternative graphical method. Figure 2.2 shows the variation in the mean square errors from the cluster analysis. This chart is referred to as the "scree" plot (the plot looks like the side of a mountain, and "scree" refers to the debris fallen from a mountain and lying at its base). When seven clusters are considered, increasing the number of clusters to eight does not contribute significantly to the reduction of the MSE. Figure 2.3 shows how the state would be subdivided into climatic regions when seven clusters are used. Researchers are of the opinion that seven clusters adequately capture the variation in climatic conditions across Texas and represent a good compromise between reducing the MSE and keeping the number of clusters small for simplicity.

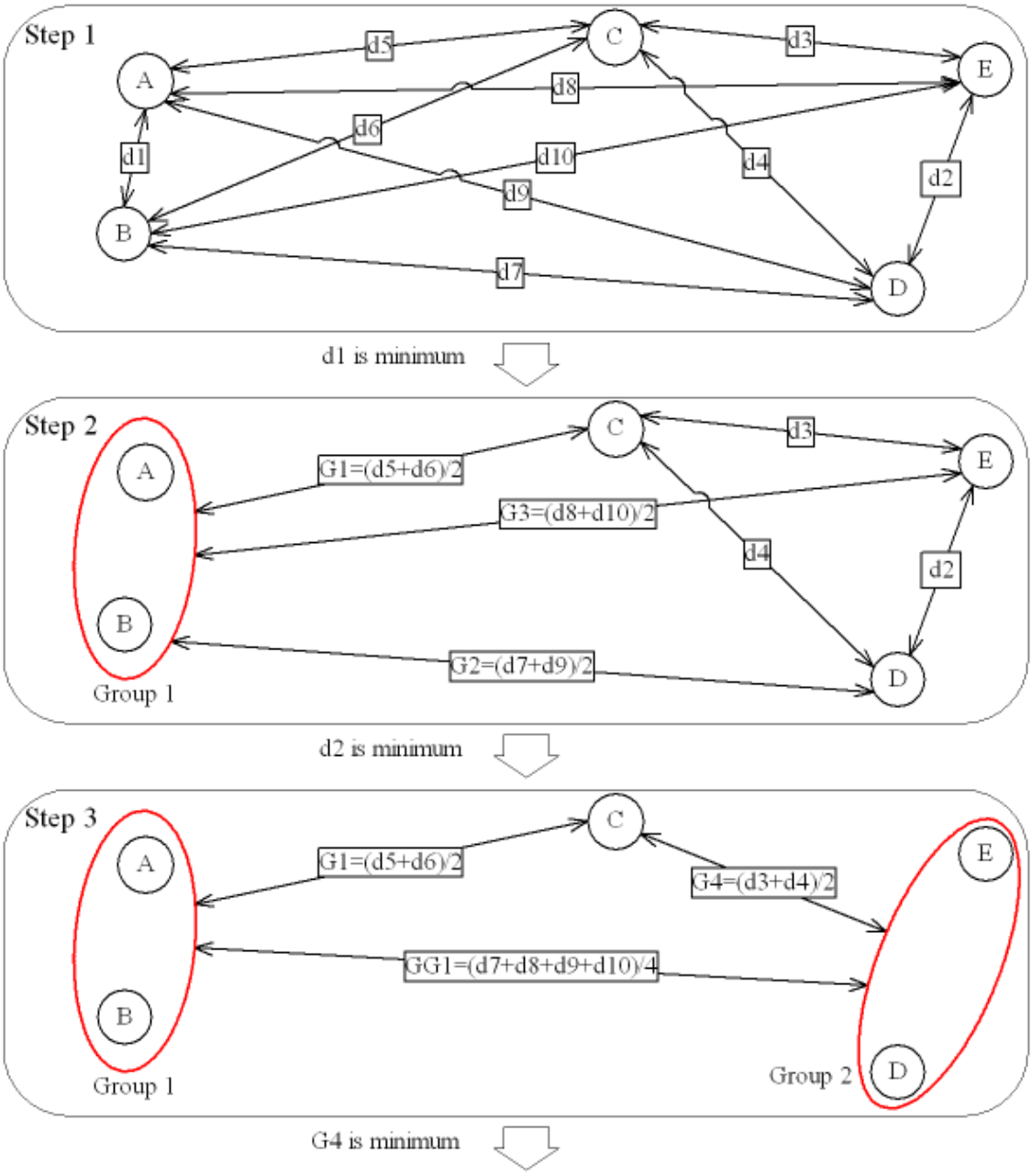

Figure 2.1. Diagram Illustrating the Cluster Analysis.

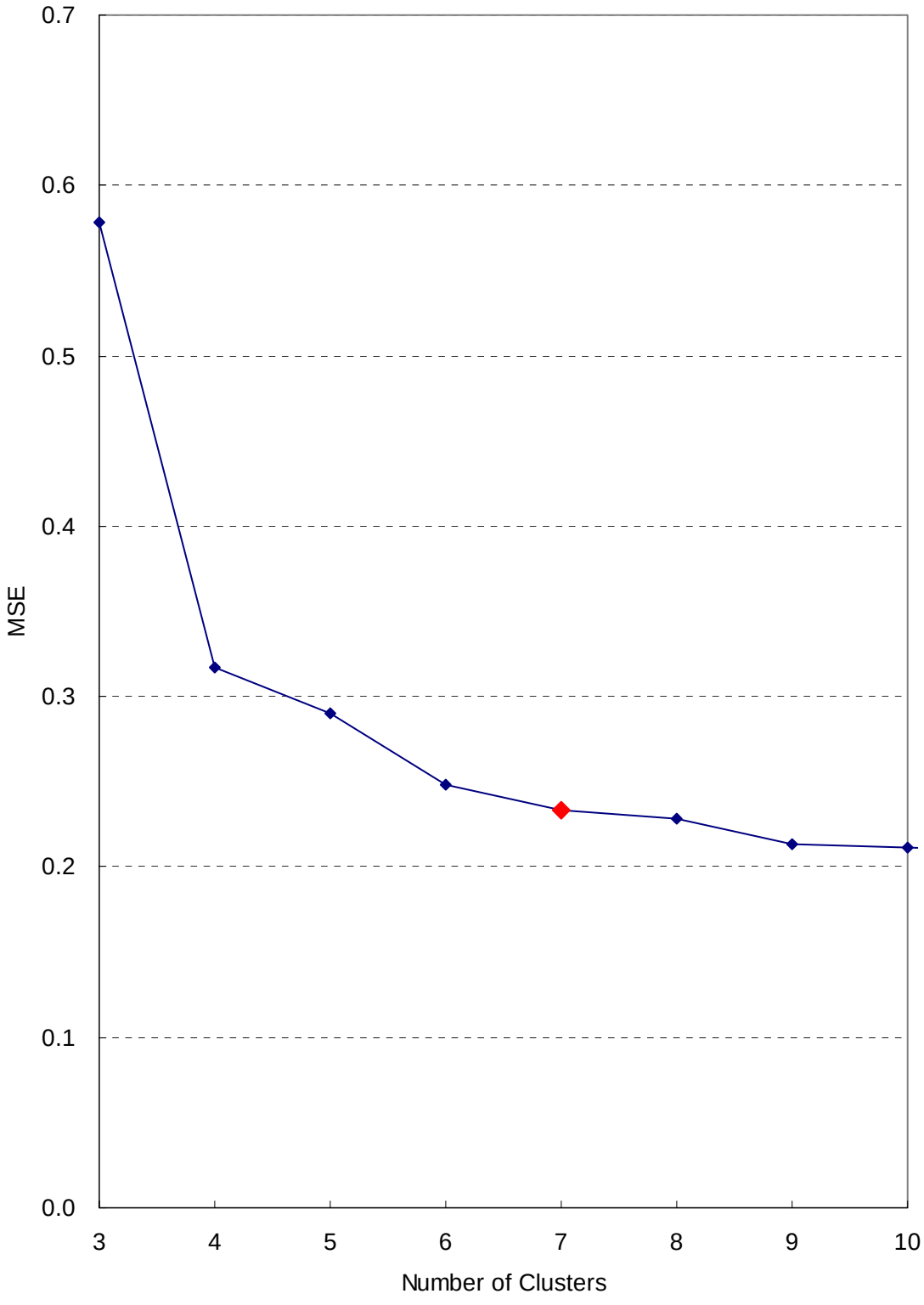

Figure 2.2. Scree Plot to Determine the Number of Climatic Regions.

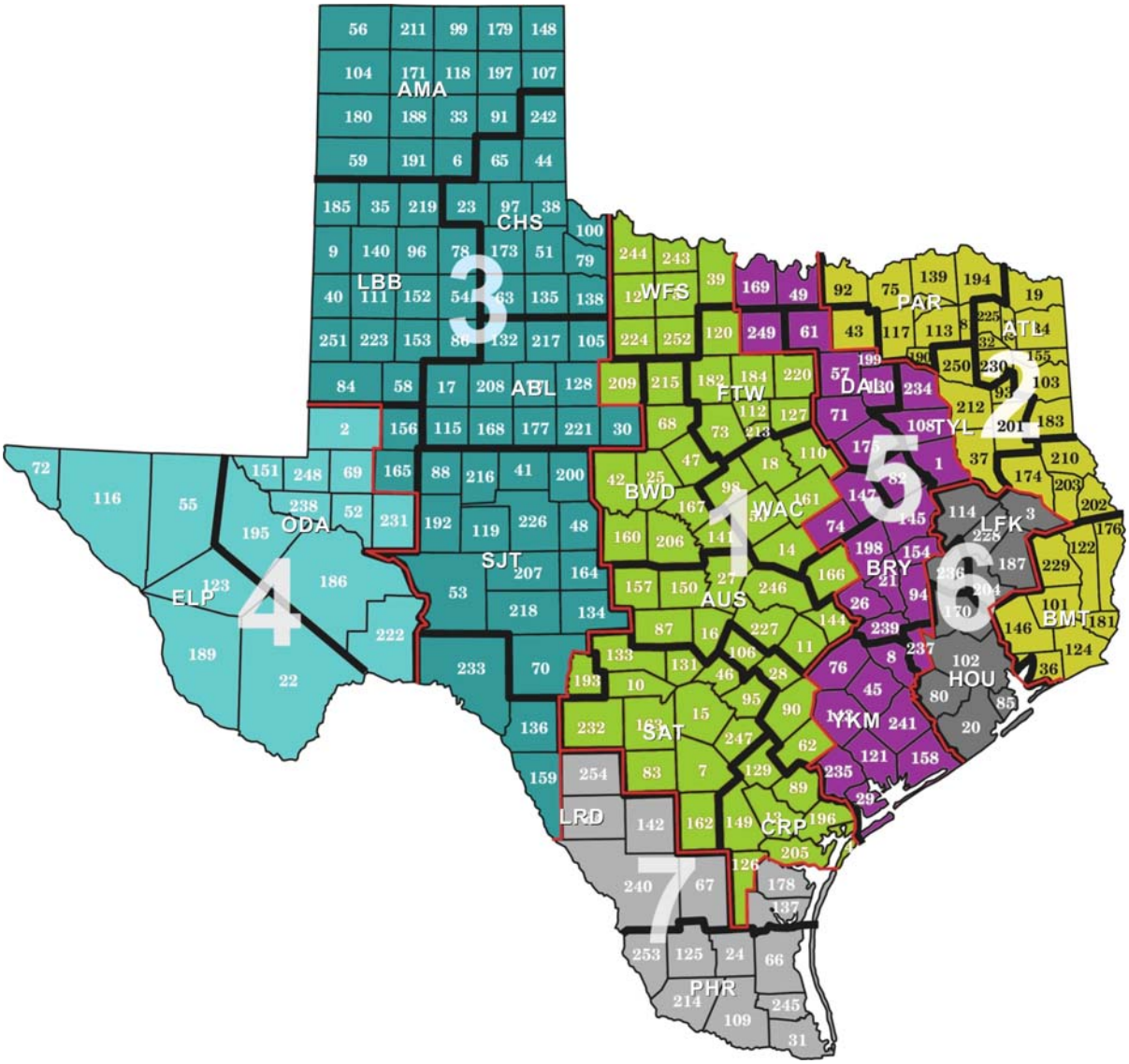

Figure 2.3. Subdivision of Texas into Seven Climatic Regions (counties on map are identified by corresponding county numbers).

SOIL REGIONS

To establish soil regions, researchers reviewed Texas county soil survey reports to identify the soil types found across the state and the predominant soils by county based on the soil volumes reported in the USDA soil surveys. Figure 2.4 shows the predominant soils based on the unified soil classification system. Given this information, researchers assigned soil-water characteristic curves to the various soil types using the catalog of soil-water characteristic curves compiled by Mason et al. (1986) and Lytton et al. (1990). For the purpose of characterizing soil regions, researchers determined the weighted average (based

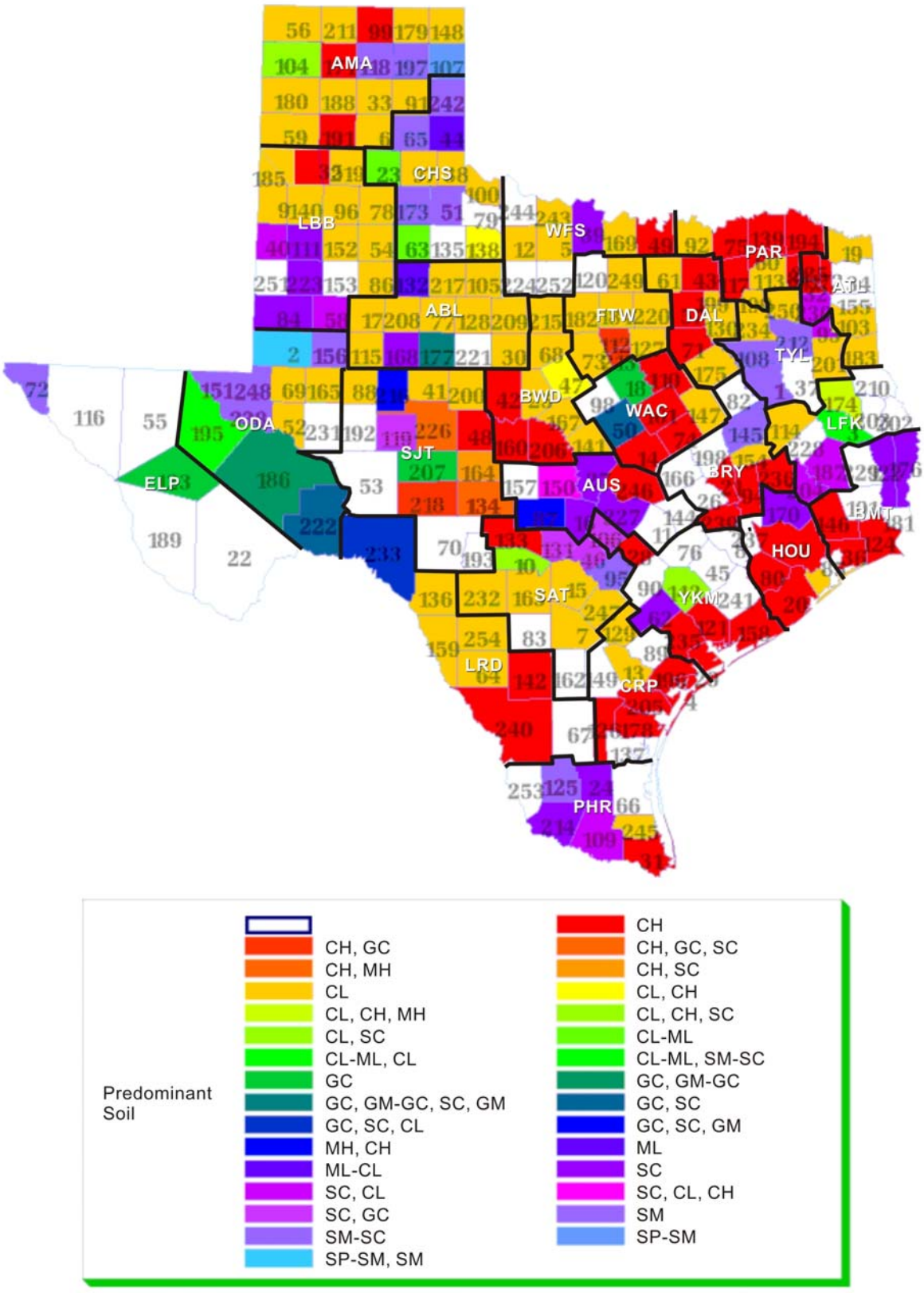

Figure 2.4. Predominant Soils Identified from County Soil Survey Reports (white areas show counties with missing information).

on soil volume) of the soil-water characteristic curves for the predominant soils in each county. Specifically, researchers computed the weighted average curve as follows:

$$\overline{w}_j = \sum_{i=1}^{m} w_{ij} \times f_i \qquad (2.3)$$

where,

$\overline{w}_j$ = the weighted average moisture content corresponding to the j^{th} level of soil suction (j = 1 to n_s, where n_s is the number of soil suction levels considered in computing the weighted average),

w_{ij} = the moisture content corresponding to the j^{th} level of soil suction for the i^{th} soil (i = 1 to m, where m is the number of predominant soils in a county), and

f_i = the weight assigned to the i^{th} soil based on soil volume.

The weighted average curves were then used in a cluster analysis to subdivide the state into soil regions. Researchers followed this approach for computational simplicity and to permit the cluster analysis to be done by county. Researchers note that this approach was used solely for the purpose of establishing the soil regions into which the state may be subdivided. With respect to considering the effect of moisture on pavement load bearing capacity, the methodology developed in this project permits engineers to use the soil-water characteristic curve applicable to a given design project.

Figure 2.4 shows counties where researchers found no published soil survey reports. For these cases, researchers computed the weighted average soil-water characteristic curves by interpolation using the data from neighboring counties. The authors considered this approach to be reasonable given that the purpose of the cluster analysis was simply to establish regional trends in the variation of the soil-water characteristic curves across the counties comprising Texas. For analyzing pavement load bearing capacity, the methodology developed in this project uses the curve applicable to a given project.

Table A3 gives data that define the weighted average soil-water characteristic curves used in the cluster analysis. For each county, the table gives the water contents corresponding to 8 soil suction levels ranging from 2.0 to 4.8 pF, where 1 pF = $\log_{10}$|suction in cm of water|. Researchers used the data in Table A3 in a bottom-up cluster analysis to subdivide the state into soil regions. This analysis used the sum of the squared differences between the weighted average curves to quantify the dissimilarity between two given counties. Figure 2.5 shows the scree plot from the cluster analysis.

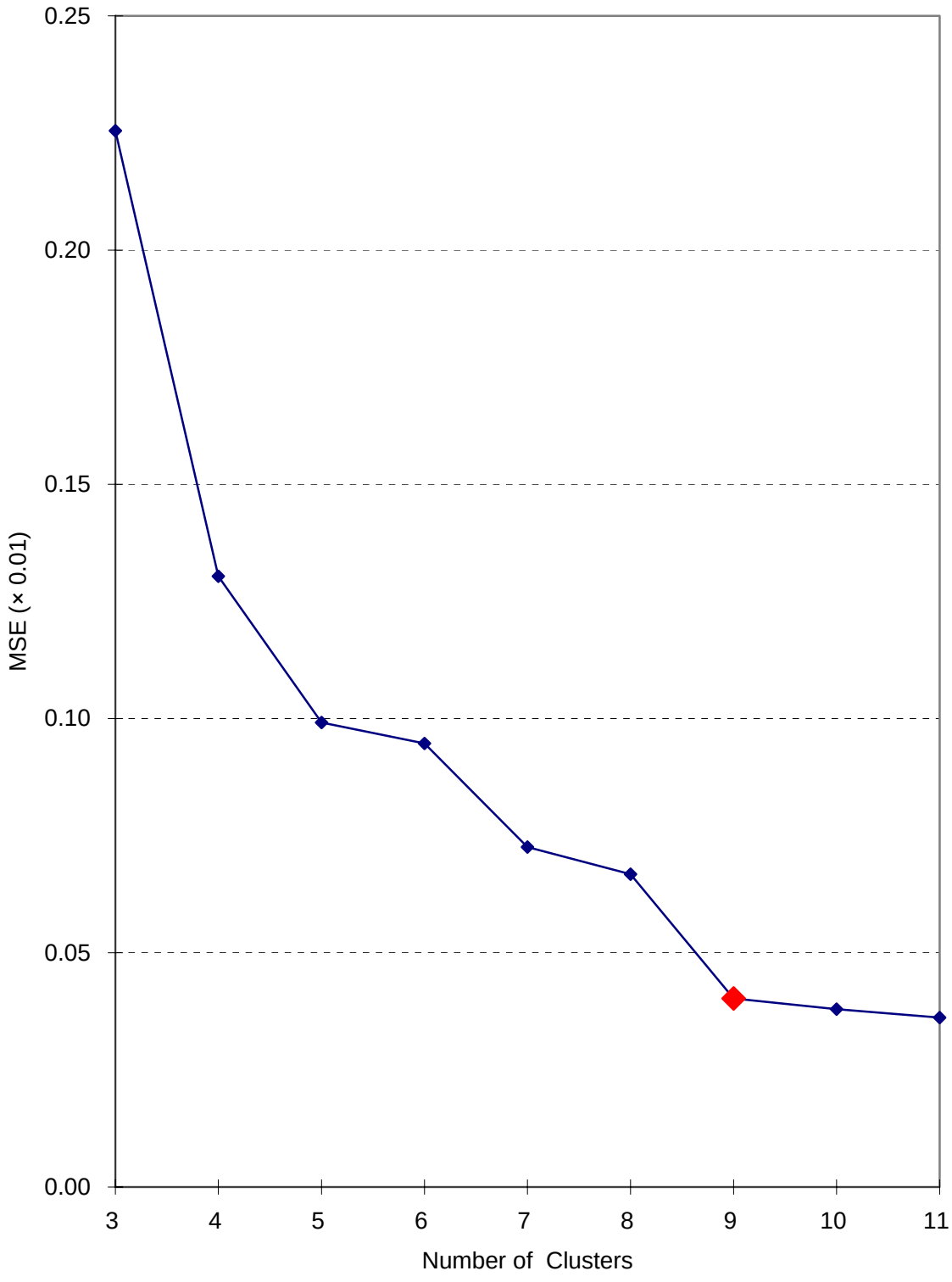

Figure 2.5. Scree Plot to Determine the Number of Soil Regions.

Based on the change in the MSEs plotted in Figure 2.5, researchers decided to use nine clusters to subdivide Texas into soil regions based on the variation of the soil-water characteristic curves. Figure 2.6 shows the nine soil regions identified from the cluster analysis. By superimposing these nine soil regions with the seven climatic regions determined previously, the climatic-soil regions given in Figure 2.7 are determined. Table 2.1 shows how the Texas counties are classified into the different climatic-soil regions.

Researchers used the results from the characterization of Texas climatic-soil regions in developing a procedure that considers the effects of environmental factors in the triaxial design check. This procedure is based on correcting soil failure envelope parameters determined from triaxial tests to values that are considered representative of expected in-service soil moisture conditions. The next chapter presents this moisture correction procedure.

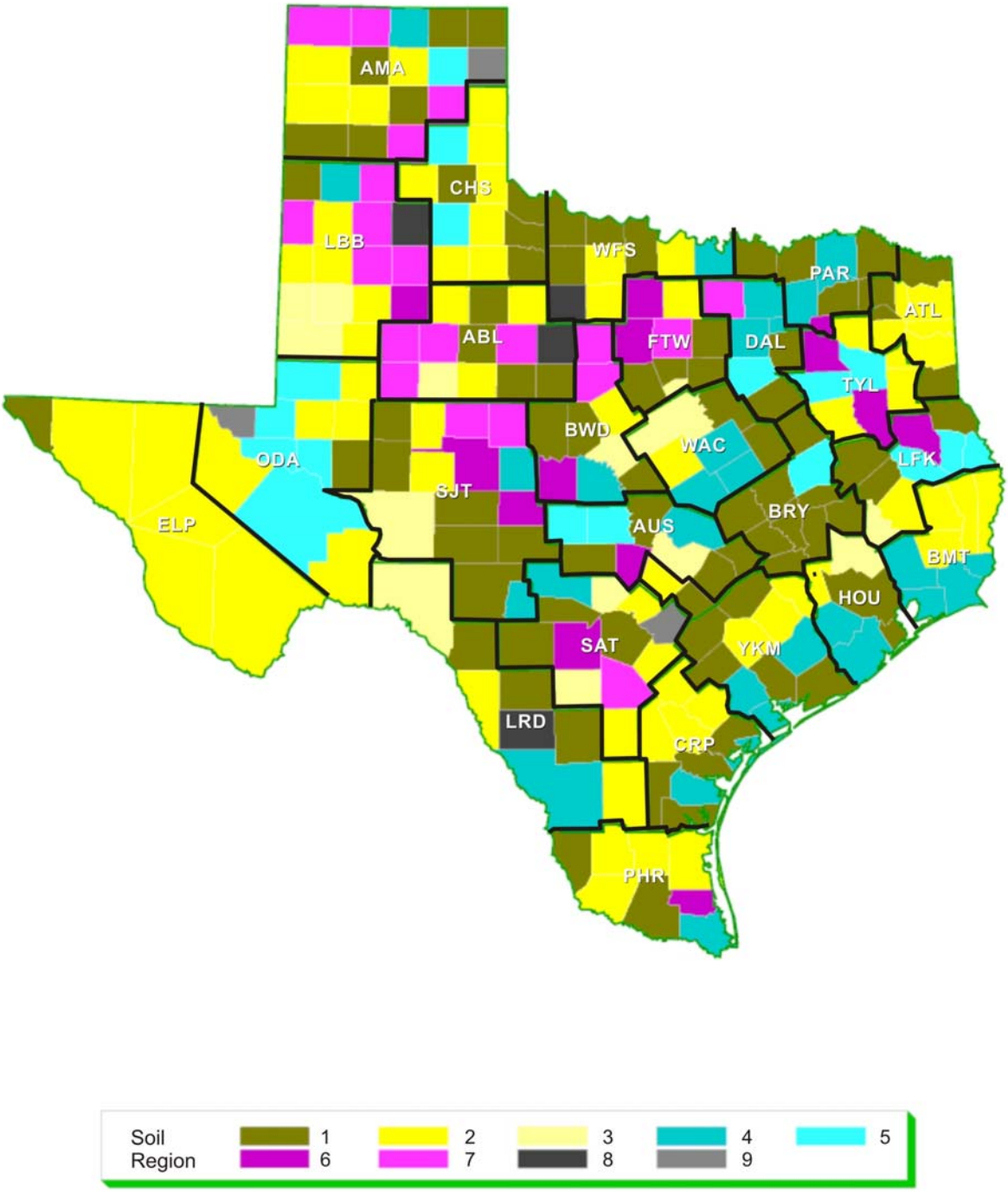

Figure 2.6. Subdivision of Texas into Nine Soil Regions.

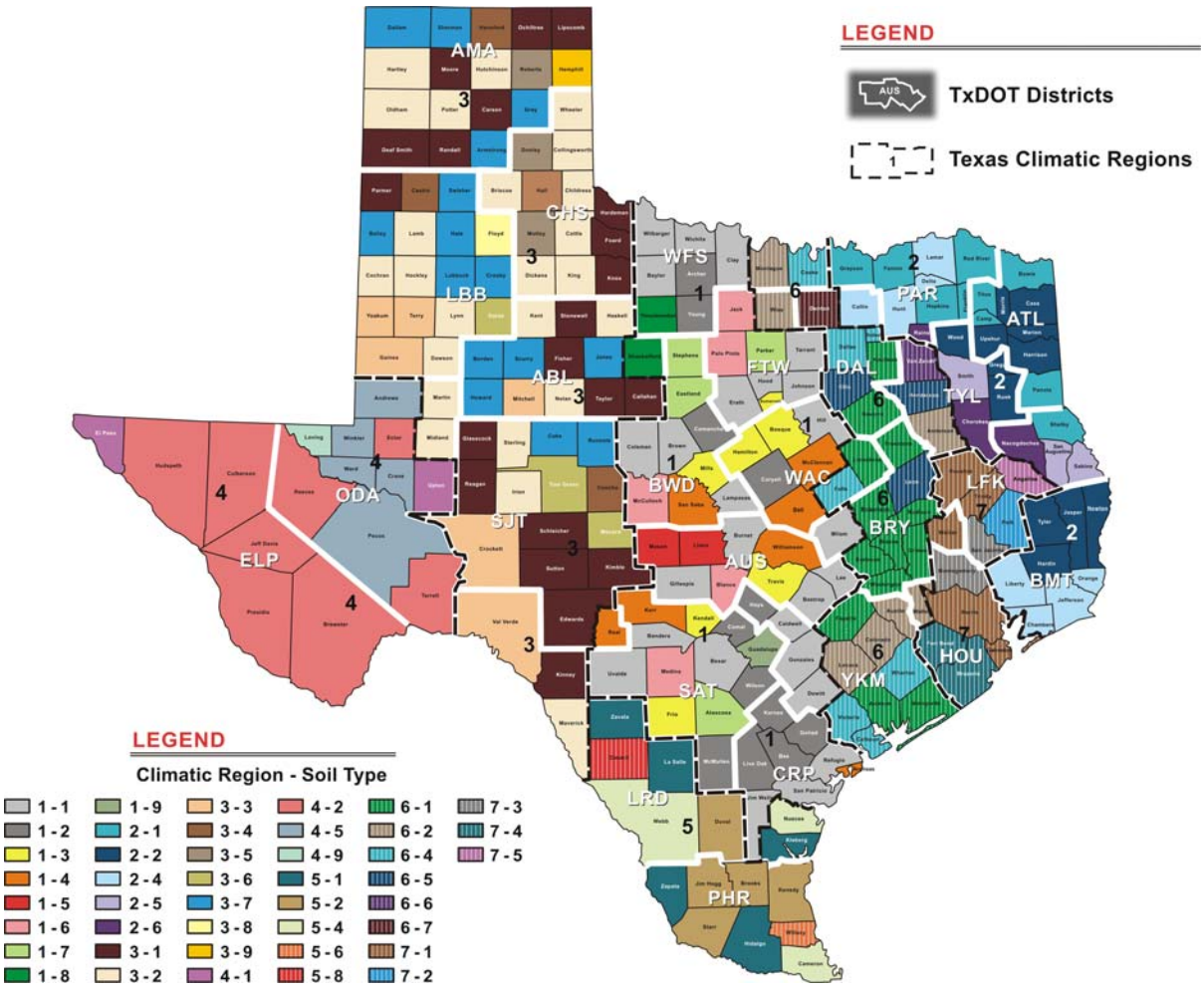

Figure 2.7. Texas Climatic-Soil Regions.

Table 2.1. Grouping of Texas Counties by Climatic-Soil Regions (counties identified by TxDOT county numbers).

Soil Region	Climatic Region							Count
	1	2	3	4	5	6	7	
1	10, 11, 12, 15, 25, 27, 28, 39, 42, 62, 73, 87, 90, 110, 112, 126, 127, 141, 144, 166, 196, 205, 220, 232, 243, 244	19, 32, 75, 81, 92, 113, 183, 194, 225	30, 33, 59, 70, 77, 79, 88, 97, 100, 134, 136, 138, 148, 171, 179, 185, 191, 192, 207, 217, 218, 221	72, 231	109, 137, 142, 253, 254	21, 26, 76, 82, 94, 121, 130, 147, 154, 158, 175, 198, 239	85, 102, 114, 210, 228, 236	83
2	5, 13, 46, 47, 50, 89, 106, 129, 149, 162, 247, 252	34, 93, 103, 155, 172, 230, 250	23, 38, 40, 44, 51, 58, 63, 104, 105, 111, 118, 119, 132, 135, 140, 153, 156, 159, 165, 177, 180, 188, 216, 242	22, 55, 69, 116, 123, 189, 195, 222	24, 66, 67, 125, 214	1, 8, 45, 143, 169, 237, 249	101, 122, 176, 187, 201, 229	69
3	18, 83, 98, 131, 167, 213, 227		53, 84, 168, 223, 233, 251				170, 204	15
4	4, 14, 133, 161, 193, 206, 246	43, 60, 117, 139	35, 48, 99		31, 178, 240	29, 49, 57, 74, 199, 235, 241	20, 36, 80, 124, 146, 181	30
5	150, 157		65, 173, 197	2, 52, 186, 238, 248		71, 108, 145	3, 202, 203, 212	17
6	16, 120, 160, 163, 182	190	86, 164, 226		245	234	37, 174	13
7	7, 68, 184, 215		6, 9, 17, 41, 54, 56, 91, 96, 115, 128, 152, 200, 208, 211, 219			61		20
8	209, 224		78		64			4
9	95		107	151				3
Count	66	21	78	16	15	32	26	254

CHAPTER III. ASSESSING THE IMPACT OF MOISTURE VARIATION ON LOAD BEARING CAPACITY OF PAVEMENTS

From the findings presented in research report 0-4519-1 (Fernando, Oh, Estakhri, and Nazarian, 2007), researchers verified that the current modified Texas triaxial design method gives very conservative estimates of load bearing capacity when compared to small- and large-scale plate bearing test results. From the analysis of UTEP test data, researchers observed significant changes in load bearing capacity with changes in the moisture condition of the base and subgrade layers. Hence, efforts were made to take the effect of moisture variation into account in a procedure to estimate or predict the load bearing capacity of pavements.

The moisture variation in the subgrade is a significant factor controlling bearing capacity, which is a function of the cohesion c, and angle of internal friction ϕ. Titus-Glover and Fernando (1995) developed equations to express strength parameters in terms of soil physical properties and soil suction. In this project, researchers used these equations to predict the effects of moisture changes on the load bearing capacity of pavements. This work led to modifications of the modified triaxial (*MTRX*) program for triaxial analysis that Fernando et al. (2001) developed in an earlier project. Researchers incorporated a procedure for adjusting strength properties to account for the effects of moisture changes on pavement load bearing capacity. This moisture correction procedure is available as an option in the *LoadGage* program developed from this project. *LoadGage* includes an extensive database of soil properties (covering all 254 Texas counties) that is used to evaluate the effects of moisture changes on soil strength properties and to account for effects of differences in moisture susceptibilities among soils in the triaxial design check. A user's guide to the program is given in a companion report to this project by Fernando, Oh, and Liu (2007).

MOISTURE CORRECTION OF STRENGTH PARAMETERS

The strength parameters c and ϕ define the Mohr-Coulomb failure envelope determined from triaxial tests on laboratory molded specimens. This failure envelope represents failure points corresponding to different levels of normal and shearing stresses. The equation for the failure envelope is given by Equation 3.1, which is the shear strength equation for a saturated soil (Fredlund and Rahardjo, 1993):

$$\tau = c + \sigma_n \tan\phi \quad (3.1)$$

where,

τ = shear stress,

σ_n = net normal stress on the failure plane at failure = $(\sigma_f - U_a)_f$,

σ_f = applied pressure at failure, and

U_a = pore air pressure.

Fredlund and Rahardjo (1993) formulated the shear strength equation of an unsaturated soil in terms of the normal stress and matric suction as given by:

$$\tau = c' + (\sigma_f - U_a)_f \tan\phi + (U_a - U_w)_f \tan\phi^b \quad (3.2)$$

where,

c' = effective cohesion defined as the intercept of the Mohr-Coulomb failure envelope on the shear stress axis when the normal stress and the matric suction are both equal to zero,

ϕ = angle of internal friction associated with the normal stress variable $(\sigma_f - U_a)$,

$(U_a - U_w)_f$ = matric suction on the failure plane at failure,

ϕ^b = angle indicating the rate of increase in shear strength relative to the matric suction, and

U_w = pore water pressure.

Equation 3.2 reduces to the shear strength equation for saturated soils when the pore water pressure U_w approaches the pore air pressure U_a and the matric suction component vanishes under saturated conditions. From examination of Equations 3.1 and 3.2, the total cohesion is determined to be:

$$c = c' + (U_a - U_w)_f \tan\phi^b \quad (3.3)$$

Titus-Glover and Fernando (1995) conducted triaxial tests on different types of base materials and subgrade (sand and clay) at three moisture levels, optimum and ± 2 percent of optimum. Additional tests were performed to obtain soil physical properties such as gradation and Atterberg limits, and the soil-water characteristic curves of the various materials tested. The final form of the equation to predict cohesion was based on Equation 3.3, which was derived from mechanistic analysis. It is given by:

$$c = c' + bU + d\,U \tan\phi \quad (3.4)$$

where,

U = suction in psi and

b, d = constants determined from test data.

Using Equation 3.4 as the functional form of the relationship between cohesion and soil suction, Titus-Glover and Fernando (1995) found the effective cohesion to be a function of the plastic limit, gradation, porosity, and specific gravity. The final form of the cohesion equation developed by these researchers is given by:

$$c = 12.167 + 0.229\,N40 - 0.373\,n - 0.006\,N40_N^2 - 0.998\,PL_N \times G_{sN} + 0.141U - 0.117U\tan\phi \quad (3.5)$$

where,

c = cohesion in psi,

$N40$ = percent of material passing the No. 40 sieve size,

n = porosity,

$N40_N$ = normalized N40 = ($N40$ – 55.889),

PL_N = normalized plastic limit = (PL – 15.896), and

G_{sN} = normalized specific gravity = (G_s – 2.608).

From examination of Equations 3.4 and 3.5, the effective cohesion c' is found to be given by the first five terms of Equation 3.5.

From a similar analysis of laboratory test data, Titus-Glover and Fernando (1995) developed an equation for predicting the angle of internal friction as follows:

$$\phi = 1.611 - 0.957\,PI - 0.881n - 4.13U_{pF} + 31.817\,G_s \quad (3.6)$$

where,

ϕ = friction angle in degrees,

PI = plasticity index, and

U_{pF} = soil suction in pF.

To convert suction in psi to suction in pF, the following relationship may be used:

$$U_{pF} = Log\,U_{psi} + 1.847 \quad (3.7)$$

Hence, as the soil moisture content varies, its strength parameters are expected to change since the moisture content is directly associated with soil suction based on Gardner's (1958) equation:

$$\theta = \frac{n}{1 + A_W \left| h_p \right|^a} \tag{3.8}$$

where,

θ = volumetric moisture content,

h_p = soil suction (or negative pore water pressure), and

A_w, a = coefficients of Gardner's equation.

From Equations 3.5 and 3.6, the following equations for adjusting strength properties due to changes in moisture content are obtained:

$$\phi_{target} = \phi_{initial} + a_0 \log\left(\frac{U_{initial}}{U_{target}}\right) \tag{3.9}$$

$$c_{target} = c_{initial} + a_1 \left(U_{target} - U_{initial}\right) + a_2 \left(U_{initial} \tan\phi_{initial} - U_{target} \tan\phi_{target}\right) \tag{3.10}$$

where,

ϕ_{target} = internal friction angle at target moisture content,

$\phi_{initial}$ = internal friction angle at initial moisture content,

U_{target} = suction (psi) at target moisture content,

$U_{initial}$ = suction (psi) at initial moisture content.

c_{target} = cohesion at target moisture content,

$c_{initial}$ = cohesion at initial moisture content,

a_0 = friction angle correction coefficient equal to 4.13, and

a_1, a_2 = cohesion correction coefficients equal to 0.141 and 0.117, respectively.

Note that the moisture correction requires the soil-water characteristic curve that gives the relationship between volumetric moisture content and soil suction for a given material. The friction angle and cohesion are adjusted based on the difference between the initial and target values of soil suction associated with the given change in moisture content. In this analysis, the initial values correspond to the moisture content at which triaxial tests on laboratory molded specimens were conducted to determine the cohesion and friction angle. These material parameters may be determined using the standard test method Tex-117E or the provisional test method Tex-143E. The target values correspond to the expected in-situ moisture content during the service life of the pavement.

EVALUATION OF LOAD BEARING CAPACITY BASED ON FIELD PLATE BEARING TEST DATA

Researchers used the moisture correction procedure described in the preceding in an evaluation of the load bearing capacity of the clay, sand, and stabilized sections that were built and tested at the Texas A&M Riverside Campus. Tables 3.1 and 3.2 identify these test sections. Three different cases were considered:

- Case I: Estimate load bearing capacity using the current modified triaxial design method given in TxDOT Test Method Tex-117E.
- Case II: Use the *LoadGage* program to estimate load bearing capacity based on subgrade strength parameters (cohesion and friction angle) obtained from Tex-117E laboratory triaxial tests (moisture correction option not used in the analysis).
- Case III: Run the *LoadGage* program to estimate load bearing capacity with the moisture correction option turned on to adjust the cohesion and friction angle based on the difference between the measured field moisture content at the time of the plate bearing tests and the moisture content of triaxial specimens tested following Test Method Tex-117E.

Case I Analysis

The load bearing capacities for Case I were evaluated in the companion report to this project by Fernando, Oh, Estakhri, and Nazarian (2007). Based on the triaxial classifications of the clay and sandy subgrades, and the nominal thicknesses of the flexible base sections, researchers used the Tex-117E flexible base design chart (Figure 3.1) to determine the allowable loads given in Table 3.3 for these sections. Researchers note that the term "allowable load" as used herein refers to a wheel load characterized by a circular footprint of uniform pressure and of load magnitude such that the subgrade shear stresses induced under load are within the Mohr-Coulomb failure envelope of the subgrade material. The term "allowable load" is not necessarily equivalent to the "design wheel load" that refers to the wheel load used for the thickness design of a given pavement. In terms of current practice, the design wheel load shown on the *x*-axis of the flexible base design chart (Figure 3.1) refers to one of the following:

Table 3.1. Flexible Base Sections Tested in Phase I of Research Project*.

Section Identifier	Subgrade	Base Material	Backcalculated Modulus (ksi)		Base Thickness (in)
			Base	Subgrade	
SSC_12	Clay	Sandstone	17.5	7.4	13
UGC_12	Clay	Uncrushed Gravel	38.6	10.3	12
CAC_12	Clay	Lime-Stabilized Caliche	18.0	8.6	12
G2C_12	Clay	Grade 2 Crushed Limestone	20.9	8.3	12
G1C_12	Clay	Grade 1 Crushed Limestone	20.3	9.6	12
SSC_6	Clay	Sandstone	22.4	9.1	6.5
UGC_6	Clay	Uncrushed Gravel	27.5	9.3	7.2
CAC_6	Clay	Lime-Stabilized Caliche	23.1	10.4	6.5
G2C_6	Clay	Grade 2 Crushed Limestone	40.8	11.4	6.7
G1C_6	Clay	Grade 1 Crushed Limestone	33.0	12.3	7
G1S_6	Sand	Grade 1 Crushed Limestone	64.6	11.2	6
G2S_6	Sand	Grade 2 Crushed Limestone	47.7	12.4	6
CAS_6	Sand	Lime-Stabilized Caliche	39.3	11.1	5
UGS_6	Sand	Uncrushed Gravel	64.9	12.0	6.8
SSS_6	Sand	Sandstone	101.5	12.5	6.6
G1S_12	Sand	Grade 1 Crushed Limestone	104.8	16.2	11
G2S_12	Sand	Grade 2 Crushed Limestone	28.0	15.5	11.8
CAS_12	Sand	Lime-Stabilized Caliche	70.6	14.8	11.5
UGS_12	Sand	Uncrushed Gravel	24.0	13.3	11
SSS_12	Sand	Sandstone	46.7	15.0	11.2

* Each section was 12 ft wide by 16 ft long.

Table 3.2. Stabilized Sections Tested in Phase II of Research Project[1].

Section Identifier	Section Composition	Backcalculated Modulus (ksi)			Thickness (in)	
		Stabilized Material	Base[2]	Subgrade	Stabilized Material	Base[2]
6B	Grade 2 with 4.5% cement on clay	580.0		14.5	5.8	
7B	Grade 2 with 3% cement on clay	272.6		13.2	6.4	
8B	Uncrushed gravel with 2% lime on clay	28.2		9.0	6.3	
9B	Thin Type D HMAC[3] over Grade 1 on clay	132.6	25.0	8.8	3.2	7.0
10B	Thick Type D HMAC over Grade 1 on clay	101.7	25.6	9.6	5.1	6.3
11B	Thick Type D HMAC over Grade 1 on sand	200.0	38.3	12.7	3.7	7.9
12B	Thin Type D HMAC over Grade 1 on sand	200.0	54.8	13.4	2.7	6.3
13B	Uncrushed gravel with 2% lime on sand	88.9		12.0	6.2	
14B	Grade 2 with 3% cement on sand	314.0		12.3	6.1	
15B	Grade 2 with 4.5% cement on sand	540.0		12.2	6.6	

[1] Each section was 12 ft wide by 16 ft long.
[2] Shaded cells indicate sections where the stabilized material is the base layer.
[3] Hot-mix asphaltic concrete pavement temperatures: 114 °F at clay site and 117 °F at sandy site.

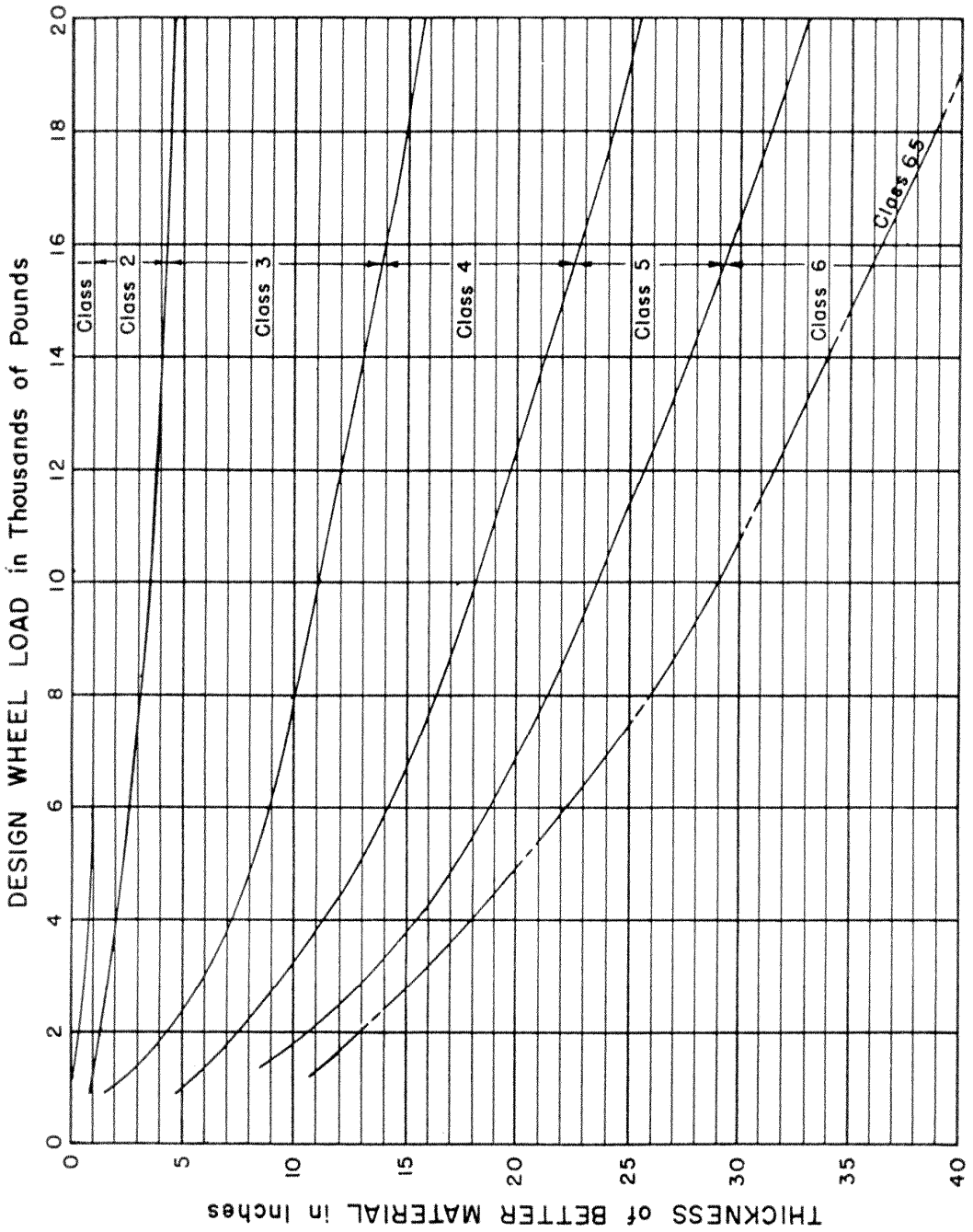

Figure 3.1. TxDOT Test Method Tex-117E Flexible Base Design Chart.

Table 3.3. Allowable Loads on Flexible Base Sections.

Material	Texas Triaxial Class	Allowable Load (kip)	
		6-inch sections	12-inch sections
Clay subgrade	6.1	1.0	2.5
Sandy subgrade	3.7	4.6	18.2

- the average of the ten heaviest wheel loads daily (ATHWLD) if the percent of tandem axles characterizing the traffic for the given design problem is less than 50 percent, or
- the ATHWLD multiplied by a load adjustment factor of 1.3 if the percent of tandem axles is equal to or greater than 50 percent.

While the allowable load and the design wheel load as used herein are based on the shear strength of the subgrade material as determined by its Mohr-Coulomb failure envelope, the difference in terminology relates to the context in which the terms are used. The design wheel load refers to the wheel load that the engineer specifies to come up with a thickness design. On the other hand, the term "allowable load" refers to the wheel load that a given pavement can structurally support without overstressing the subgrade based on its Mohr-Coulomb failure envelope. In this report, researchers use the term "allowable load" to quantify the load bearing capacity of the sections tested in this project. This load is determined from analyzing test data collected on a given section. Given this distinction, the results from this analysis should not be misinterpreted as loads used for designing the test sections.

To determine the allowable loads on the stabilized sections, researchers used the Texas triaxial design check module in TxDOT's FPS-19 program (with tandem loads less than 50 percent) to get the allowable load for an equivalent flexible base section determined in accordance with the Tex-117E thickness design charts. As an example, consider Section 9B, which consists of 3.2 inches of Type D HMAC, over 7 inches of Grade 1 crushed limestone base, over clay subgrade with a Texas triaxial class of 6.1. Using FPS-19, researchers determined this section to be equivalent to about a 12-inch flexible base section on the same clay subgrade as illustrated below:

- Flexible base thickness required: 12 inches
- Thickness reduction for HMAC: 1.8 inches
- Modified triaxial thickness required: 10.2 inches

The thickness reduction of 1.8 inches is determined from the Tex-117 thickness reduction chart (Figure 3.2), given the equivalent flexible base thickness of 12 inches and the cohesiometer value of 300 for the 3.2-inch thick HMAC layer. The cohesiometer value of 300 is taken from Table 3.4, which shows typical values used by TxDOT engineers for design of flexible pavements. Allowing for a thickness reduction of 1.8 inches, the required modified triaxial thickness is determined to be 10.2 inches, which equals the total as-built

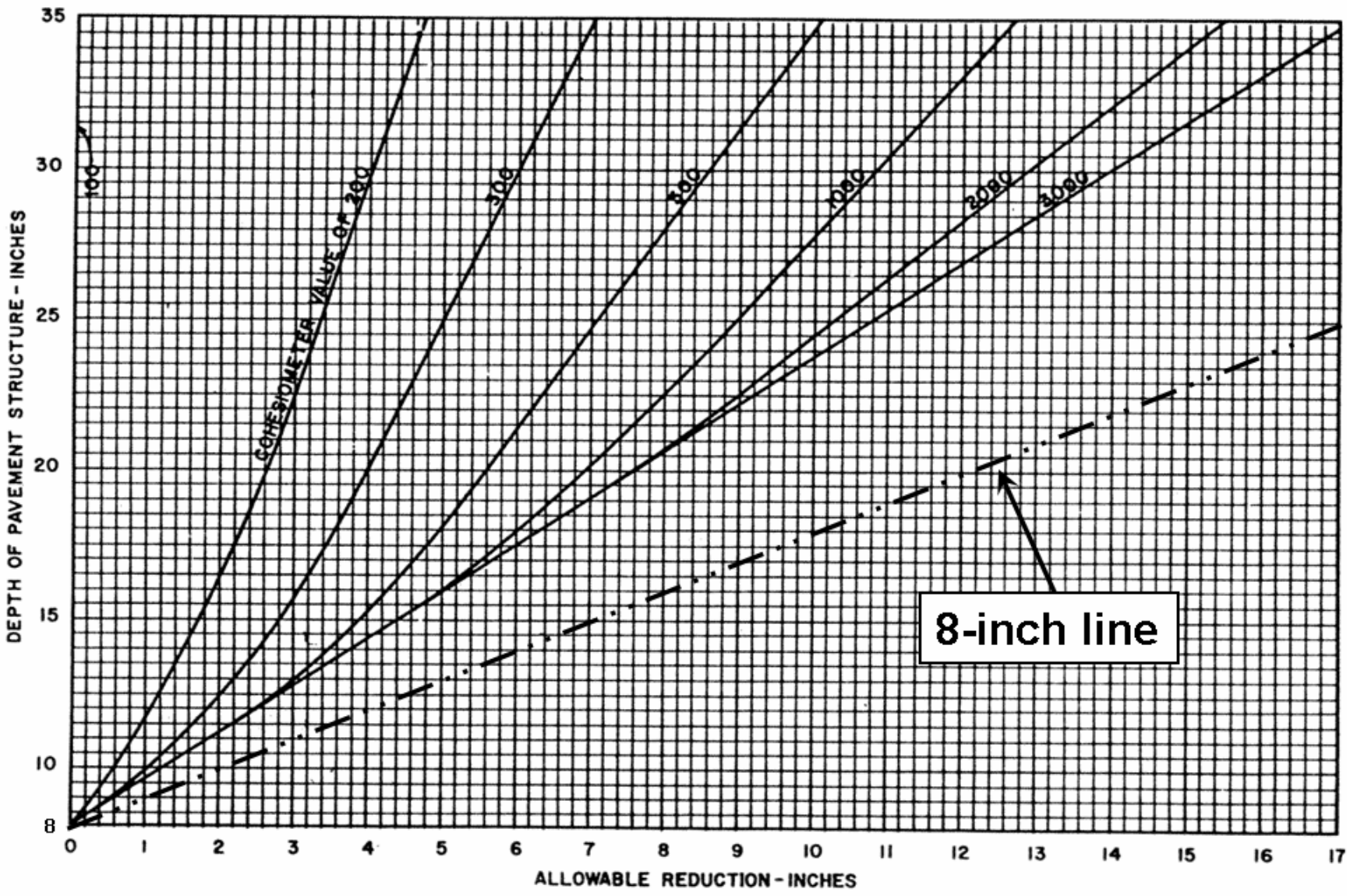

Figure 3.2. Tex-117E Thickness Reduction Chart for Stabilized Layers.

Table 3.4. Cohesiometer Values for Different Materials.

Material Type	Modified Cohesiometer Value
Lime-treated base greater than 3 inches thick	300
Lime-treated subgrade greater than 3 inches thick	250
Cement-treated base greater than 3 inches thick	1000
Cold-mix bituminous materials greater than 3 inches thick	300
Hot-mix bituminous materials greater than 6 inches thick	800
Hot-mix bituminous materials 4 to 6 inches thick	550
Hot-mix bituminous materials 2 to 4 inches thick	300

thickness of the stabilized section. Thus, for the equivalent flexible base section thickness of 12 inches and a subgrade triaxial class of 6.1, researchers determined the allowable load to be 2500 lb from the Tex-117 flexible base design chart given in Figure 3.1.

Researchers note that the above process involves a reversed application of the modified triaxial design method in Tex-117E. For flexible pavement design using this method, one would normally determine the required thickness of better material above the subgrade using the flexible base design chart given the design wheel load and the subgrade triaxial class. Thus, for the example given, the required depth of cover is determined to be 12 inches for a design wheel load of 2500 lb (assuming tandem loads less than 50 percent) and a subgrade triaxial class of 6.1. Since the pavement would have a stabilized layer, the engineer would then use the chart shown in Figure 3.2 to determine the applicable thickness reduction. From this chart, the thickness reduction is determined to be 1.8 inches, given the 12-inch depth of cover from the flexible base design chart and the cohesiometer value of 300 for the 3.2-inch thick HMAC layer. Thus, a modified triaxial thickness of (12.0 – 1.8) = 10.2 inches is determined, of which 3.2 inches is HMAC and the remaining 7 inches is flexible base.

Researchers used FPS-19 following the same procedure as described above to determine the allowable loads for the other stabilized sections. Table 3.5 shows the results from this analysis. Except for the HMAC sections, no thickness reductions were determined for the other stabilized sections, which have base thicknesses of less than 8 inches. Researchers note that the Tex-117E thickness reduction chart does not provide reductions for depths of cover below 8 inches as shown in Figure 3.2. In addition, examination of the cohesiometer curves in this figure shows that the thickness reductions from the curves will never result in a modified depth of cover less than 8 inches. Note that the cohesiometer curves are all to the left of the 8-inch line drawn in Figure 3.2 that gives the correction factors resulting in a modified triaxial thickness of 8 inches. Since no thickness reductions

Table 3.5. Allowable Loads on Stabilized Sections.

Section Identifier	Section Composition	Allowable Load* (kip)
6B	Grade 2 with 4.5% cement on clay soil	1.0
7B	Grade 2 with 3% cement on clay soil	1.0
8B	Uncrushed gravel with 2% lime on clay soil	1.0
9B	Thin Type D HMAC over Grade 1 on clay soil	2.5
10B	Thick Type D HMAC over Grade 1 on clay soil	4.2
11B	Thick Type D HMAC over Grade 1 on sandy soil	36.0
12B	Thin Type D HMAC over Grade 1 on sandy soil	13.0
13B	Uncrushed gravel with 2% lime on sandy soil	4.6
14B	Grade 2 with 3% cement on sandy soil	4.6
15B	Grade 2 with 4.5% cement on sandy soil	4.6

*Does not include correction for stabilized material on non-HMAC section

were determined for the non-HMAC stabilized sections using Tex-117E, the allowable loads given in Table 3.5 do not incorporate corrections for the stabilized materials on these sections.

Case II Analysis

For the Case II analysis, researchers used the cohesion and friction angle determined from Tex-117E triaxial tests on clay and sandy specimens, along with the backcalculated layer moduli and thicknesses of the sections built to predict the allowable loads based on the Mohr-Coulomb failure envelope. From triaxial test results, researchers determined the failure envelopes for the clay and sandy subgrades. The clay was found to have a cohesion of 1.7 psi and a friction angle of 10.3°. The sandy subgrade was characterized to have a cohesion of 6 psi and a friction angle of 32.8°. Tables 3.1 and 3.2 give the layer moduli backcalculated from falling weight deflectometer measurements taken on the flexible base and stabilized sections, respectively. Researchers performed the backcalculations using the MODULUS program (Michalak and Scullion, 1995). In addition, the tables show the layer thicknesses of the sections built.

Table 3.2 shows that the backcalculated asphalt and base moduli are rather low for the HMAC sections built on the clay subgrade. Researchers examined the FWD data from these sections and found that the deflections are rather high for the given sections. Table 3.6 shows the normalized deflections from these sections as well as the assessments of layer strengths as determined from the remaining life analysis module within the MODULUS program. In this table, UPR is an indicator of the strength of the upper pavement layers that

Table 3.6. Layer Strength Assessment Based on FWD Deflections.

Section	Station*	Normalized Sensor Deflection (mils)					SCI (mils)	Layer Strength		
		1	2	3	4	7		UPR	LWR	SGR
9B	1	37.93	19.99	8.34	5.08	2.51	17.94	PR	VP	VP
	2	45.14	24.66	10.70	6.04	2.66	20.48	VP	VP	VP
	3	39.31	20.21	8.75	5.50	2.53	19.10	PR	VP	VP
	4	41.14	23.44	10.16	6.15	2.55	17.70	PR	VP	VP
	Mean	40.88	22.07	9.49	5.69	2.56	18.81	PR	VP	VP
10B	1	36.63	19.00	8.48	5.20	2.37	17.63	PR	VP	VP
	2	45.01	24.15	10.03	5.64	2.55	20.86	VP	VP	VP
	3	31.25	16.16	7.80	4.84	2.45	15.10	PR	PR	VP
	4	33.69	18.59	9.14	5.67	2.33	15.11	PR	PR	VP
	Mean	36.64	19.47	8.86	5.34	2.43	17.17	PR	VP	VP

* FWD deflections taken along the longitudinal centerline of the section with plate positioned at ±2 and ±6 ft from the mid-point of the section. Front of trailer was positioned towards mid-point of section at each test location.

comprise the top eight inches of the pavement structure. This quantity is determined from the surface curvature index (SCI), which is the difference between the sensor 1 and sensor 2 FWD deflections.

It is observed from Table 3.6 that the SCIs are all high resulting in UPRs that range from poor (PR) to very poor (VP) for the HMAC sections on the clay subgrade. This assessment of the upper pavement strength is consistent with the low HMAC and base moduli backcalculated from the FWD deflections taken on these sections. In addition, researchers note that the strength of the lower pavement layers (LWR) and that of the subgrade (SGR) are generally very poor as determined from the base curvature indices (BCIs) and the sensor 7 FWD deflections. Considering these results, the authors are of the opinion that the backcalculated values for the HMAC and base layers are indicative of the poor support provided by the clay subgrade on these sections.

It is noted that that no pavement temperatures were available from the plate bearing tests on the HMAC sections. Thus, researchers used the HMAC backcalculated moduli without temperature correction to evaluate the load bearing capacities on the HMAC sections. While temperature correction was not possible, researchers note that the plate bearing tests were completed within a week of the FWD tests, and that tests on the HMAC sections were conducted from about noon to late afternoon under prevailing atmospheric conditions similar to the FWD tests.

Case III Analysis

For the Case III analysis, researchers characterized the soil-water characteristic curves of the clay and sandy materials on which the sections were built. Figures 3.3 and 3.4 show the data from soil-suction tests conducted on the clay and sandy materials, respectively. Researchers conducted these tests following the filter paper method described by Bulut, Lytton, and Wray (2001). The fitted curves and the coefficients of Gardner's equation for the soils tested are also shown in Figures 3.3 and 3.4. These coefficients relate the volumetric water content to the measured soil suction according to Equation 3.8.

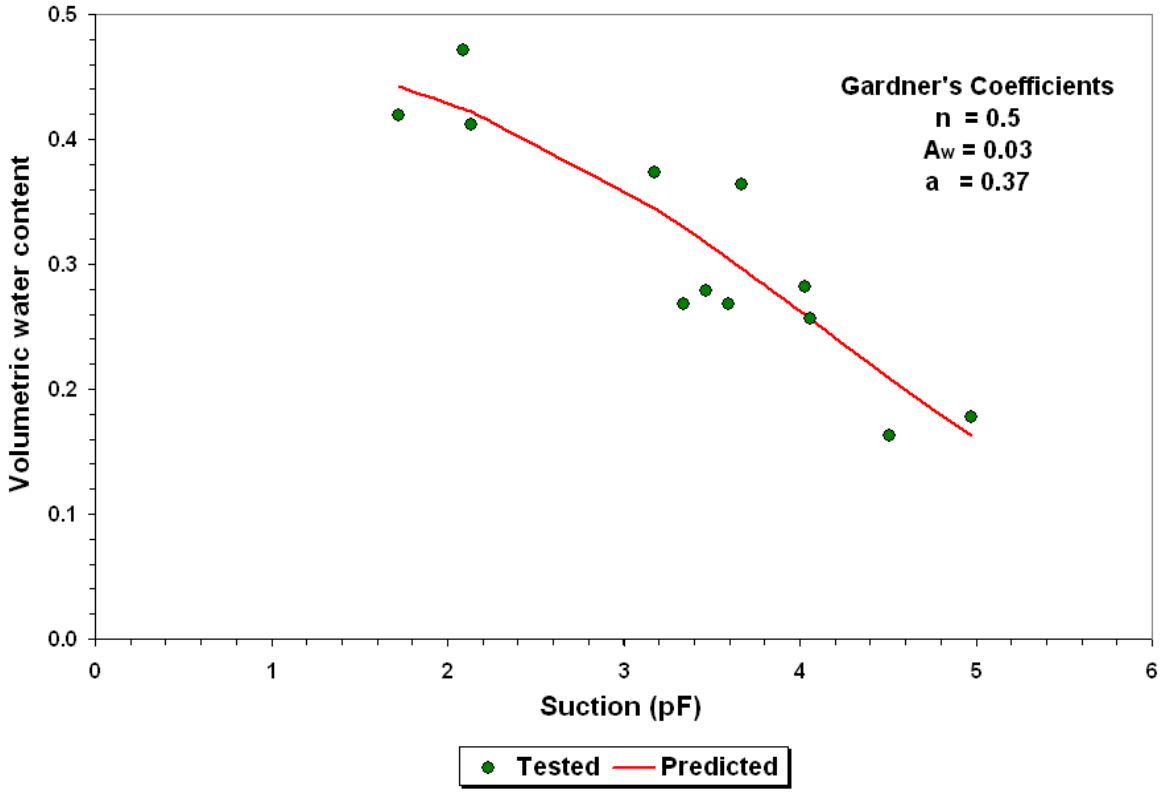

Figure 3.3. Results from Soil Suction Tests on Clay Subgrade.

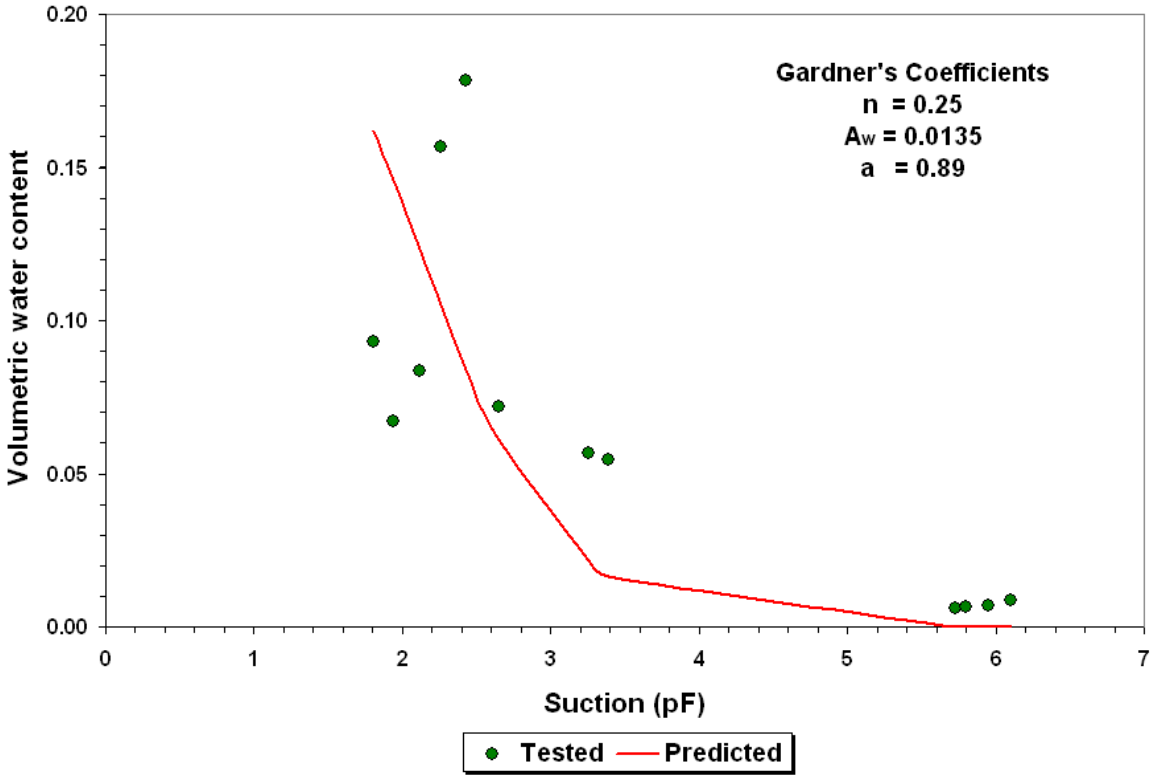

Figure 3.4. Results from Soil Suction Tests on Sandy Subgrade.

Figure 3.5 shows a run-time screen from the *LoadGage* program that illustrates the adjustment of subgrade strength properties due to changes in soil suction arising from moisture content variations. The program gives users the option to view the soil suction curve for a given material. From the specified initial and field moisture contents, the program shows on the chart the corresponding soil suction values that are used in Equations 3.9 and 3.10 to adjust the strength properties from the prescribed initial values to the in-situ values corresponding to the specified field moisture content. The reader is referred to the *LoadGage* user's guide by Fernando, Oh, and Liu (2007) for more details on the application of the program to perform a triaxial design check with the moisture correction option.

Researchers used the *LoadGage* program for the Case III analysis. In this analysis, the strength properties of the subgrade materials were determined according to Test Method Tex-117E (following current practice). Thus, the initial moisture contents correspond to the condition of the specimens after capillary wetting as prescribed in Tex-117E. For the clay material, researchers measured the moisture content to be 25 percent for the triaxial specimens. The corresponding moisture content for the sand specimens was 12.3 percent.

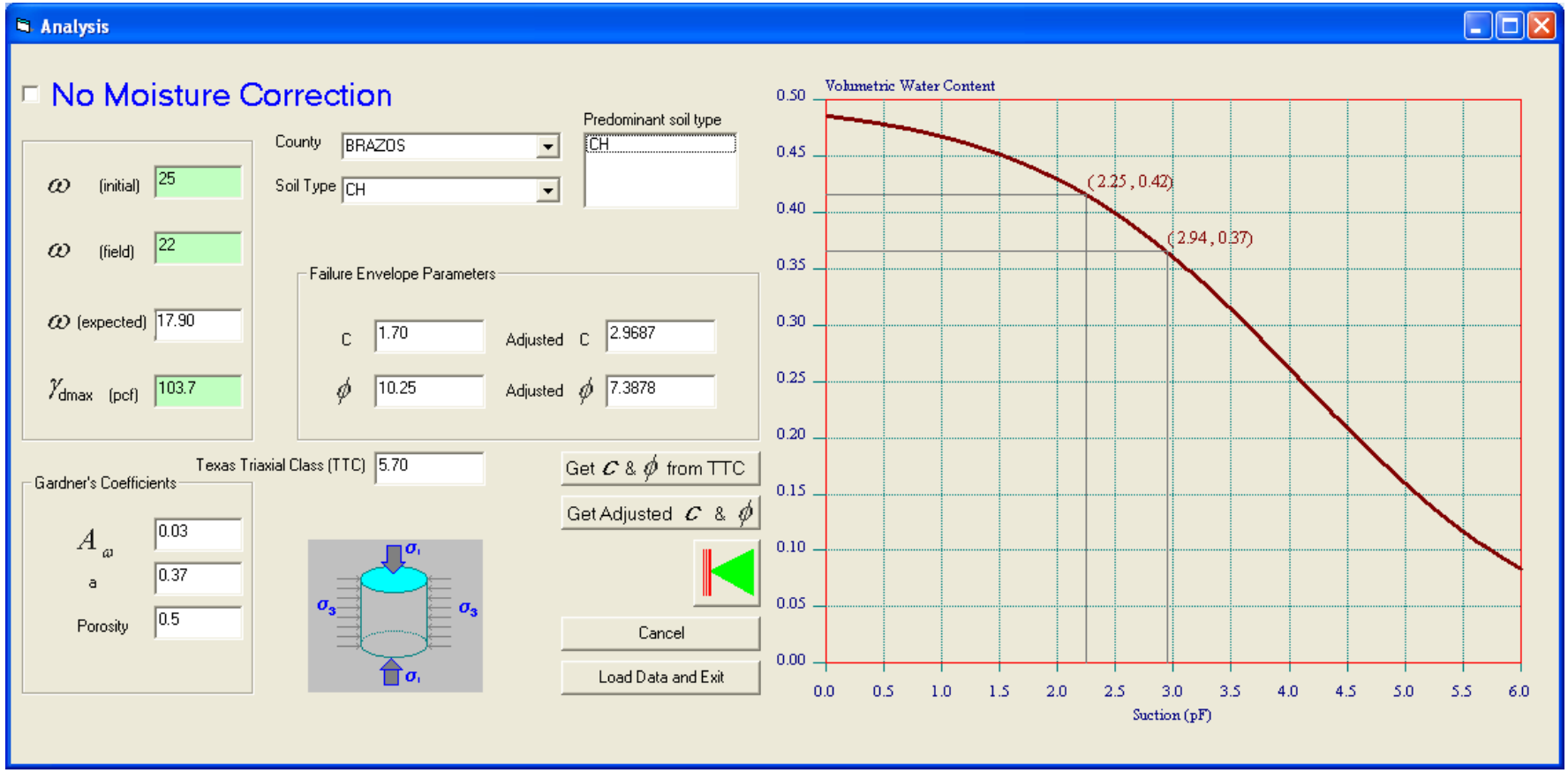

Figure 3.5. ***LoadGage*** **Run-Time Screen Illustrating Effect of Moisture Change on Soil Suction.**

After plate bearing tests were conducted on the flexible base sections, researchers took soil samples for determination of moisture content in the laboratory. From these tests, the average field moisture contents were determined to be 22 and 7 percent at the clay and sandy sites, respectively. Similar measurements made on these sites after field tests on the stabilized sections showed the average moisture contents to be 17.4 (clay) and 7 percent (sandy site). Given this information, researchers used the moisture correction procedure described previously to adjust the strength properties of the subgrade materials and estimate representative in-situ values for the Case III analysis.

Comparison of Load Bearing Capacity Estimates

Tables 3.7 to 3.9 show the load bearing capacity estimates for the three cases considered. For comparison purposes, the tables also show the load bearing capacity estimates corresponding to a permanent displacement of 50 mils on the sections tested. These estimates are based on an analysis of the measured deformation response from plate bearing tests done on these sections that is presented in the companion report to this project by Fernando, Oh, Estakhri, and Nazarian (2007).

A deformation of 50 mils is hard to discern with the naked eye, and is within the range of macro-texture of pavement surfaces. Thus, researchers used the load corresponding to a 50-mil permanent displacement as a reference in comparing the three methods used to predict pavement load bearing capacity under static loading. For each method, researchers determined the differences between the load bearing capacity predictions on the sections tested, and the corresponding reference values based on the 50-mil permanent displacement tolerance. Tables 3.7 to 3.9 show these differences. In these tables, a negative difference means that a given method underestimates the load bearing capacity based on the 50-mil criterion while a positive difference means just the opposite. To facilitate the comparison of the three methods, researchers plotted the differences from the 50-mil reference loads in Figures 3.6 to 3.8. The following observations are noted from these figures:

Table 3.7. Load Bearing Capacity Estimates for Sections on Clay Subgrade.

Section	Load Bearing Capacity (kip)				Difference from 50-mil Reference (kip)		
	50-mil	Case I	Case II	Case III	Case I	Case II	Case III
SSC_12	2	2.5	2.8	4.6	0.5	0.8	2.6
UGC_12	4.5	2.5	3.1	5	-2	-1.4	0.5
CAC_12	3.2	2.5	2.4	4	-0.7	-0.8	0.8
G2C_12	2.5	2.5	2.6	4.2	0	0.1	1.7
G1C_12	4.9	2.5	2.4	3.9	-2.4	-2.5	-1
SSC_6	2.4	1	1.6	2.6	-1.4	-0.8	0.2
UGC_6	2.6	1	1.6	2.5	-1.6	-1	-0.1
CAC_6	3	1	1.3	2.1	-2	-1.7	-0.9
G2C_6	4.7	1	1.6	2.5	-3.7	-3.1	-2.2
G1C_6	5.3	1	1.5	2.4	-4.3	-3.8	-2.9
Average difference (kip)					-1.8	-1.4	-0.1
Minimum difference (kip)					-4.3	-3.8	-2.9
Maximum difference (kip)					0.5	0.8	2.6
Average of absolute differences (kip)					1.9	1.6	1.3

Table 3.8. Load Bearing Capacity Estimates for Sections on Sandy Subgrade.

Section	Load Bearing Capacity (kip)				Difference from 50-mil Reference (kip)		
	50-mil	Case I	Case II	Case III	Case I	Case II	Case III
G1S_6	12.6	4.6	12.1	12.5	-8	-0.5	-0.1
G2S_6	11.5	4.6	10.1	10.3	-6.9	-1.4	-1.2
CAS_6	11.5	4.6	9.6	10.2	-6.9	-1.9	-1.3
UGS_6	10	4.6	11.8	12.1	-5.4	1.8	2.1
SSS_6	18.5	4.6	15	15.3	-13.9	-3.5	-3.2
G1S_12	20	18.2	19.5	20	-1.8	-0.5	0.0
G2S_12	12.5	18.2	11.8	12.5	5.7	-0.7	0.0
CAS_12	21.8	18.2	17	17.3	-3.6	-4.8	-4.5
UGS_12	6.5	18.2	11.2	11.3	11.7	4.7	4.8
SSS_12	12.3	18.2	13	13.5	5.9	0.7	1.2
Average difference (kip)					-2.3	-0.6	-0.2
Minimum difference (kip)					-13.9	-4.8	-4.5
Maximum difference (kip)					11.7	4.7	4.8
Average of absolute differences (kip)					7.0	2.1	1.8

Table 3.9. Load Bearing Capacity Estimates for Stabilized Sections.

Section	Load Bearing Capacity (kip)				Difference from 50-mil Reference (kip)		
	50-mil	Case I	Case II	Case III	Case I	Case II	Case III
6B	27.5	1	5.4	27.1	-26.5	-22.1	-0.4
7B	20	1	4	22.7	-19	-16	2.7
8B	12.5	1	1.5	8.5	-11.5	-11	-4
9B	13.3	2.5	2.7	15.6	-10.8	-10.6	2.3
10B	17	4.2	3	18.1	-12.8	-14	1.1
11B	14.5	36	20.6	21	21.5	6.1	6.5
12B	17.5	13	17.2	17.4	-4.5	-0.3	-0.1
13B	21	4.6	13.8	14.3	-16.4	-7.2	-6.7
14B	42.6	4.6	39	39.7	-38	-3.6	-2.9
15B	44.3	4.6	50	50	-39.7	5.7	5.7
Average difference (kip)					-15.8	-7.3	0.4
Minimum difference (kip)					-39.7	-22.1	-6.7
Maximum difference (kip)					21.5	6.1	6.5
Average of absolute differences (kip)					20.1	9.7	3.2

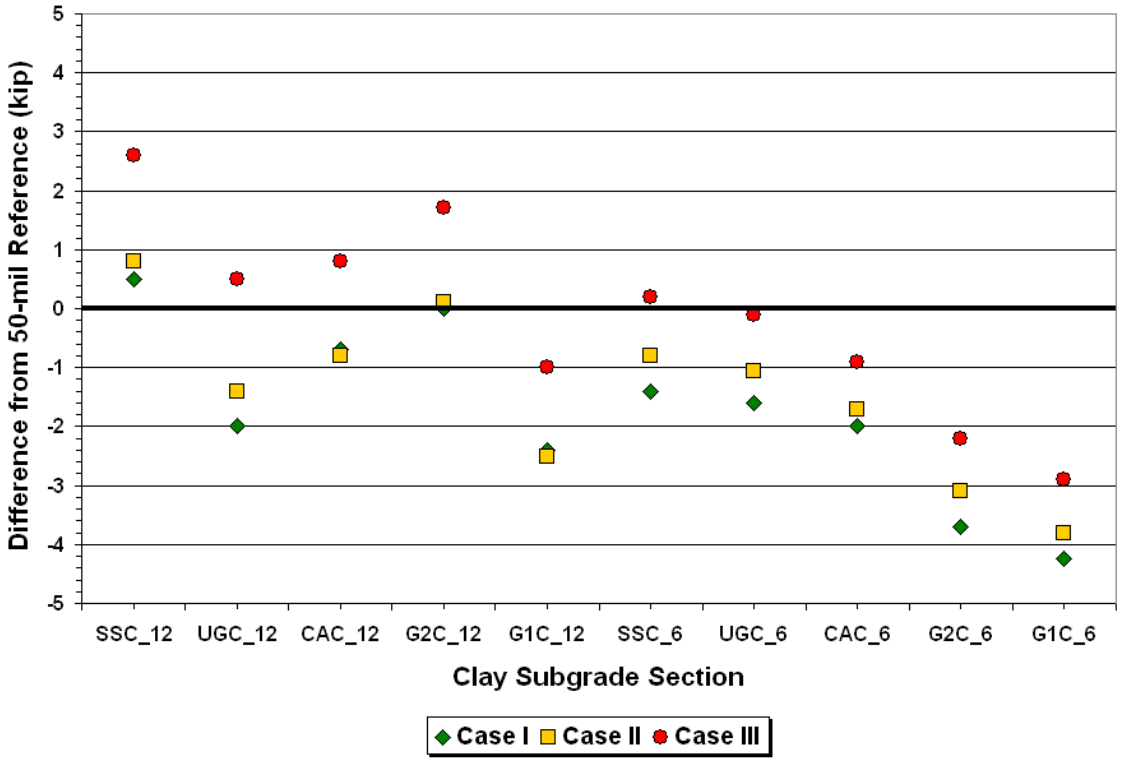

Figure 3.6. Differences between Case I, Case II, and Case III Load Bearing Capacity Estimates and 50-mil Reference Loads on Clay Subgrade Sections.

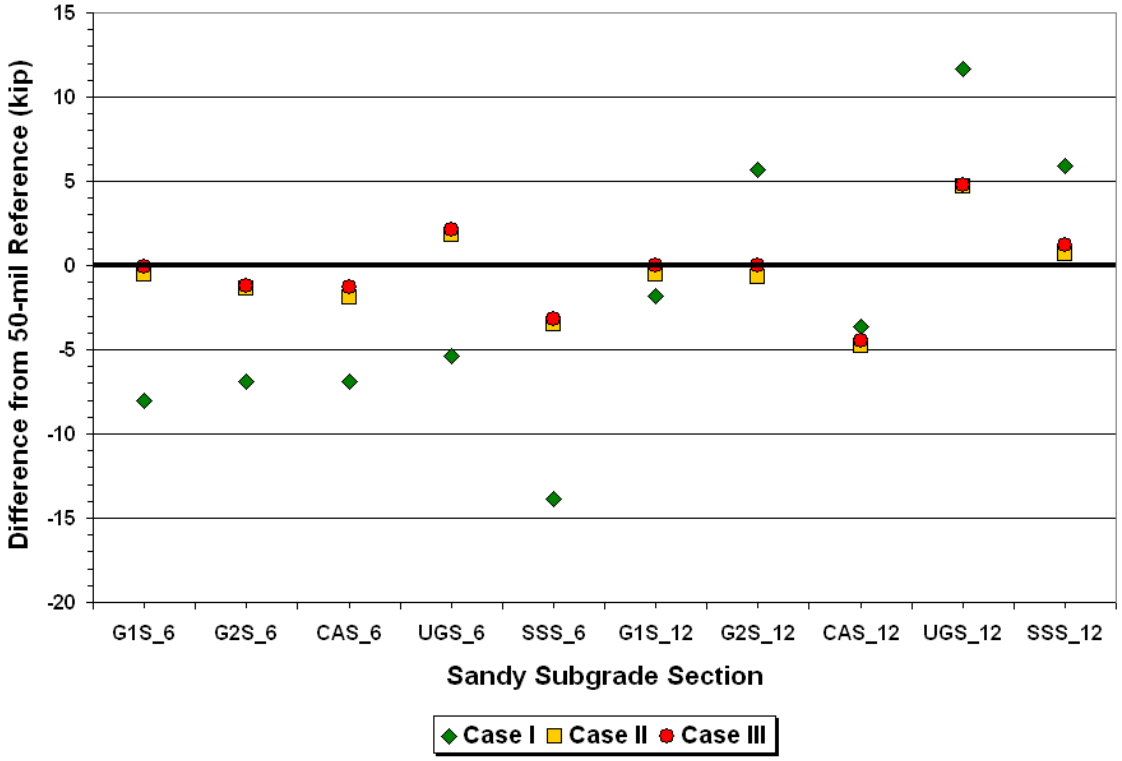

Figure 3.7. Differences between Case I, Case II, and Case III Load Bearing Capacity Estimates and 50-mil Reference Loads on Sandy Subgrade Sections.

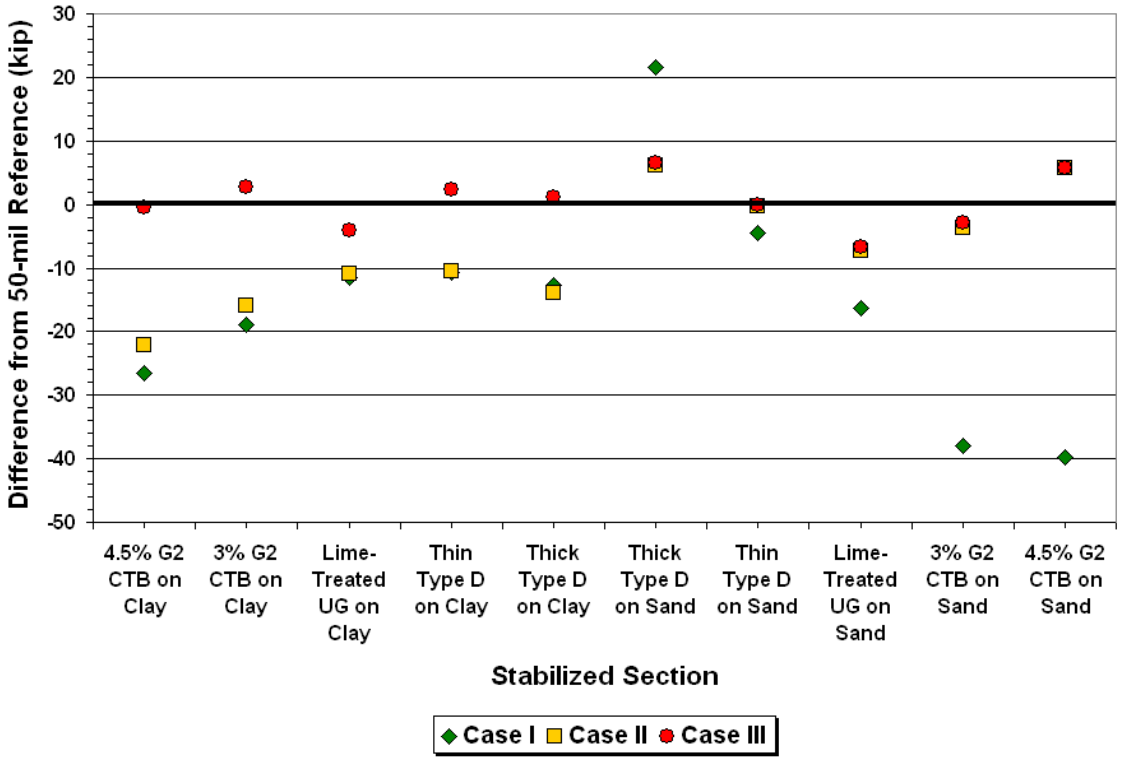

Figure 3.8. Differences between Case I, Case II, and Case III Load Bearing Capacity Estimates and 50-mil Reference Loads on Stabilized Sections.

- Overall, Figures 3.6 to 3.8 show that Case III exhibits the best agreement with the 50-mil reference loads. The differences associated with Case III are observed to plot closest to zero for most of the sections tested.
- For the flexible base sections built on clay subgrade, the Case III analysis gave the best agreement with the reference values on all but two of the sections, SSC_12 and G2C_12, where the estimates are higher than the reference loads by 2.6 and 1.7 kips, respectively (Table 3.7). On the 6-inch flexible base sections, Figure 3.6 shows that Case III gave the best results among the three methods.
- For the same clay subgrade, Figure 3.8 also shows that Case III gave the best agreement with the 50-mil reference loads on the stabilized sections.
- In general, Figures 3.6 to 3.8 show that Case I and Case II gave similar estimates of load bearing capacity on the clay subgrade sections. On the sandy subgrade sections, the estimates from Case II and Case III are more comparable. These observations apply to both the flexible base and stabilized sections.

The last bullet item reflects the effect of soil suction on the bearing capacity predictions. As explained in the beginning of this chapter, changes in soil moisture affect the strength properties of soils in accordance with the soil-water characteristic curve. For the clay and sandy subgrade materials investigated in this project, the soil-water characteristic curves are shown in Figures 3.3 and 3.4, respectively. Given these curves and the soil moisture contents corresponding to the laboratory and field test conditions, researchers predicted the change in soil suction with change in moisture content for each material.

Table 3.10 shows the results of this analysis using the *LoadGage* program. This table shows the moisture contents of the triaxial soil specimens as well as the subgrade materials at the times researchers performed the plate bearing tests on the full-scale field sections. At the measured moisture contents, researchers predicted the corresponding soil suction levels using the soil-water characteristic curves of the clay and sandy subgrade soils. Note the wider range in the predicted soil suctions and strength properties for the clay material compared to the sandy subgrade. Table 3.10 explains why the Case II and Case III analyses show more differences in bearing capacity estimates on the clay subgrade sections (where the effect of moisture change is more pronounced), and closer predictions on the sandy subgrade sections, where the effect of moisture is less significant.

Table 3.10. Variation of Soil Suction and Strength Properties with Moisture Content.

Subgrade	Test	Gravimetric moisture content (%)	Soil suction (psi)	Strength properties	
				Cohesion (psi)	Friction angle (degree)
Clay	Triaxial test	25	2.2	1.7	10.3
	Plate bearing (flexible base sections)	22	11.3	2.9	7.3
	Plate bearing (stabilized sections)	17.4	74.6	11.3	3.9
Sand	Triaxial test	12.3	0.1	6	32.8
	Plate bearing (flexible base and stabilized sections)	7	1.5	6.1	32.8

It is worth noting the similarity in the Case I and Case II predictions on the flexible base sections at the clay site (Table 3.7). Of the three methods, Case I and Case II are conceptually, the most similar in terms of the underlying theory used for computing load induced stresses, and the characterization of the Mohr-Coulomb failure envelope based on triaxial test data obtained in accordance with Test Method Tex-117E on moisture-conditioned specimens. However, on the sandy subgrade sections, Case I and Case II show more differences in load bearing capacity predictions. In the opinion of the authors, the differences observed are due to the approximate nature of the existing triaxial design method (Case I), which characterizes the strength of a given material in terms of the Texas triaxial class in lieu of c and ϕ. Note that a given Texas triaxial class can correspond to a range of failure envelopes defined by different cohesions and friction angles. In contrast, the Case II analysis is based on the specific c and ϕ parameters determined from triaxial tests on a given material. Another likely reason for the observed differences is that the existing thickness design curves in Test Method Tex-117E are based on certain assumptions regarding the variation of modular ratios with pavement depth. To the extent that the assumed modular ratios are in variance with ratios of the layer moduli specified in a Case II analysis, differences in predictions of load induced pavement stresses and the resulting bearing capacity estimates will arise. In the researchers' opinion, the Case II analysis represents a more refined method of evaluating pavement load bearing capacity compared to the existing thickness design curves, which are approximate in nature due to the assumptions made in

their development. The reader is referred to the review conducted by Fernando, Oh, Estakhri, and Nazarian (2007) for a detailed discussion of the development of these curves.

Based on the results presented in Tables 3.7 to 3.9, the Case II analysis appears to be more appropriate for assessment of pavement load bearing capacity compared to Case I. On the flexible base sections at the clay site, the authors consider the Case I and Case II predictions to be comparable, with the Case II predictions showing slightly better agreement with the 50-mil reference loads on the 6-inch sections. However, on the sandy subgrade and stabilized sections, the Case II predictions show better agreement with the reference loads compared to Case I, where the load bearing capacity estimates are quite conservative for the majority of the sections, particularly the 6-inch flexible base sections on the sandy subgrade (Table 3.8), and the stabilized sections (Table 3.9).

While the Case I results are generally the most conservative relative to the reference load bearing capacities corresponding to the 50-mil limiting permanent displacement criterion, there are four sections, SSS_12, UGS_12, G2S_12, and 11B (thick HMAC section on sandy subgrade) where the Case I predictions are higher than the 50-mil reference loads and the corresponding Case II and Case IIII load bearing capacity predictions. Based on the plate bearing test data, researchers estimated the permanent displacements associated with the Case I predictions on these sections to be 64, 120, 72, and 136 mils, respectively. On two of the three sandy subgrade sections (SSS_12, and G2S_12), the Case II and Case III predictions are significantly lower than the Case I allowable loads, and closer to the pavement load bearing capacities corresponding to the 50-mil permanent displacement tolerance.

Comparing the Case II predictions with those from Case III, the authors note the following observations from the results presented in Tables 3.7 to 3.9:

- The Case III analysis with moisture correction of the failure envelope parameters generally gave predictions that are closer to the reference loads corresponding to the 50-mil permanent displacement tolerance for flexible base sections on clay (in particular, the 6-inch sections).
- For the flexible base sections on sand, the Case II and Case III analyses gave similar results, with Case III being slightly better, in the authors' opinion. The Case I predictions significantly underestimate the 50-mil reference loads on the 6-inch flexible base sections at the sand site, and significantly overestimate the reference

loads on three of the five 12-inch flexible base sections, SSS_12, UGS_12 and G2S_12. On these sections, the estimated permanent displacements associated with the Case I predictions are 64, 120, and 72 mils, respectively.

- On the stabilized sections, the Case I and Case II predictions are quite conservative for the sections built on clay (Table 3.9). For these stabilized sections, the Case III results are better in the researchers' opinion. For the stabilized sections built on sand, the Case II and Case III analyses gave similar results. The Case I predictions for the stabilized sections are generally too conservative, with the exception of the thick HMAC section on the sandy subgrade, where Case I significantly overestimates the 50-mil reference load.

Considering the above findings, the authors offer the following recommendations with respect to revising the existing triaxial design check done in accordance with Tex-117E:

- The researchers recommend using a Case II analysis for thin-surfaced roads with flexible base and no stabilized layers.
- For design of pavement sections with stabilized materials, the researchers recommend using a Case III analysis for roadways underlain by fine-grained soils such as clays and silts. For stabilized sections founded on coarse-grained materials such as sandy soils and gravels, the researchers recommend a Case II analysis.

The results of the evaluation presented herein demonstrated the influence that soil moisture can have on subgrade strength properties and the predicted load bearing capacity. In view of this finding, the researchers recommend that the engineer consider running a Case III analysis to check the Case II analysis results on thin-surfaced roads with flexible base and no stabilized layers. This check is particularly recommended on thin-surfaced roads founded on moisture-susceptible fine-grained soils, i.e., clays and silts. On projects (such as in west Texas) where the expected in-service soil moisture content might be drier than the moisture content corresponding to the Texas triaxial class or subgrade failure envelope based on Tex-117E, running a Case III analysis would give the engineer an indication of the factor of safety associated with the Case II analysis. On the other hand, if the subgrade failure envelope corresponds to a different moisture content (such as the optimum condition proposed in Tex-143E), and the expected in-service moisture content is higher than the value used for triaxial testing, the researchers recommend a Case III analysis (in lieu of Case II) to check the FPS design on thin-surfaced pavements founded on moisture-susceptible soils.

This analysis would permit the engineer to consider the potential reduction in load bearing capacity arising from a wetter soil condition.

EVALUATION OF LOAD BEARING CAPACITY BASED ON UTEP DATA FROM TESTS ON SMALL-SCALE PAVEMENT MODELS

The University of Texas at El Paso carried out laboratory plate bearing tests on small-scale pavement models during this project. UTEP researchers conducted these tests on models fabricated with the same base and subgrade materials used for construction of the full-scale pavement sections tested at the Texas A&M Riverside Campus. The fabrication of these models and the setup used for the laboratory plate bearing tests are documented in research report 0-4519-1 by Fernando, Oh, Estakhri, and Nazarian (2007).

Small-scale pavement tests provided researchers the opportunity to study the effects of moisture on load bearing capacity under controlled laboratory conditions. As described in research report 0-4519-1, UTEP fabricated small-scale pavement models and ran plate bearing tests at three different moisture conditions. Moisture conditioning was achieved by adding water in stages, carefully measuring the amount of water added to the small-scale model so that the bulk moisture content of the soil in the tank could be calculated during moisture conditioning. UTEP researchers tested each model at three different times corresponding to:

- three days after model fabrication (representing optimum condition),
- after moisture conditioning of the subgrade, and
- after moisture conditioning of the base and subgrade.

For the second item, the moisture conditioning was considered complete after the resistance from the resistivity probes became constant for about 48 hours. For the third item, moisture conditioning was terminated when either the small-scale model would not absorb moisture as judged by the volume of water in the container supplying moisture to the model, or when the surface of the model was completely moist. Tables 3.11 and 3.12 show the moisture contents of the small-scale models as determined by UTEP from their tests. It is observed that the clay and caliche materials exhibited significant changes in moisture content as the models underwent moisture conditioning as compared to the other materials.

Table 3.11. Measured Moisture Contents of Subgrade Soils from Tests on Small-Scale Pavement Models.

Small-Scale Pavement Model		Subgrade Soil Moisture Content (%)	
Subgrade Material	Base Material	Optimum	After Moisture Conditioning
Sandy	Caliche	10.6	14.7
	Grade 1 Crushed Limestone	11.6	14.8
	Grade 2 Crushed Limestone	10.7	15.2
	Sandstone	10.1	14.7
	Uncrushed Gravel	11.3	13.5
Clay	Caliche	18.3	32.7
	Grade 1 Crushed Limestone	20.5	29.4
	Grade 2 Crushed Limestone	16.9	28.9
	Sandstone	15.0	32.9
	Uncrushed Gravel	17.4	26.6

Table 3.12. Measured Moisture Contents of Base Materials from Tests on Small-Scale Pavement Models.

Subgrade Material	Model Condition	Base Moisture Content (%)				
		Caliche	Crushed Limestone		Sandstone	Uncrushed Gravel
			Grade 1	Grade 2		
Sandy	Optimum	13.2	7.5	6.1	6.1	7.0
	Moisture-Conditioned Subgrade	19.0	9.8	6.4	6.2	8.1
	Moisture-Conditioned Base/Subgrade	21.1	10.7	7.3	7.6	9.2
Clay	Optimum	11.6	7.7	7.7	6.2	6.1
	Moisture-Conditioned Subgrade	19.0	9.4	8.7	7.4	6.3
	Moisture-Conditioned Base/Subgrade.	21.3	9.9	8.9	9.5	8.8

Similar to the analysis of data from full-scale plate bearing tests, researchers determined the loads corresponding to a permanent displacement of 50 mils using the data from small-scale pavement tests conducted at UTEP. Figures 3.9 and 3.10 show the results from these calculations. For comparison, laboratory equivalent values of allowable loads based on the current triaxial design curves are also shown on the charts. These values were determined by dividing the Tex-117E allowable loads by four, corresponding to the ratio of the loaded areas between full-scale and small-scale testing, following similitude rules.

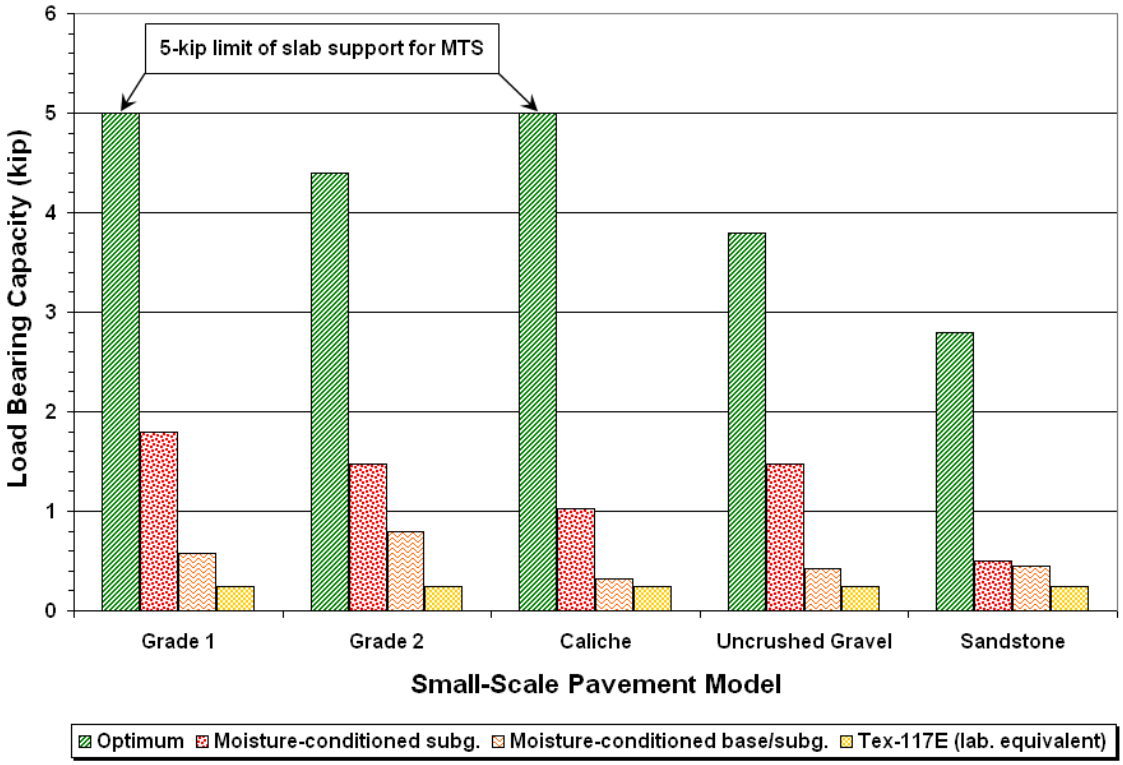

Figure 3.9. Variation of Load Bearing Capacity with Moisture Condition from Small-Scale Tests of Models with Base Materials on Clay.

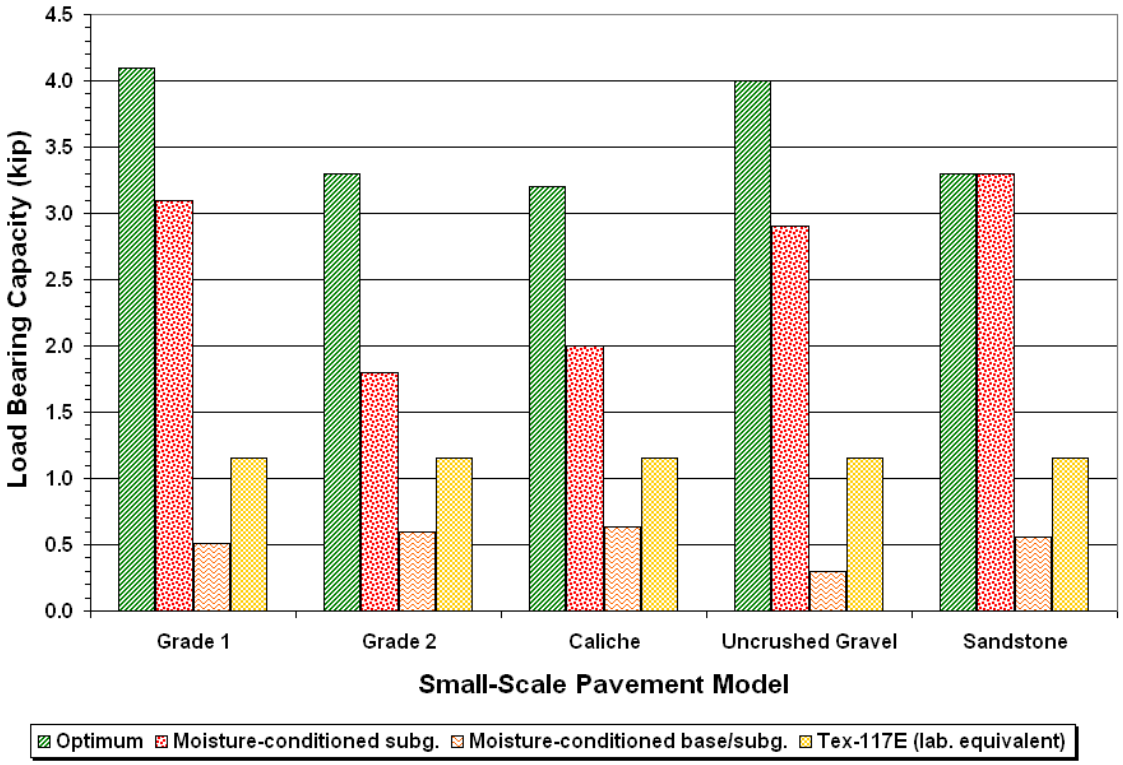

Figure 3.10. Variation of Load Bearing Capacity with Moisture Condition from Small-Scale Tests of Models with Base Materials on Sandy Subgrade.

Figure 3.9 shows drastic reductions in load bearing capacity between the optimum moisture condition and after moisture conditioning of the subgrade for small-scale models where the base materials are placed on clay. On the sand specimens, the reductions in load bearing capacity are not as dramatic (see Figure 3.10), reflecting lesser susceptibility to moisture of the sandy subgrade material compared to the clay. It is interesting to note that the laboratory equivalent Tex-117E loads are more comparable with the results from tests after the base and subgrade are moisture conditioned, particularly for the clay specimens. This observation reflects the high degree of conservatism in the current test method. In the authors' opinion, the observed differences in the load bearing capacities at various moisture conditions suggest the need to properly account for these effects in the existing triaxial design method, considering the range of climatic and soil conditions found across the state.

Researchers used the UTEP data to verify the moisture correction procedure presented earlier in this chapter. Given the soil suction curves as well as the strength properties (cohesion and friction angle) of the clay and sandy materials from Tex-117E triaxial testing, researchers applied the moisture correction procedure (Case III analysis) to adjust the strength properties determined to values corresponding to the optimum moisture contents at which plate bearing tests were conducted on small-scale pavement models. Researchers then used the corrected properties to predict load bearing capacity and compared the predictions with the allowable loads corresponding to a permanent displacement of 50 mils from the plate bearing test data.

Resilient modulus data for this evaluation were obtained from laboratory resilient modulus tests conducted at UTEP on the five flexible base materials and two subgrade soils used for fabricating the small-scale pavement models. Based on the test data collected for a given material, researchers characterized its modulus as stress-dependent according to the following relationship proposed by Uzan (1985):

$$M_R = K_1 P_a \left(\frac{I_1}{P_a} \right)^{K_2} \left(\frac{\tau_{oct}}{P_a} \right)^{K_3} \qquad (3.11)$$

where,

M_R = resilient modulus,

P_a = atmospheric pressure (14.5 psi),

I_1 = first stress invariant,

τ_{oct} = octahedral shear stress, and

K_1, K_2, K_3 = stress-dependent material coefficients.

Researchers fitted the above model to the resilient modulus data to determine the stress-dependent material coefficients for each material. Table 3.13 gives these coefficients for the two conditions (optimum and after moisture conditioning) at which tests were conducted.

Figure 3.11 compares the predicted load bearing capacities with the corresponding allowable loads based on the 50-mil limiting permanent displacement criterion. In the analyses, materials were characterized as stress-dependent using the corresponding K_1, K_2, and K_3 coefficients in the *LoadGage* program. The results from the Case III analysis (with moisture correction) show that the predicted load bearing capacities compare reasonably with the allowable loads corresponding to the 50-mil permanent displacement criterion, particularly for the sand specimens. However, the predictions tend to be conservative, particularly for the clay models where the average of the differences between the predicted and reference allowable loads is -1 kip. For the sand specimens, the average difference is -0.34 kip. These differences can arise because of measurement errors during testing, errors in modeling the response of the small-scale pavement models, and other unexplained or unaccounted sources of variation. While the predictions reflect some conservatism, researchers note that even more conservative estimates would have been determined had the moisture condition of the subgrade soil not been considered in the analysis, as is presently the case in practice. The proposed moisture correction procedure provides engineers the option to consider the effect of moisture on load bearing capacity in the triaxial design check. In the authors' opinion, the results from this limited laboratory evaluation verified that the procedure gave reasonable predictions that are in accord with the expected change in load bearing capacity as the soil moisture condition changes from wet (corresponding to Tex-117E moisture conditioning) to optimum.

Table 3.13. Resilient Modulus Parameters of Base and Subgrade Materials.

Test Condition	Parameter	Base Material					Subgrade Material	
		Caliche	Limestone		Sandstone	Uncr. Gravel	Sand	Clay
			Gr. 1	Gr. 2				
Optimum	K_1	2434	3423	657	1901	669	919	1927
	K_2	-0.2	0.35	0.7	0.35	0.7	0.60	0.0
	K_3	-0.2	-0.2	-0.3	-0.1	-0.6	0.0	-0.1
	R^2	0.91	0.89	0.94	0.91	0.91	0.86	0.97
After moisture conditioning	K_1	281	1699	367	2196	490	437	2916
	K_2	0.5	0.20	0.5	0.0	1.0	1.0	0.9
	K_3	-0.4	-0.11	-0.3	0.2	-0.5	-0.24	0.8
	R^2	0.99	0.97	0.90	0.96	0.94	0.81	0.93

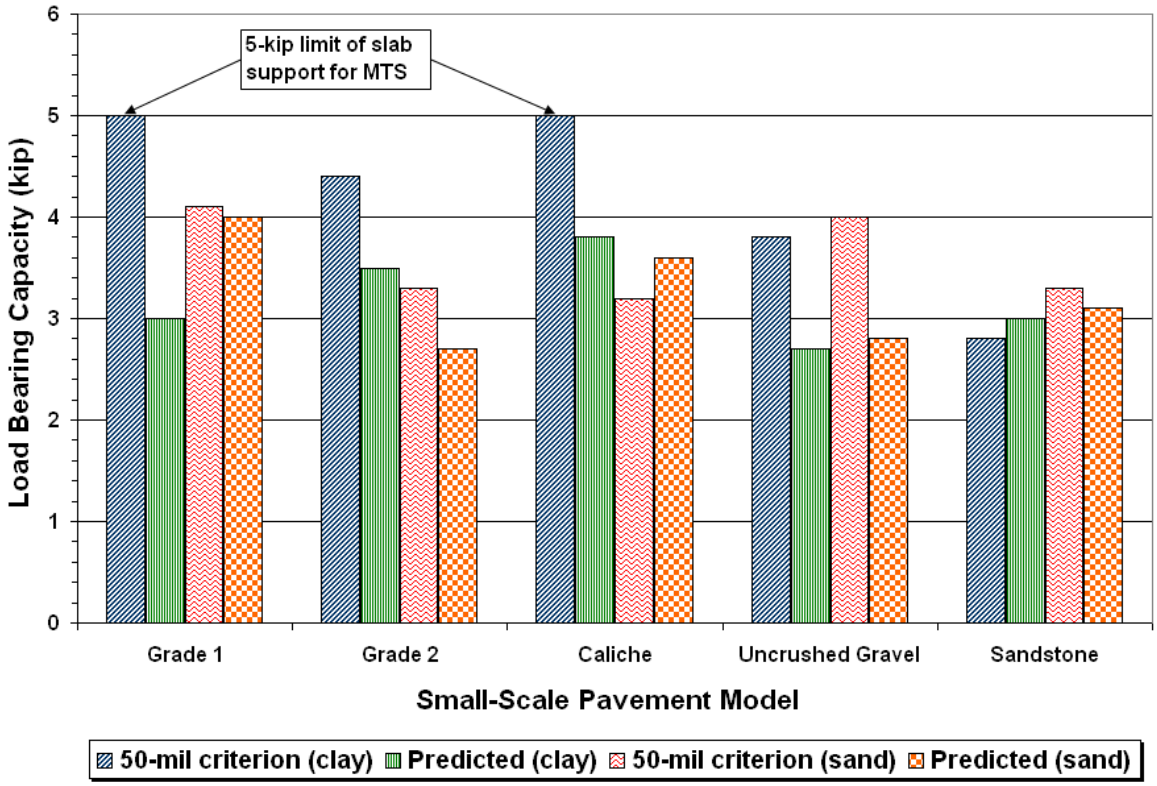

Figure 3.11. Comparison of Load Bearing Capacity Predictions Corresponding to Optimum Moisture Conditions for Small-Scale Models Built using Clay and Sandy Subgrade Soils.

CHAPTER IV. EVALUATION OF EXPECTED IN-SERVICE SOIL MOISTURE CONTENTS

INTRODUCTION

To support implementation of the revised methodology incorporated in *LoadGage* for conducting a triaxial design check on FPS pavement designs, researchers compiled a database of soil characteristics covering all 254 Texas counties. For each county, the database includes information on Texas triaxial classifications, soil water characteristic curves, and expected in-service soil moisture contents. To compile this comprehensive database, researchers first reviewed published county soil survey reports to identify the different soils (based on the Unified Soil Classification system) found in a given county. This review identified the predominant soils from the acreage information given in the soil survey reports. Once the soil types were established, researchers undertook the task of compiling data on soil characteristics that are needed to run a triaxial design check using *LoadGage*. The intent was to compile information that the engineer can use at his or her discretion in the absence of site-specific data for a given analysis. For the most part, this task consisted of finding and compiling published information. However, the development of the database also included analyses of the expected in-service moisture content by soil type and climatic region. These analyses were done in order to provide information useful for moisture correction should the engineer decide to take this option. The expected in-service soil moisture contents were evaluated using a comprehensive model of climatic effects initially developed by Lytton et al. (1990) for the Federal Highway Administration. Researchers used an updated version of this model, referred to as the Enhanced Integrated Climatic Model (EICM), to evaluate expected soil moisture contents in this project. The present chapter describes this evaluation, which was done as part of developing the soils database in the *LoadGage* program.

COMPILATION OF DATA FOR SOIL MOISTURE PREDICTION

Climatic data collected in this project included air temperatures, precipitation, relative humidity, and Thornthwaite moisture index. Researchers used these variables to characterize the state into climatic regions as documented in Chapter II of this report. In addition, representative Texas triaxial classifications, soil-water characteristic curves, and soil permeability characteristics were compiled for the different soil types identified in each

county. For this task, the project director provided researchers with an electronic spreadsheet of Texas triaxial classifications by soil series, which were compiled over the years from triaxial tests conducted by TxDOT. Researchers used this information to assign representative Texas triaxial classifications for the different soil types identified by county. Similarly, soil suction and permeability characteristics (Tables A3 and A4) were established from published information given by Mason et al. (1986) and Lytton et al. (1990), and from data on soil suction tests conducted at the Texas Transportation Institute (TTI) during this project.

Having compiled a statewide database on climatic and soil characteristics, researchers used EICM to evaluate expected soil moisture content variations for a representative range of pavements found in Texas (Oh et al., 2006). For this purpose, TxDOT provided information on pavement geometric characteristics (structural layers and thicknesses) as well as material types characterizing typical pavement structures found in the different Texas climatic regions. Figure 4.1 illustrates typical cross-sections of Farm-to-Market roads considered in this evaluation. Researchers focused on FM roads because these roads are expected to be the most susceptible to moisture and environmental effects because of the types of materials used and the relatively thinner layer thicknesses in comparison to Interstate, U.S., or state highways. In addition, researchers obtained data through a web search on groundwater table depths in Texas (National Water Information System, 2006). This parameter significantly affects the moisture content predictions, and hence, the equilibrium modulus values of the underlying pavement layers. The groundwater table is used to calculate lower boundary suction for the entire day. Lower boundary suction data represents the position of the water table. If the water table is at the bottom of the soil profile, the value of lower boundary suction is set to zero at that location or node in the EICM program. If the water table is higher than the bottom node of the soil profile, a positive value for suction is used based on the hydrostatic pressure (Larson and Dempsey, 1997). If the water table is beneath the bottom node, the user should input the current suction at that node, which is computed as a negative hydrostatic pressure.

Previous research has found that, in arid climates, if the water table exists within a depth of 30 ft below the pavement surface, it will dominate the moisture conditions in the subgrade (Lytton et al., 1990). In this case, the suction profiles are calculated using hydrostatic pressure. Where the water table is below 30 ft, moisture movement will largely

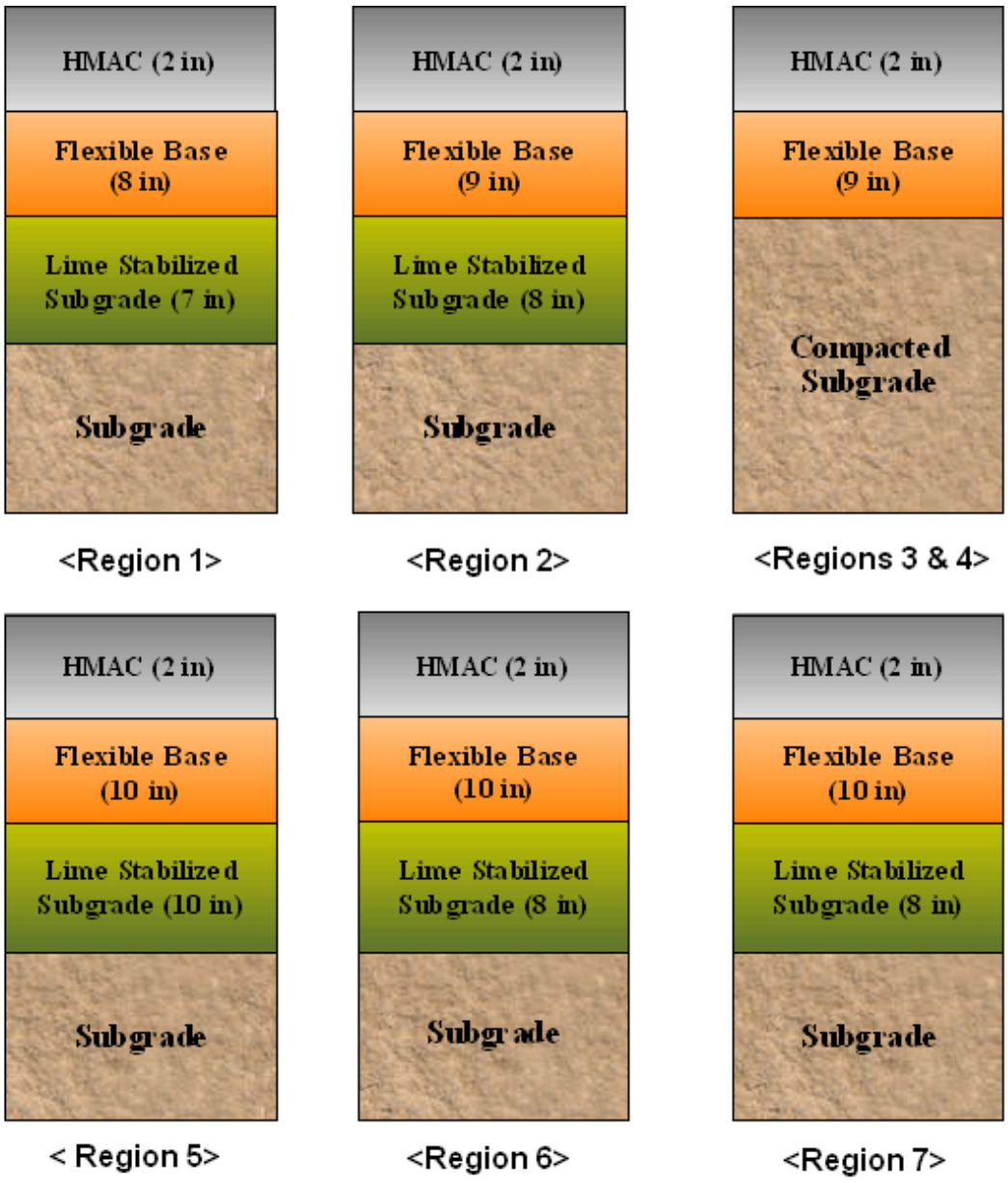

Figure 4.1. Typical Pavement Structures for FM Roads in Different Climatic Regions.

be controlled by unsaturated flow theory. For these conditions, the Thornthwaite moisture index may be used to predict the equilibrium soil suction value at the bottom node of the pavement for the purpose of estimating the initial soil suction profile that is an input to EICM. This profile affects the predicted moisture variations in the pavement layers. Researchers used the following equation by Lytton, Aubeny, and Bulut (2004) to predict the equilibrium soil suction value under unsaturated conditions:

$$U_e = 3.5633e^{-0.0051TMI} \quad (4.1)$$

where U_e is the equilibrium boundary suction at the bottom node. Once this parameter was determined, researchers computed the suction profile from the bottom node to the top of the base using the WinPRES (Windows™ version of Pavement Roughness in Expansive Soils) program by Lytton, Aubeny, and Bulut (2004). The internal boundary condition in EICM determines how moisture enters the subgrade. For this analysis, the assumption was made that the subgrade receives most of the water from suction induced by the groundwater table.

Figure 4.2 illustrates initial suction profiles predicted by WinPRES for two different climatic-soil conditions representing a dry region (El Paso County) and a wet region (Brazos County). As shown, the program computes two suction profiles for a given analysis — one representing a drying condition, and the other representing a wetting condition. The suction profile for Brazos County indicates a wetter condition as reflected in the lower equilibrium suction value of about 3.7 pF for the bottom node. Researchers used the initial suction profiles corresponding to a wetting condition in the verification of the EICM program that is presented subsequently.

VERIFICATION OF THE EICM PROGRAM

Prior to predicting soil moisture contents using EICM, researchers verified the program by comparing its predictions with field measurements. For this verification, researchers used Long Term Pavement Performance (LTPP) seasonal monitoring data on field moisture content measured by Time Domain Reflectometry (TDR) probes installed at different depths on Texas LTPP seasonal monitoring sites. Figure 4.3 shows the results from one verification conducted by researchers using LTPP data from test sections located at six different Texas counties. For these analyses, soil suction and permeability characteristics for the soils found at the LTPP sites were obtained from the database compiled by researchers. These properties were used in EICM along with the climatic data compiled for the six counties to predict subgrade moisture contents at the LTPP sites. It is observed that the predicted subgrade moisture contents from EICM compare favorably with the TDR measurements.

Another verification involved the application of EICM to predict the moisture contents at different depths of an in-service flexible pavement section located along the northbound lane of US77 near Victoria, Texas. This section consisted of a 7.5-inch hot-mix asphalt layer, 12 inches of crushed stone base, and 6 inches of lime-stabilized subbase overlying a silty sand subgrade. Researchers used the soils and climatic data compiled in this

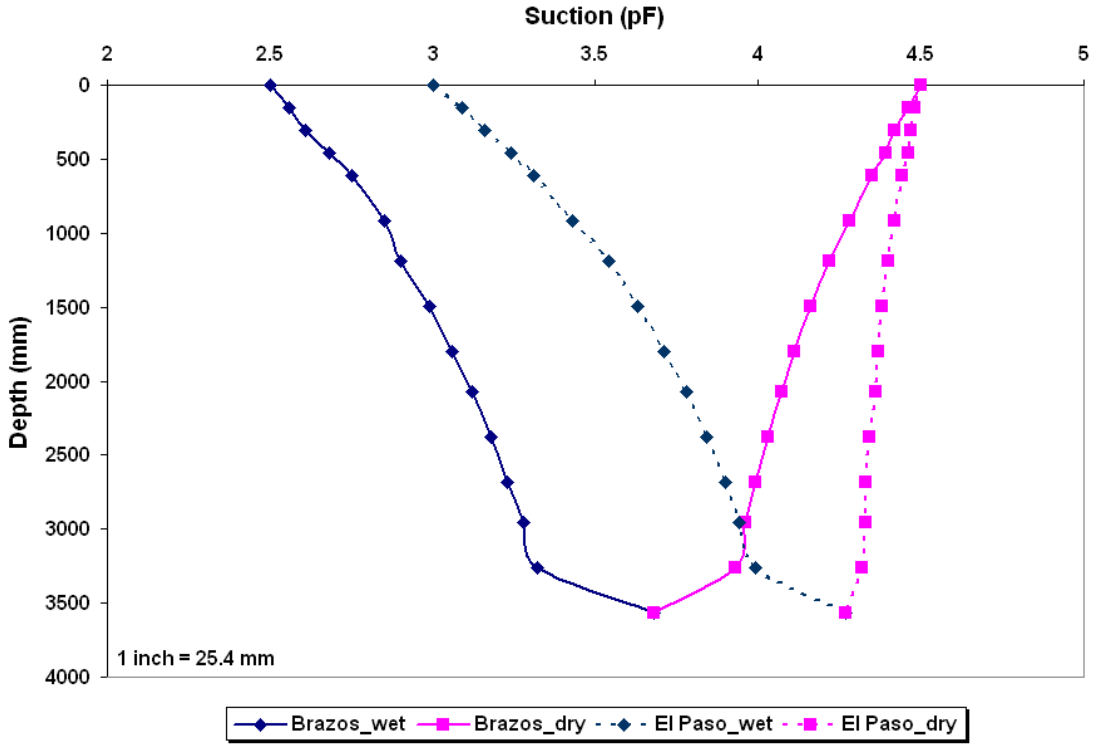

Figure 4.2. Comparison of Predicted Initial Soil Suction Profiles for Counties with Different Climates.

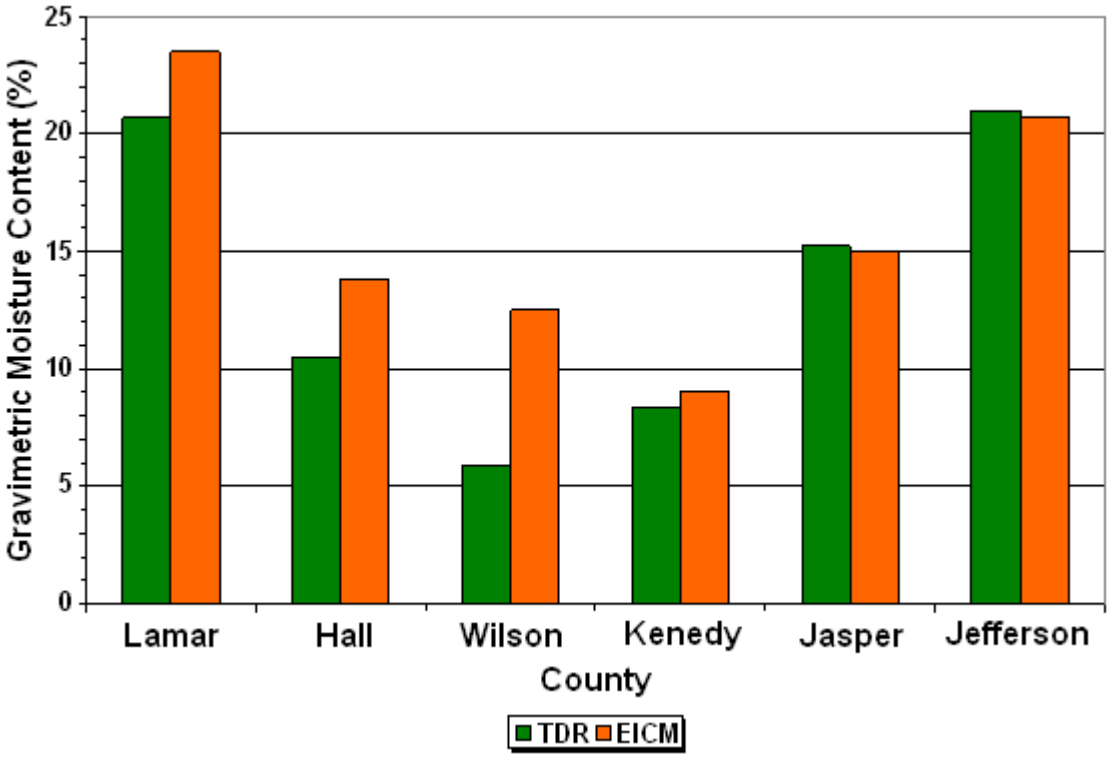

Figure 4.3. Comparison of EICM Predictions with TDR Measurements from LTPP Test Sections Located in Different Counties.

project to verify the EICM program on this Victoria test section. Figure 4.4 compares the soil moisture contents predicted at different depths with the corresponding measurements from TDR probes buried under the section. Once more, the predictions compare reasonably with the TDR measurements, in the authors' opinion.

Researchers also used the EICM program to predict the soil moisture variations on a flexible pavement test section located along SH48 in Brownsville. TTI staff instrumented this test section with multi-depth deflectometers, thermocouples, and TDR probes on another TxDOT project that evaluated the effects of routine overweight truck traffic on pavement life (Fernando, et al., 2006). Figure 4.5 shows the average of monthly moisture contents measured with the TDR probes placed in the base layer. It is observed that the average of the predicted moisture contents from EICM compare favorably with the average of the TDR measurements.

PREDICTION OF EXPECTED SOIL MOISTURE CONTENTS

Given the reasonable results from the verifications performed on EICM, researchers used the program to predict expected in-service subgrade moisture contents for the range of pavements and climatic-soil conditions considered in this project. Figure 4.6 illustrates predicted gravimetric subgrade moisture contents for the different Texas climatic-soil regions presented in Chapter II. For comparison purposes, the plastic limits (PLs) obtained from county soil survey reports are also shown. The range of in-situ moisture contents may be estimated as PL ± 3 percent. In Figure 4.6, the tick marks represent the high and low limits of the range of in situ moisture contents estimated from the plastic limits. The dots denote the predictions from EICM. On the basis of the plastic limits reported for different soils, the predicted gravimetric moisture contents appear to be reasonable, and plot within the range of in situ moisture contents estimated from the plastic limits.

The results given in Figure 4.6 are based on the representative soil suction and permeability characteristics for a given soil region and the corresponding climatic conditions. For developing the database of soil characteristics, researchers took a more comprehensive approach wherein EICM was used to predict expected in-service soil moisture contents for the different soil types found in each county, and for the range of pavements and climatic conditions considered in this evaluation. Researchers used the predictions from EICM to group counties into regions and developed the color-coded map shown in Figure 4.7 based on the predicted soil moisture contents for the predominant soils found in the different counties.

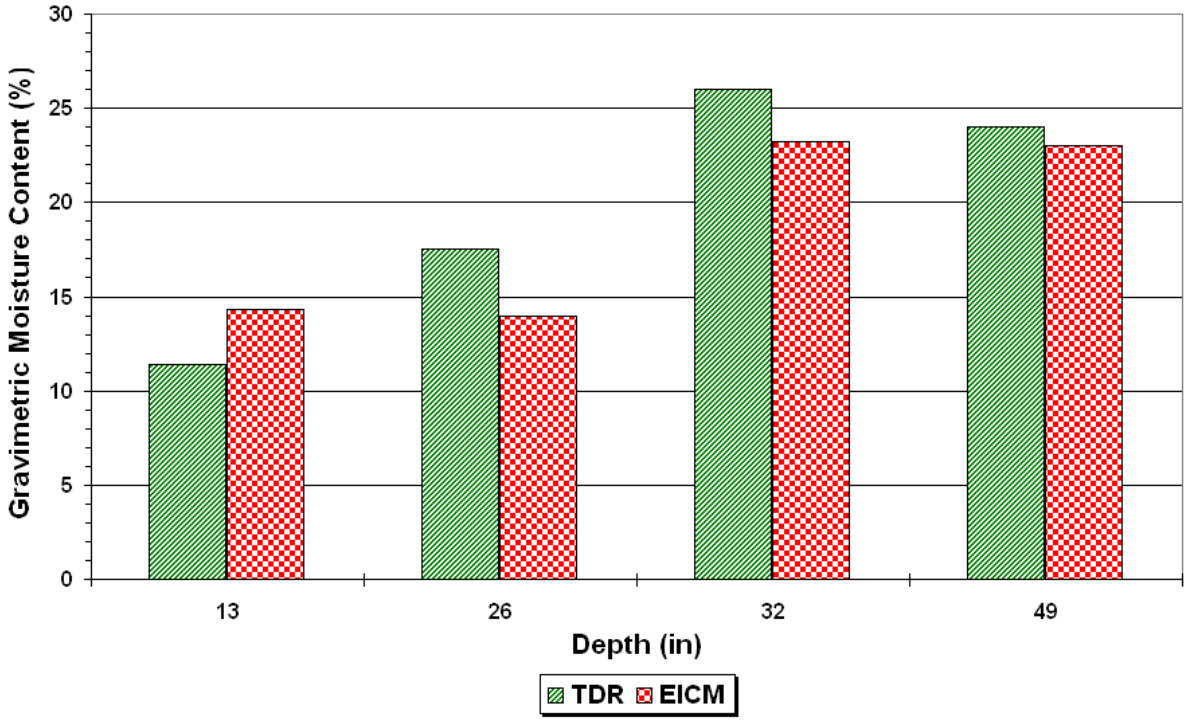

Figure 4.4. Comparison of EICM Predictions with TDR Measurements at Different Depths on Victoria Flexible Pavement Section.

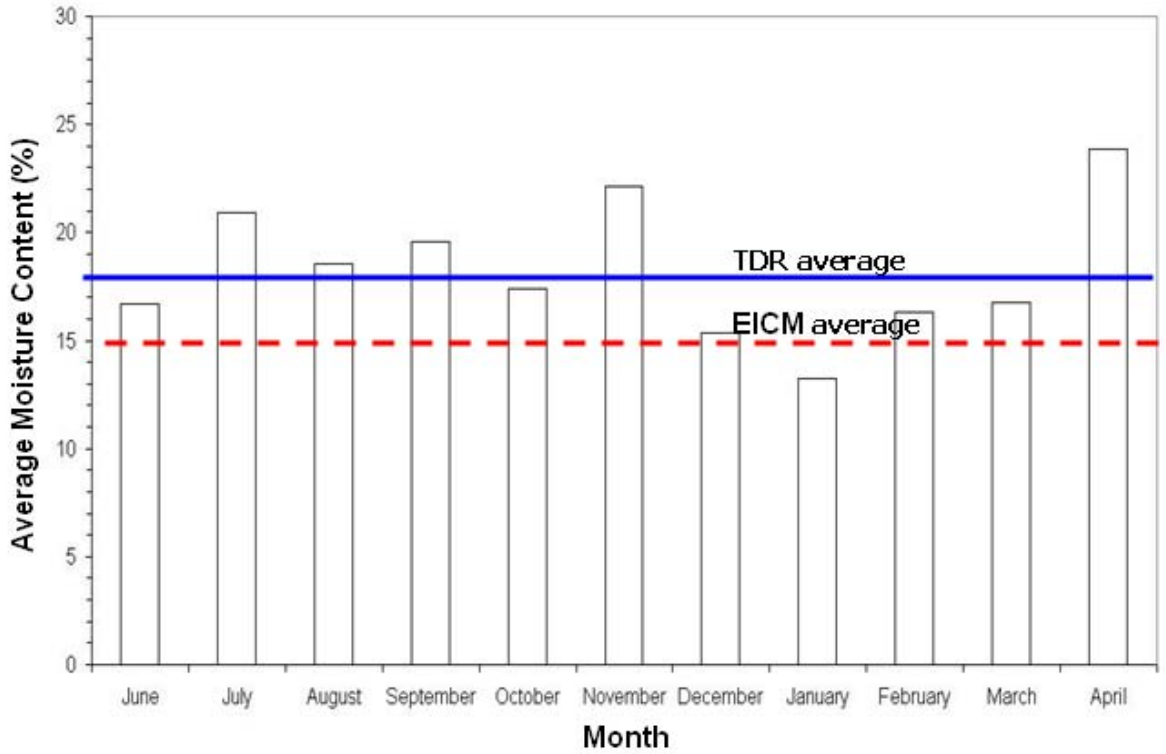

Figure 4.5. Comparison of EICM Predictions with TDR Measurements from Base Layer of Flexible Pavement Test Section in Brownsville.

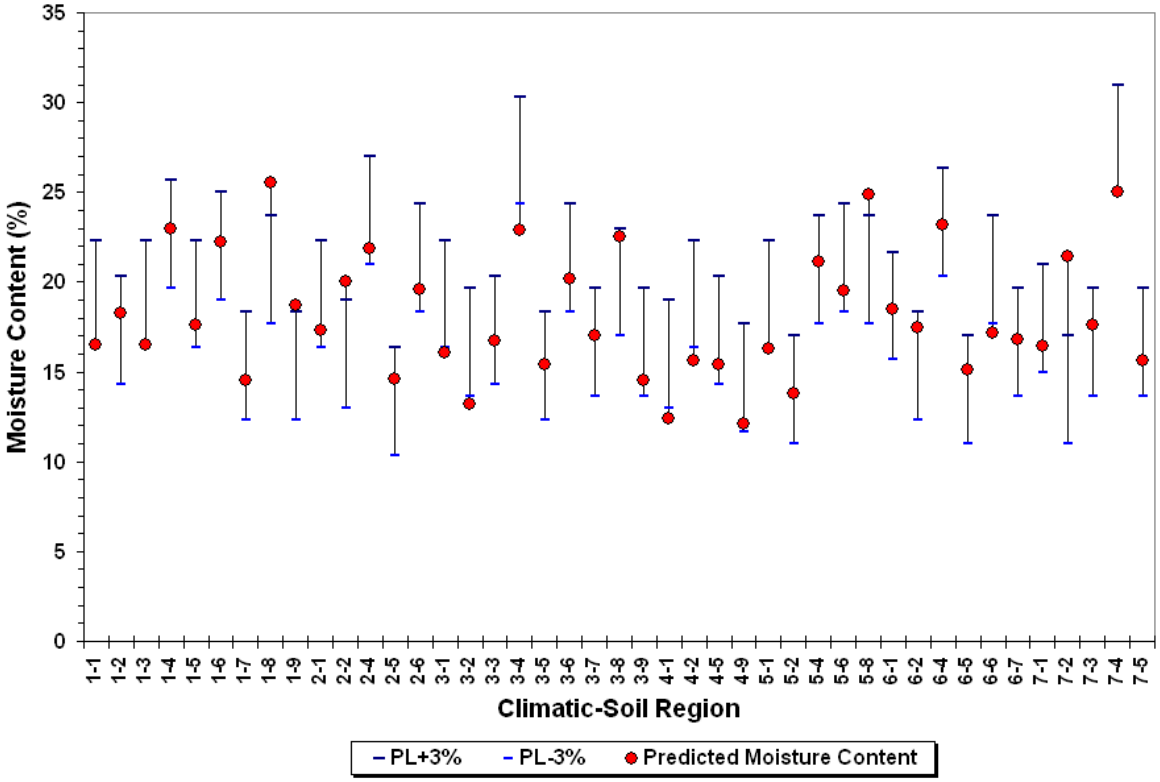

Figure 4.6. Comparison of Predicted Subgrade Moisture Contents from EICM with Estimates Based on Soil Plastic Limits.

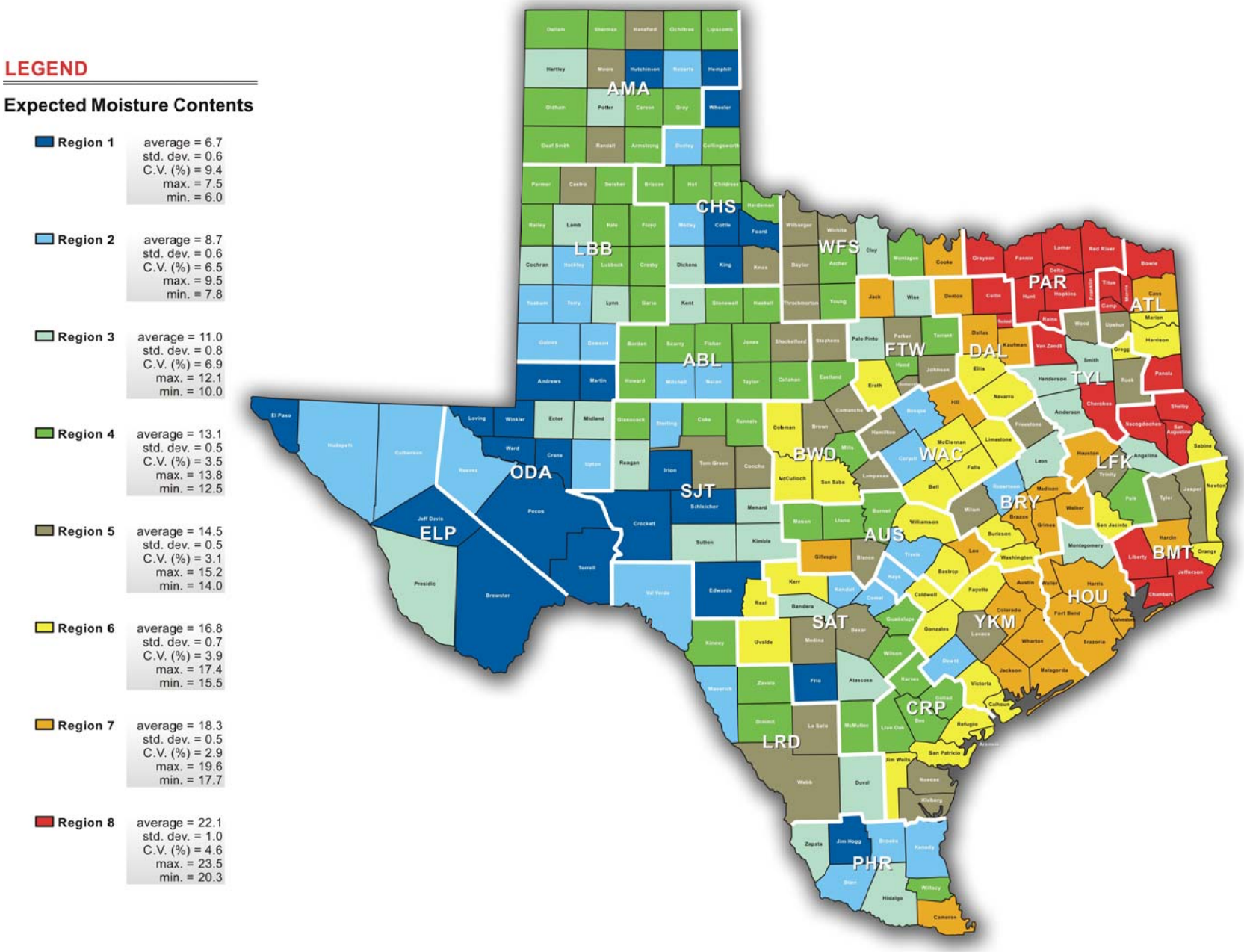

Figure 4.7 Map Showing Variation of Expected Soil Moisture Contents across Texas.

CHAPTER V. SUMMARY OF FINDINGS AND RECOMMENDATIONS

The major objectives of this project were to verify the load-thickness design chart in Test Method Tex-117E and to develop a methodology that accounts for variations in climatic and soil conditions in the triaxial design check of pavement designs from TxDOT's FPS program. To carry out this investigation, researchers executed a comprehensive work plan that included:

- a literature review of the modified Texas triaxial design method,
- development and execution of a plan to verify the load-thickness design curves based on testing full-scale field sections and small-scale pavement models,
- investigation of the correspondence between small-scale and full-scale pavement test results,
- analysis of plate bearing test data to evaluate the deformation response of field sections and small-scale laboratory specimens,
- assessment of the existing load-thickness design curves against plate bearing test results,
- compilation of climatic and soils data on the counties comprising the state,
- investigation of the relationships between soil moisture and soil strength properties and development of a procedure to correct strength properties to consider moisture effects in the triaxial design check,
- evaluation of expected soil moisture contents using a comprehensive model of climatic effects to support applications of the moisture correction procedure proposed in this project for cases where the engineer deems that such corrections are appropriate, and
- development of a computerized method of triaxial design analysis that offers greater versatility in modeling pavement systems and load configurations compared to the limited range of approximate solutions represented in the existing thickness design curves.

The findings from this project are documented in two research reports covering the verification of the existing design method (0-4519-1) and the development of a methodology to account for moisture effects and differences in moisture susceptibilities among soils in the triaxial design check. This report documents the tasks conducted by researchers to improve the existing design procedure by providing a more realistic method of modeling pavement

systems and load configurations in the analysis, and providing the option of correcting strength properties for cases where such adjustments are deemed approriate. Based on the research presented in this report, the following findings are noted:

- Three different methods of estimating load bearing capacity (Cases I, II, and III) were evaluated using the plate bearing test data collected on full-scale pavement sections. In this evaluation, researchers compared the load bearing capacity estimates on the sections tested with the loads corresponding to a 50-mil permanent displacement threshold. Overall, the predictions of load bearing capacity from Case III gave the best agreement with the 50-mil reference loads. For the flexible base sections built on clay subgrade, the Case III analysis gave the best agreement with the reference values on all but two of the sections. For the same clay subgrade, Case III also gave the best agreement with the 50-mil reference loads on the stabilized sections.
- In general, the analysis results show that Case I and Case II gave similar estimates of load bearing capacity on the clay subgrade sections. On the sandy subgrade sections, the estimates from Case II and Case III are more comparable. These observations apply to both the flexible base and stabilized sections, and reflect the effect of soil suction on the bearing capacity predictions. For moisture-susceptible soils, changes in moisture content can have a significant influence on the load bearing capacity of pavements founded on these soils.
- While Case I and Case II are conceptually the most similar of the three methods in terms of the underlying theory used to compute load induced stresses and the characterization of the failure envelope based on Test Method Tex-117E, it was interesting to observe differences between the Case I and Case II predictions. In the opinion of the authors, these differences are due to the approximate nature of the existing triaxial design method (Case I), which characterizes the strength of a given material in terms of the Texas triaxial class in lieu of the soil failure envelope parameters that are directly used in the Case II and Case III analyses. Another likely reason for the observed differences between Case I and Case II is that the existing thickness design curves are based on certain assumptions regarding the variation of modular ratios with pavement depth. To the extent that the assumed modular ratios are in variance with ratios of the layer moduli specified in the Case II analysis, differences in predictions of load induced stresses and the resulting allowable loads

will arise. In the researchers' opinion, the Case II analysis represents a more refined method of evaluating pavement load bearing capacity compared to the existing thickness design curves, which are approximate in nature due to the assumptions made in their development.

- Based on comparisons with the reference loads corresponding to the 50-mil permanent displacement tolerance, the Case II analysis appears to be more appropriate for assessment of pavement load bearing capacity compared to Case I. On the flexible base sections at the clay site, the Case I and Case II predictions are generally comparable, with the Case II predictions showing slightly better agreement with the 50-mil reference loads on the 6-inch sections. However, on the sandy subgrade and stabilized sections, the Case II predictions show better agreement with the reference loads compared to Case I, where the load bearing capacity estimates are quite conservative for the majority of the sections, particularly the 6-inch flexible base sections on the sandy subgrade, and the stabilized sections.
- While the Case I results are generally the most conservative, there are four sections, SSS_12, UGS_12, G2S_12, and 11B (thick HMAC section on sandy subgrade), where the Case I predictions are higher than the 50-mil allowable loads. Based on the plate bearing test data, researchers estimated the permanent displacements associated with the Case I predictions on these sections to be 64, 120, 72, and 136 mils, respectively. On two of the three sandy subgrade sections (SSS_12, and G2S_12), the Case II and Case III predictions are significantly lower than the Case I allowable loads, and are closer to the pavement load bearing capacities corresponding to the 50-mil limiting permanent displacement criterion.
- Comparing the Case II predictions with those from Case III, researchers observed that the Case III analysis with moisture correction of the failure envelope parameters generally gave predictions that are closer to the reference loads corresponding to the 50-mil limiting permanent displacement tolerance for flexible base sections on clay (in particular, the 6-inch sections). For the flexible base sections on sand, the Case II and Case III analyses gave similar results, with Case III being slightly better, in the authors' opinion.
- The Case I predictions significantly underestimate the 50-mil reference loads on the 6-inch flexible base sections at the sand site, and significantly overestimate the

reference loads on three of the five 12-inch flexible base sections, SSS_12, UGS_12 and G2S_12. On these sections, the estimated permanent displacements associated with the Case I predictions are 64, 120, and 72 mils, respectively.

- On the stabilized sections, the Case I and Case II predictions are quite conservative for the sections built on clay. For these stabilized sections, the Case III results are better in the researchers' opinion. For the stabilized sections built on sand, the Case II and Case III analyses gave similar results. The Case I predictions for the stabilized sections are generally too conservative, with the exception of the thick HMAC section on the sandy subgrade, where Case I significantly overestimated the 50-mil reference load.
- Small-scale tests carried out under different moisture conditions demonstrated the detrimental impact of moisture on the deformation response of small-scale pavement models fabricated with the same base and subgrade materials used on the full-scale pavement sections tested in this project. In particular, test results showed drastic reductions in load bearing capacity between the optimum moisture condition and after moisture conditioning of the subgrade for small-scale models where the base materials were placed on clay. On the sand specimens, the reductions in load bearing capacity were not as dramatic, reflecting lesser susceptibility to moisture in the sandy subgrade material compared to the clay.
- The verification of the moisture correction procedure (Case III analysis) using plate bearing test data collected on small-scale pavement models showed that the predicted load bearing capacities compare reasonably with the allowable loads corresponding to the 50-mil permanent displacement tolerance, particularly for the small-scale pavement models fabricated with the sandy subgrade material. However, the predictions tend to be conservative, particularly for the clay models. While the predictions reflect some conservatism, researchers note that even more conservative estimates would have been determined had the moisture condition of the subgrade soil not been considered in the analysis, as is presently the case in practice. In the authors' opinion, the results from this limited laboratory evaluation verified that the procedure gave reasonable predictions that are in accord with the expected change in load bearing capacity as the soil moisture condition changes from wet (corresponding to Tex-117E moisture conditioning) to optimum.

- Verification of the soil moisture predictions from EICM showed that this program reasonably predicts the moisture contents measured with TDR probes on instrumented pavement sections. Researchers used this program to predict subgrade moisture contents for the different Texas climatic-soil regions and found the predictions to be within the range of in situ moisture contents estimated from soil plastic limits obtained from county soil survey reports reviewed in this project. In addition, the evaluation of expected soil moisture contents revealed that the predictions from EICM approach equilibrium values over time. This observation implies that the moisture content of each underlying pavement layer can be expected to reach equilibrium some time after initial construction and that a representative moisture content value may be recommended for the purpose of pavement design.

Considering the findings from the investigations presented in this report, researchers offer the following recommendations with respect to implementing the *LoadGage* program developed from this project:

- The findings from field and laboratory tests conducted in this project verified the conservatism in the existing design method that TxDOT engineers have previously recognized. For the near term, researchers recommend that TxDOT consider dropping the load adjustment factor of 1.3 when using the existing design method to check FPS pavement designs. If an analysis of wheel load stresses under tandem axles is needed, such an analysis can be accomplished more realistically with the *LoadGage* program, which provides the capability for specifying a tandem axle configuration in the analysis.
- Given the conservatism observed in the existing design method (Case I), and the range in climatic and soil conditions found across Texas, there will be applications where the engineer should use the more refined analysis offered by the *LoadGage* program, even if simply to check the results from the existing triaxial design method. Based on the findings from comparisons of the Case I, Case II, and Case III methods of estimating load bearing capacity, researchers recommend the following:
    - For thin-surfaced roads with flexible base and no stabilized layers, use a Case II analysis with subgrade strength properties (cohesion and friction angle) determined from triaxial tests based on Tex-117E. Since moisture correction is not done in Case II, this approach would tend to produce

conservative results for design checks on thin-surfaced roads founded on moisture-susceptible soils where the expected in-service moisture content is drier than the moisture content associated with the soil strength properties from Tex-117E triaxial tests. However, for design problems where the soil failure envelope corresponds to a different moisture content (such as the optimum condition proposed in Tex-143E), and the in-service moisture content is expected to be higher than the value used for triaxial testing, the researchers recommend a Case III analysis (in lieu of Case II) to check the FPS design on thin-surfaced pavements founded on moisture-susceptible soils. This analysis would permit the engineer to consider the potential reduction in load bearing capacity arising from a wetter soil condition.

- For design of pavement sections with stabilized materials, use a Case III analysis for roadways underlain by fine-grained soils such as clays and silts. For stabilized sections founded on coarse-grained materials such as sandy soils and gravels, use Case II.

The authors recommend an implementation project to provide a phased transition from the current triaxial design check to the *LoadGage* program developed from this project. For implementation, researchers recommend integrating *LoadGage* into TxDOT's flexible pavement system program. The implementation project should include a *LoadGage* training course to provide users with the necessary information to properly use the program in practical applications. As implementation proceeds, pavement design engineers are encouraged to run *LoadGage* side-by-side with the existing modified triaxial design method to assess the potential impact of implementing the program in their Districts.

REFERENCES

Applied Research Associates. *Guide for Mechanistic-Empirical Design of New and Rehabilitated Pavement Structures*. Final Report, National Cooperative Highway Research Program Project 1-37A, Transportation Research Board, Washington, D.C., 2004.

Bulut, R., R. L. Lytton, and W. K. Wray. *Suction Measurements by Filter Paper*. Expansive Clay Soils and Vegetative Influence on Shallow Foundations, ASCE Geotechnical Special Publication No. 115 (eds. C. Vipulanandan, M. B. Addison, and M. Hasen), American Society of Civil Engineers, Reston, VA, pp. 243-261, 2001.

Fernando, E. G., W. Liu, T. Lee, and T. Scullion. *The Texas Modified Triaxial (MTRX) Design Program*. Research Report 1869-3, Texas Transportation Institute, The Texas A&M University System, College Station, TX, 2001.

Fernando, E. G., S. Ramos, J. Oh, J. Ragsdale, Z. Xie, R. Atkins, and H. Taylor. *Characterizing the Effects of Routine Overweight Truck Traffic on SH4/48*. Research Report 0-4184-1, Texas Transportation Institute, The Texas A&M University System, College Station, TX, 2006.

Fernando, E. G., J. Oh, and W. Liu. *LoadGage User's Manual*. Product 0-4519-P3, Texas Transportation Institute, The Texas A&M University System, College Station, TX, 2007.

Fernando, E. G., J. Oh, C. Estakhri, and S. Nazarian. *Verification of the Load-Thickness Design Curves in the Modified Triaxial Design Method*. Research Report 0-4519-1, Texas Transportation Institute, The Texas A&M University System, College Station, TX, 2007.

Fredlund, D. G., and H. Rahardjo. *Soil Mechanics for Unsaturated Soils*. John Wiley & Sons, Inc., NY, 1993.

Gardner, W. R. *Some Steady State Solutions of the Unsaturated Moisture Flow Equation with Application of Evaporation from a Water Table*. Soil Science, Vol. 85, pp. 223-232, 1958.

Larson, G., and B. J. Dempsey. *Enhanced Integrated Climatic Model Version 2.0, Final Report*. Report No. DTFA MN/DOT 72114, University of Illinois at Urbana-Champaign, 1997.

Lytton, R. L., C. P. Aubeny, and R. Bulut. *Design Procedures for Pavements on Expansive Soils*. Research Report 0-4518-1, Texas Transportation Institute, The Texas A&M University System, College Station, TX, 2004.

Lytton, R. L., D. E. Pufahl, C. H. Michalak, H. S. Liang, and B. J. Dempsey. *An Integrated Model of the Climatic Effects on Pavement*. Report No. FHWA-RD-90-033, Texas Transportation Institute, The Texas A&M University System, College Station, TX, 1990.

Mason, J. G., C. W. Ollayos, G. L. Guymon, and R. L. Berg. *User's Guide for the Mathematical Model of Frost Heave and Thaw Settlement in Pavements*. Cold Regions Research Engineering Laboratory, Hanover, NH, 1986.

Michalak, C. H., and T. Scullion. *MODULUS 5.0: User's Manual*. Research Report 1987-1, Texas Transportation Institute, The Texas A&M University System, College Station, TX, 1995.

National Water Information System. *USGS Ground-Water Data for the Nation*. http://nwis.waterdata.usgs.gov/nwis/gw, accessed June 22, 2006.

Oh, J., D. Ryu, E. G. Fernando, and R. L. Lytton. *Estimation of Expected Moisture Contents for Pavements by Environmental and Soil Characteristics*. Transportation Research Record, Journal of the Transportation Research Board, No. 1967, Transportation Research Board, Washington, D.C., pp. 135-147, 2006.

Titus-Glover, L., and E. G. Fernando. *Evaluation of Pavement Base and Subgrade Material Properties and Test Procedures*. Research Report 1335-2, Texas Transportation Institute, The Texas A&M University System, College Station, TX, 1995.

Uzan, J. *Granular Material Characterization*. Transportation Research Record 1022, Transportation Research Board, Washington, D.C., pp. 52-59, 1985.

APPENDIX A.
DATA FOR CHARACTERIZING CLIMATIC AND SOIL VARIATIONS ACROSS TEXAS

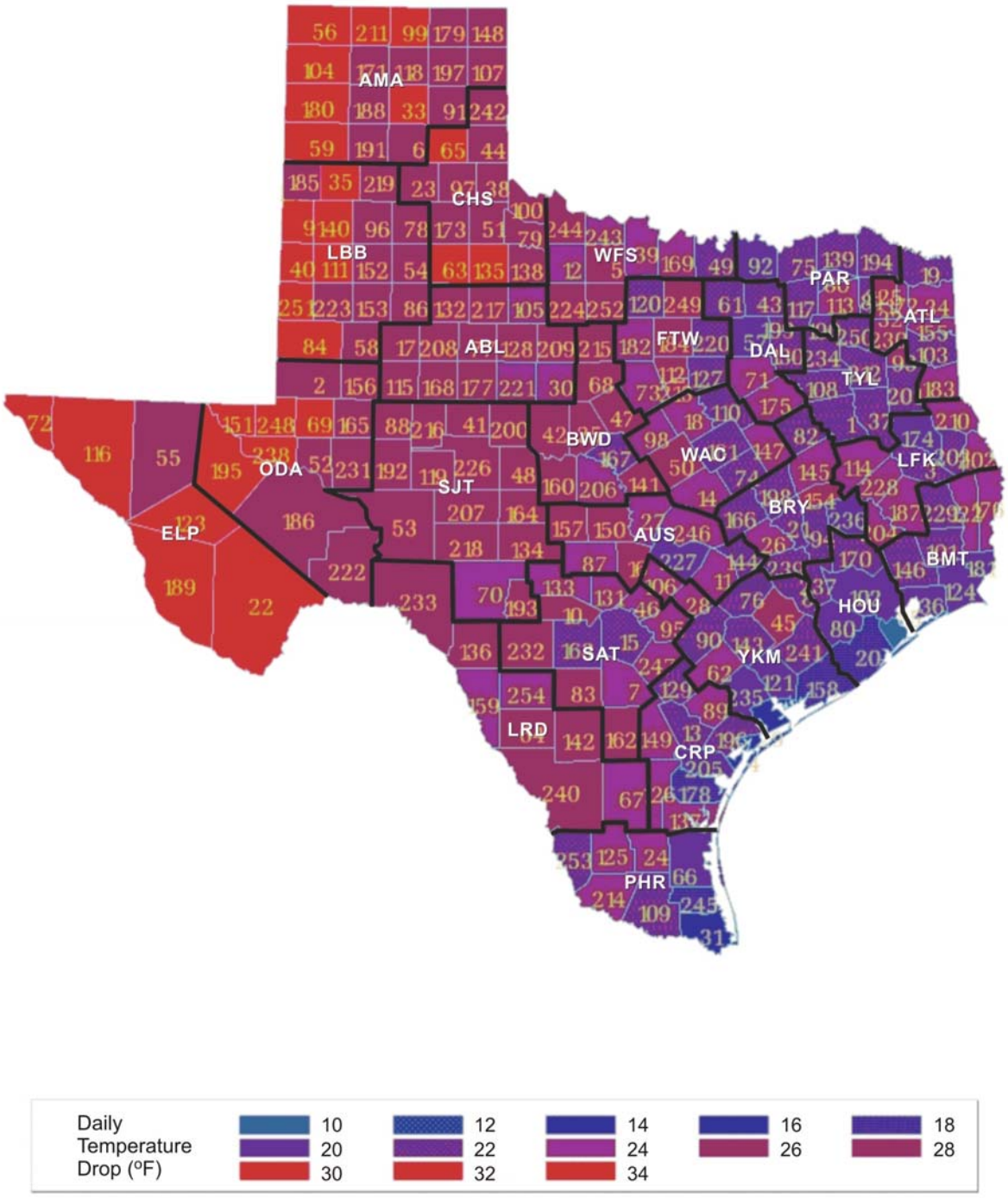

Figure A1. Variation in Daily Temperature Drops (°F) across Texas Counties (identified by corresponding county numbers on map).

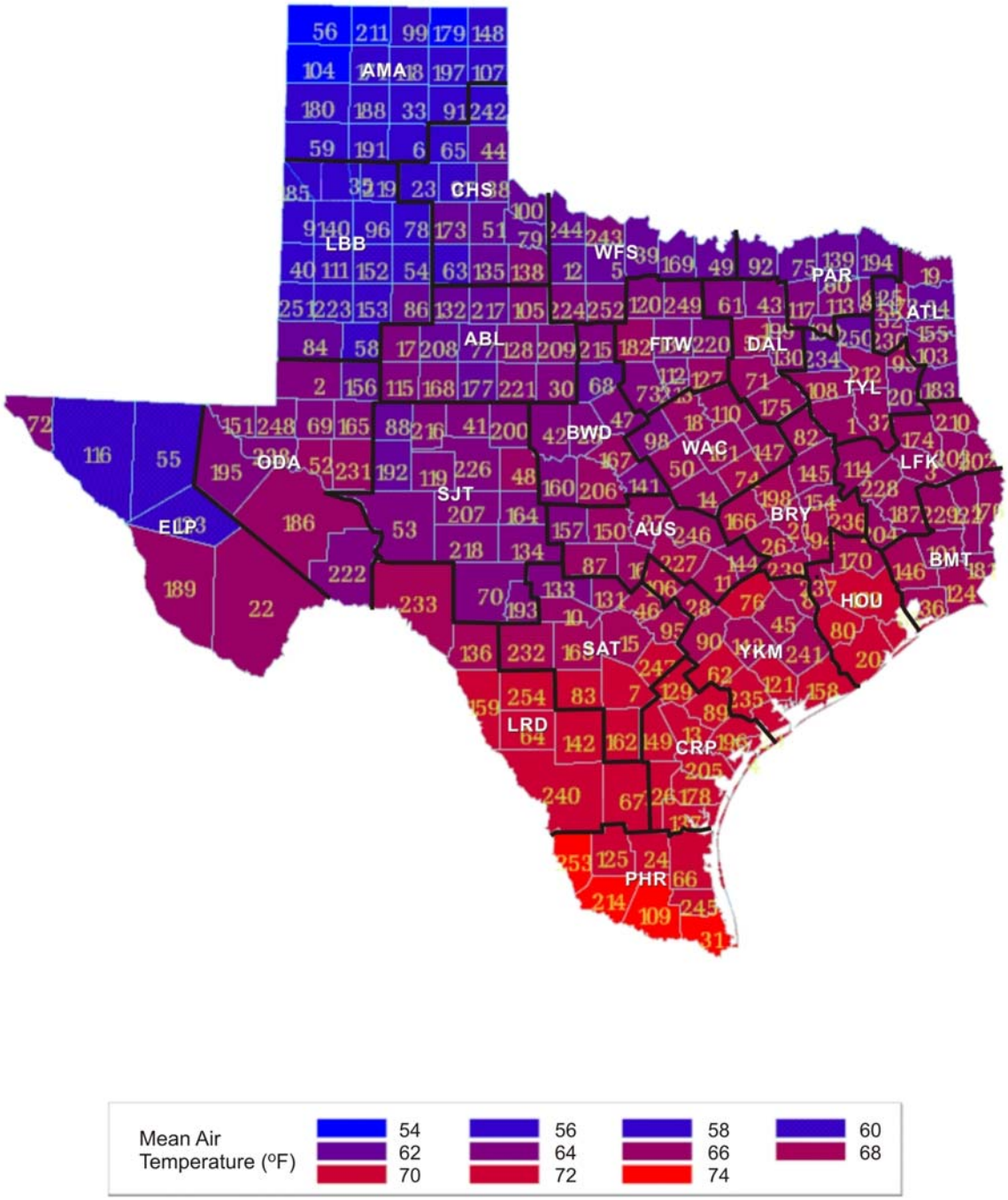

Figure A2. Variation in Mean Air Temperatures (°F) across Texas Counties (identified by corresponding county numbers on map).

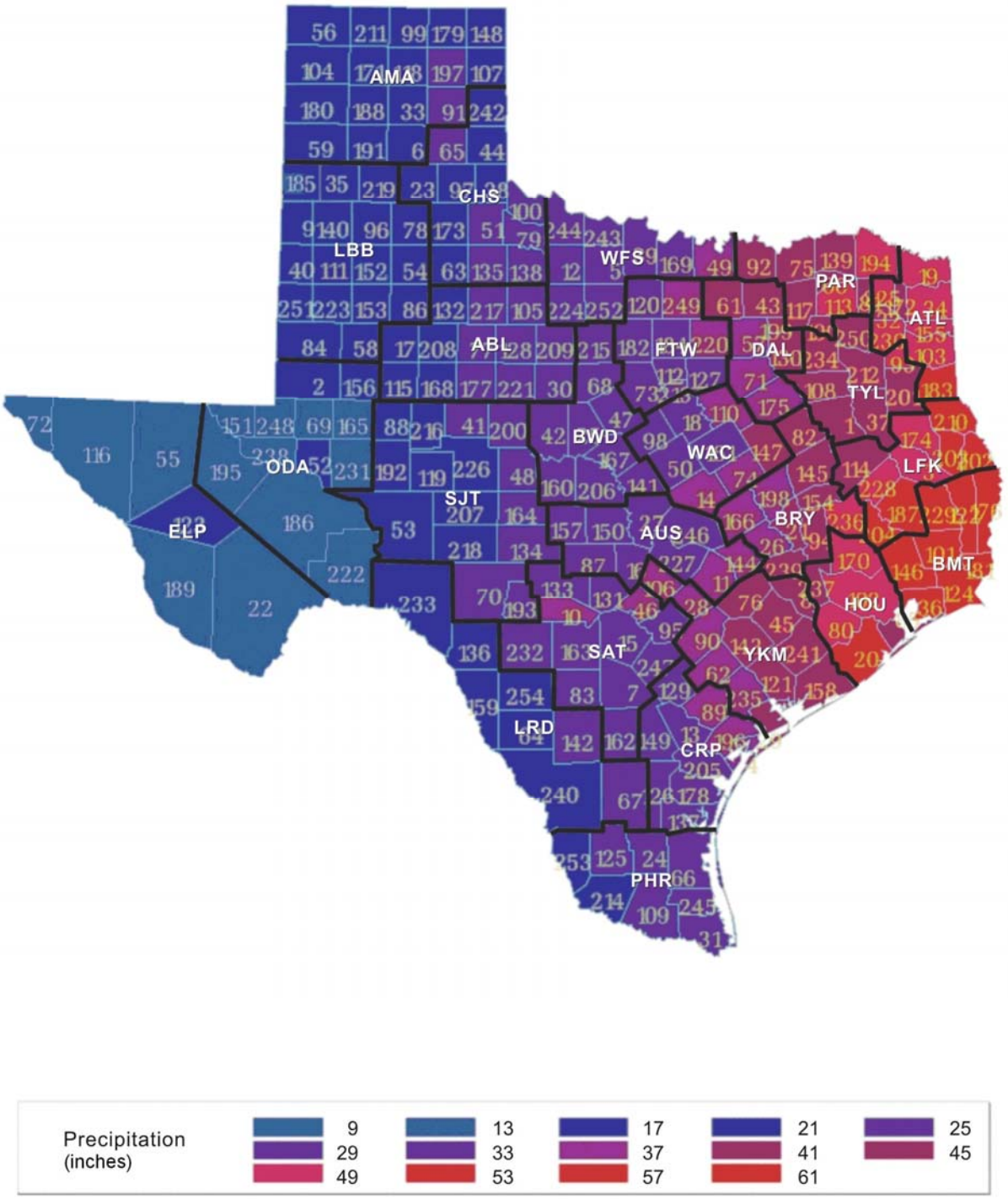

Figure A3. Variation in Mean Precipitations across Texas Counties (identified by corresponding county numbers on map).

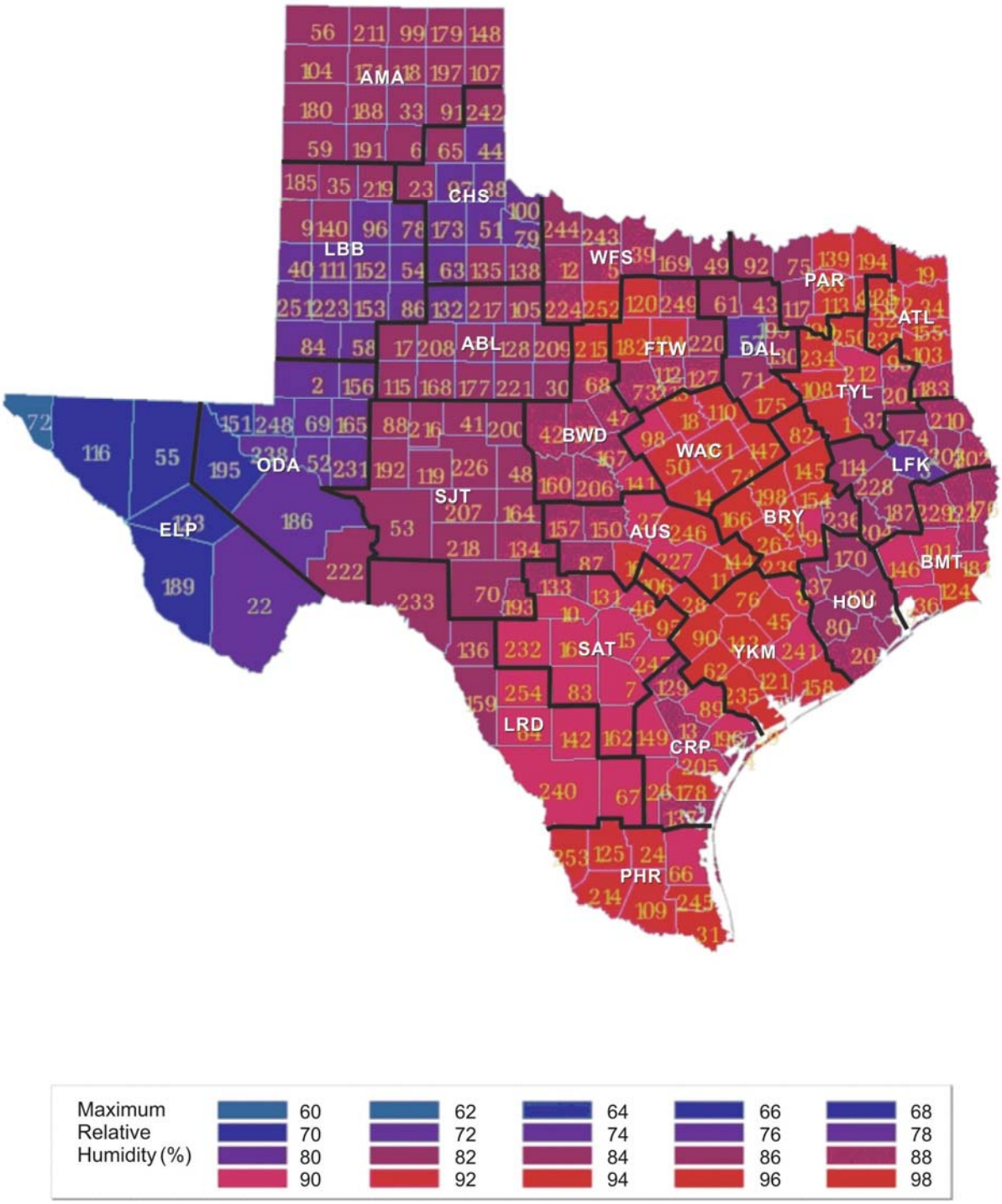

Figure A4. Variation in Maximum Relative Humidities across Texas Counties (identified by corresponding county numbers on map).

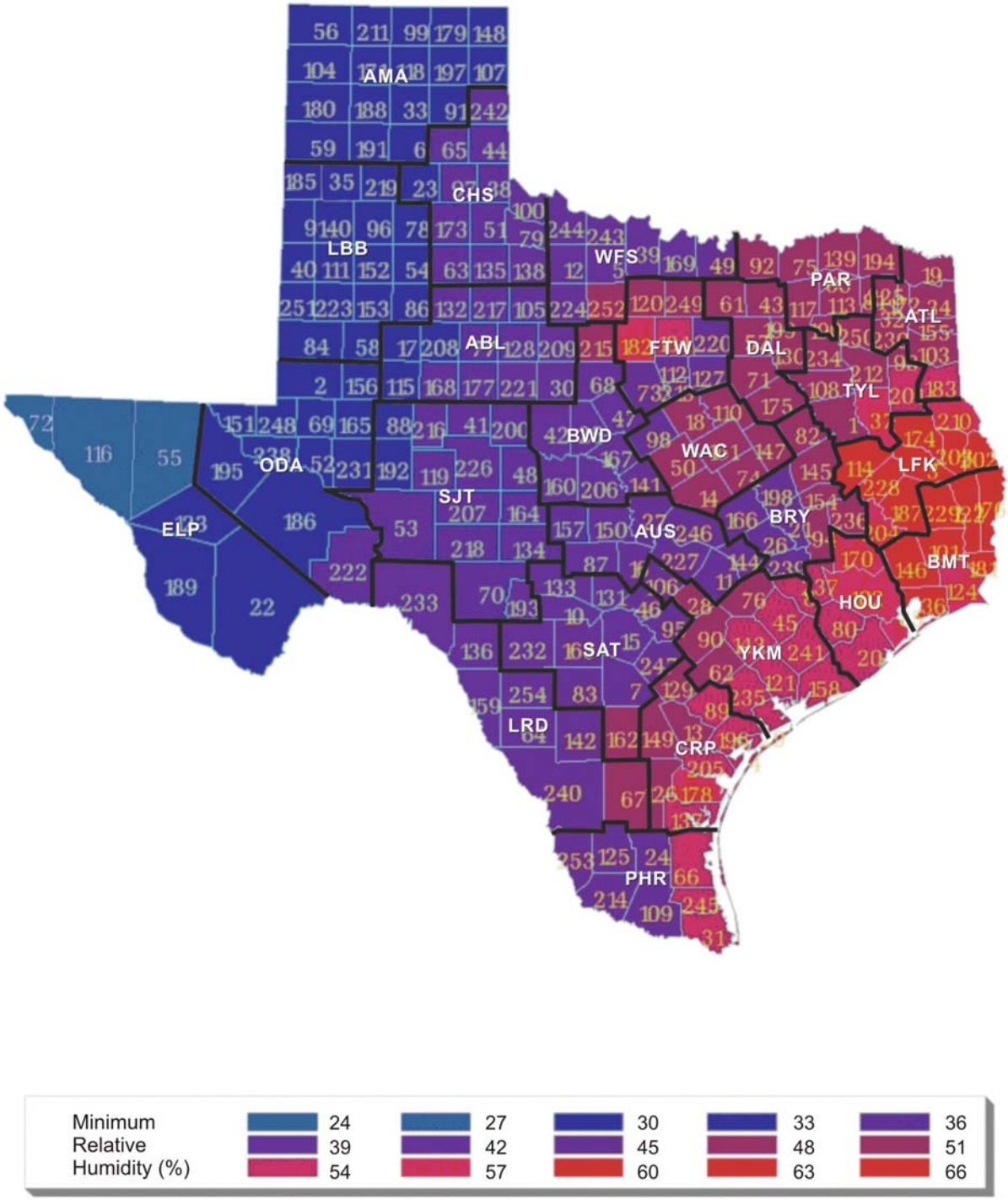

Figure A5. Variation in Minimum Relative Humidities across Texas Counties (identified by corresponding county numbers on map).

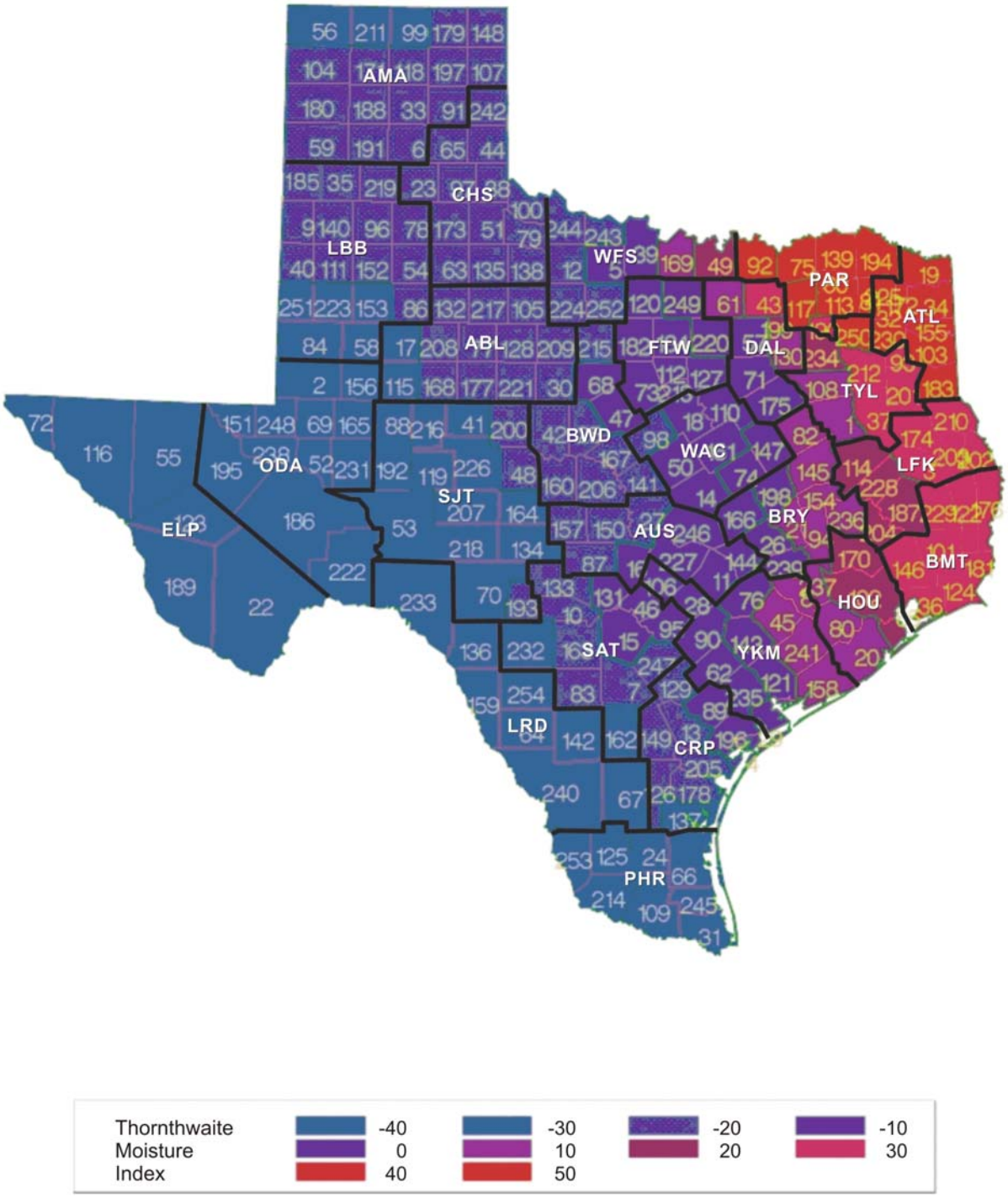

Figure A6. Variation in Thornthwaite Moisture Indices across Texas Counties (identified by corresponding county numbers on map).

Table A1. TxDOT List of Districts and Counties.

DISTRICT 1
(Paris)
60 Delta
75 Fannin
81 Franklin
92 Grayson
113 Hopkins
117 Hunt
139 Lamar
190 Rains
194 Red River

DISTRICT 2
(Fort Worth)
73 Erath
112 Hood
120 Jack
127 Johnson
182 Palo Pinto
184 Parker
213 Somervell
220 Tarrant
249 Wise

DISTRICT 3
(Wichita Falls)
5 Archer
12 Baylor
39 Clay
49 Cook
169 Montague
224 Throckmorton
243 Wichita
244 Wilbarger
252 Young

DISTRICT 4
(Amarillo)
6 Armstrong
33 Carson
56 Dallam
59 Deaf Smith
91 Gray
99 Hansford
104 Hartley
107 Hemphill
118 Hutchinson
148 Lipscomb
171 Moore
179 Ochiltree
180 Oldham
188 Potter
191 Randall
197 Roberts
211 Sherman

DISTRICT 5
(Lubbock)
9 Bailey
35 Castro
40 Cochran
54 Crosby
58 Dawson
78 Floyd
84 Gaines
86 Garza
96 Hale
111 Hockley
140 Lamb
152 Lubbock
153 Lynn
185 Parmer
219 Swisher
223 Terry
251 Yoakum

DISTRICT 6
(Odessa)
2 Andrews
52 Crane
69 Ector
151 Loving
156 Martin
165 Midland
186 Pecos
195 Reeves
222 Terrell
231 Upton
238 Ward
248 Winkler

DISTRICT 7
(San Angelo)
41 Coke
48 Concho
53 Crockett
70 Edwards
88 Glasscock
119 Irion
134 Kimble
164 Menard
192 Reagan
193 Real
200 Runnels
207 Schleicher
216 Sterling
218 Sutton
226 Tom Green

DISTRICT 8
(Abilene)
17 Borden
30 Callahan
77 Fisher
105 Haskell
115 Howard
128 Jones
132 Kent
168 Mitchell
177 Nolan
208 Scurry
209 Shackelford
217 Stonewall
221 Taylor

DISTRICT 9
(Waco)
14 Bell
18 Bosque
50 Coryell
74 Falls
98 Hamilton
110 Hill
147 Limestone
161 McLennan

DISTRICT 10
(Tyler)
1 Anderson
37 Cherokee
93 Gregg
108 Henderson
201 Rusk
212 Smith
234 Van Zandt
250 Wood

DISTRICT 11
(Lufkin)
3 Angelina
114 Houston
174 Nacogdoches
187 Polk
202 Sabine
203 San Augustine
204 San Jacinto
210 Shelby
228 Trinity

DISTRICT 12
(Houston)
20 Brazoria
80 Fort Bend
85 Galveston
102 Harris
170 Montgomery
237 Waller

DISTRICT 13
(Yoakum)
8 Austin
29 Calhoun
45 Colorado
62 DeWitt
76 Fayette
90 Gonzales
121 Jackson
143 Lavaca
158 Matagorda
235 Victoria
241 Warton

DISTRICT 14
(Austin)
11 Bastrop
16 Blanco
27 Burnett
28 Caldwell
87 Gillespie
106 Hays
144 Lee
150 Llano
157 Mason
227 Travis
246 Williamson

DISTRICT 15
(San Antonio)
7 Atascosa
10 Bandera
15 Bexar
46 Comal
83 Frio
95 Guadalupe
131 Kendall
133 Kerr
162 McMullen
163 Medina
232 Uvalde
247 Wilson

DISTRICT 16
(Corpus Christi)
4 Aransas
13 Bee
89 Goliad
126 Jim Wells
129 Karnes
137 Kleberg
149 Live Oak
178 Nueces
196 Refugio
205 San Patricio

DISTRICT 17
(Bryan)
21 Brazos
26 Burleson
82 Freestone
94 Grimes
145 Leon
154 Madison
166 Milam
198 Robertson
236 Walker
239 Washington

DISTRICT 18
(Dallas)
43 Collin
57 Dallas
61 Denton
71 Ellis
130 Kaufman
175 Navarro
199 Rockwall

DISTRICT 19
(Atlanta)
19 Bowie
32 Camp
34 Cass
103 Harrison
155 Marion
172 Morris
183 Panola
225 Titus
230 Upshur

DISTRICT 20
(Beaumont)
36 Chambers
101 Hardin
122 Jasper
124 Jefferson
146 Liberty
176 Newton
181 Orange
229 Tyler

DISTRICT 21
(Pharr)
24 Brooks
31 Cameron
109 Hildago
125 Jim Hogg
66 Kenedy
214 Starr
245 Willacy
253 Zapata

DISTRICT 22
(Laredo)
64 Dimmit
67 Duval
136 Kinney
142 La Salle
159 Maverick
233 Val Verde
240 Webb
254 Zavala

DISTRICT 23
(Brownwood)
25 Brown
42 Coleman
47 Comanche
68 Eastland
141 Lampasas
160 McCulloch
167 Mills
206 San Saba
215 Stephens

DISTRICT 24
(El Paso)
22 Brewster
55 Culberson
72 El Paso
116 Hudspeth
123 Jeff Davis
189 Presidio

DISTRICT 25
(Childress)
23 Briscoe
38 Childress
44 Collingsworth
51 Cottle
63 Dickens
65 Donley
79 Foard
97 Hall
100 Hardeman
135 King
138 Knox
173 Motley
242 Wheeler

Table A2. Thirty-Year Averages of Climatic Variables.

County Number	Daily Temperature Drop (°F)	Mean Temperature (°F)	Precipitation (in.)	Maximum Relative Humidity (%)	Minimum Relative Humidity (%)	Thornthwaite Moisture Index	County Number	Daily Temperature Drop (°F)	Mean Temperature (°F)	Precipitation (in.)	Maximum Relative Humidity (%)	Minimum Relative Humidity (%)	Thornthwaite Moisture Index
1	22	66	46	91	48	14	2	28	64	15	79	30	-40
3	23	67	49	74	63	25	4	15	70	38	88	53	-10
5	27	63	28	88	43	-13	6	28	56	22	82	34	-20
7	25	70	28	89	45	-20	8	22	67	41	90	55	9
9	32	57	17	81	33	-20	10	27	66	36	89	40	-15
11	24	68	36	93	46	-10	12	25	63	26	88	40	-20
13	21	70	33	88	50	-15	14	24	66	35	91	47	-10
15	22	69	30	90	43	-14	16	26	66	33	91	44	-10
17	27	64	20	81	32	-30	18	24	65	34	91	47	-11
19	23	63	51	91	50	43	20	18	69	53	88	55	10
21	22	69	40	94	45	5	22	30	66	13	75	31	-30
23	28	57	22	81	34	-20	24	24	72	25	91	45	-30
25	26	64	28	88	40	-20	26	24	68	39	93	45	0
27	24	65	32	90	45	-15	28	25	68	36	92	47	-10
29	14	71	39	96	53	0	30	24	64	26	82	40	-20
31	17	73	28	95	55	-30	32	23	63	45	91	50	43
33	29	55	22	82	34	-21	34	24	63	49	91	50	40
35	30	56	19	81	33	-20	36	19	69	54	90	61	30
37	21	66	47	85	57	25	38	25	62	23	80	37	-23
39	25	62	32	88	43	-5	40	30	58	18	80	32	-20
41	27	65	23	84	36	-30	42	26	63	27	88	38	-20
43	22	63	41	86	48	29	44	28	63	23	80	36	-20
45	27	68	45	93	53	5	46	24	67	36	90	44	-10
47	26	65	30	88	43	-13	48	29	66	26	84	36	-23
49	23	63	38	86	45	20	50	25	65	32	91	47	-14
51	28	62	24	80	37	-23	52	27	66	15	77	33	-40
53	28	63	19	81	35	-35	54	27	60	21	80	33	-23
55	26	60	14	67	28	-40	56	30	55	15	83	34	-25
57	20	67	38	74	48	3	58	29	61	19	80	31	-30
59	30	57	19	82	34	-20	60	22	63	45	91	50	50
61	23	64	39	86	47	10	62	24	70	36	94	51	-10
63	29	61	20	80	36	-23	64	25	71	21	89	43	-30
65	30	59	24	82	35	-20	66	20	72	28	90	54	-25
67	24	72	25	90	50	-30	68	27	63	29	88	43	-13
69	29	64	14	75	30	-40	70	24	64	24	86	37	-30
71	23	65	38	86	48	0	72	31	64	9	62	24	-40
73	24	63	32	88	46	-10	74	23	68	38	93	47	0
75	22	62	45	86	48	50	76	21	69	39	95	50	0
77	27	62	24	82	37	-23	78	27	58	21	80	33	-20

Table A2. Thirty-Year Averages of Climatic Variables (continued).

County Number	Daily Temperature Drop (°F)	Mean Temperature (°F)	Precipitation (in.)	Maximum Relative Humidity (%)	Minimum Relative Humidity (%)	Thornthwaite Moisture Index	County Number	Daily Temperature Drop (°F)	Mean Temperature (°F)	Precipitation (in.)	Maximum Relative Humidity (%)	Minimum Relative Humidity (%)	Thornthwaite Moisture Index
79	27	62	26	80	38	-21	80	20	69	48	86	55	10
81	22	64	47	91	50	47	82	23	66	41	91	48	9
83	25	70	25	89	45	-23	84	29	61	18	80	31	-30
85	11	71	44	86	56	17	86	27	62	21	80	33	-23
87	24	66	31	88	38	-18	88	29	62	17	83	33	-33
89	24	71	37	90	55	-13	90	22	68	35	93	50	-10
91	26	58	24	82	34	-20	92	21	63	42	86	48	40
93	24	65	49	91	50	33	94	22	68	44	90	48	10
95	23	68	34	91	45	-10	96	25	58	20	80	33	-20
97	28	61	21	80	36	-21	98	24	64	31	90	46	-15
99	30	57	20	83	34	-25	100	28	62	26	80	38	-21
101	22	67	56	90	65	31	102	20	69	50	85	56	15
103	22	64	51	91	50	38	104	30	55	17	83	34	-23
105	25	64	25	82	37	-21	106	23	68	36	91	45	-10
107	29	57	22	83	34	-20	108	22	65	42	91	49	13
109	22	74	23	92	44	-30	110	22	66	37	91	48	-5
111	30	59	20	80	32	-20	112	25	65	32	88	46	-9
113	24	64	48	91	50	50	114	23	66	44	85	60	15
115	26	64	20	81	33	-30	116	33	61	11	65	26	-40
117	22	63	44	86	48	38	118	27	58	22	83	34	-23
119	28	63	20	84	36	-30	120	23	63	31	91	51	-11
121	20	69	42	94	54	3	122	24	66	57	88	63	31
123	29	60	15	69	29	-30	124	20	68	58	96	57	30
125	24	72	24	91	45	-35	126	23	72	28	90	50	-20
127	23	66	35	88	46	-10	128	26	64	25	82	37	-21
129	23	69	29	88	49	-15	130	22	64	39	86	49	10
131	25	65	34	90	40	-10	132	28	61	23	80	36	-23
133	24	64	30	88	38	-15	134	29	65	25	87	36	-25
135	30	61	24	82	37	-23	136	25	69	22	86	40	-30
137	23	72	29	89	53	-25	138	27	63	26	82	38	-21
139	23	63	47	91	50	50	140	30	58	18	81	33	-20
141	26	64	32	90	44	-20	142	26	71	24	89	45	-30
143	22	69	43	95	54	0	144	22	67	37	93	46	-7
145	23	66	42	93	47	9	146	22	67	58	90	61	29
147	25	66	40	93	47	0	148	28	56	23	83	34	-20
149	24	71	25	90	50	-20	150	26	66	27	88	41	-20
151	32	64	13	70	29	-40	152	27	60	17	80	32	-20
153	28	60	21	80	32	-30	154	25	67	43	93	47	7
155	24	63	49	91	50	40	156	28	63	18	79	31	-35

Table A2. Thirty-Year Averages of Climatic Variables (continued).

County Number	Daily Temperature Drop (°F)	Mean Temperature (°F)	Precipitation (in.)	Maximum Relative Humidity (%)	Minimum Relative Humidity (%)	Thornthwaite Moisture Index	County Number	Daily Temperature Drop (°F)	Mean Temperature (°F)	Precipitation (in.)	Maximum Relative Humidity (%)	Minimum Relative Humidity (%)	Thornthwaite Moisture Index
157	28	65	28	88	36	-20	158	17	70	46	92	55	5
159	24	71	21	86	40	-30	160	26	65	28	88	38	-20
161	23	66	35	92	48	-10	162	27	71	23	89	48	-25
163	23	69	28	90	46	-20	164	29	65	25	86	36	-25
165	29	64	15	79	30	-35	166	23	69	35	93	46	-10
167	22	65	29	88	43	-20	168	27	63	19	82	36	-23
169	24	62	33	86	43	8	170	21	68	49	85	57	16
171	28	56	18	83	34	-23	172	23	65	47	91	50	40
173	26	62	22	80	36	-23	174	21	66	50	85	60	30
175	24	65	37	91	49	0	176	24	65	56	88	63	32
177	26	63	24	82	37	-23	178	18	72	32	92	57	-20
179	27	55	21	83	34	-23	180	30	57	18	83	34	-21
181	20	67	61	90	66	31	182	25	66	31	94	56	-10
183	24	65	52	88	53	35	184	25	63	35	91	53	-10
185	29	56	18	81	33	-23	186	29	66	14	75	31	-40
187	25	66	52	85	60	20	188	27	57	20	83	34	-21
189	34	66	14	69	29	-30	190	22	63	44	91	50	30
191	29	59	19	82	34	-20	192	28	63	19	83	33	-35
193	26	65	28	88	40	-20	194	22	63	49	91	50	47
195	32	64	13	69	29	-40	196	22	71	37	90	54	-10
197	27	56	23	83	34	-20	198	22	67	39	93	46	0
199	22	64	39	86	48	18	200	27	65	24	82	37	-21
201	22	65	47	88	55	30	202	24	65	54	88	62	32
203	23	66	52	85	62	31	204	24	67	52	85	58	20
205	20	71	35	90	55	-15	206	25	66	28	88	41	-20
207	28	64	22	85	36	-30	208	28	62	22	82	34	-23
209	26	63	28	85	40	-20	210	24	65	53	88	58	33
211	29	54	18	83	34	-25	212	21	67	45	91	50	25
213	29	64	33	88	46	-10	214	24	74	21	91	45	-40
215	26	65	27	91	48	-15	216	29	63	20	84	36	-30
217	28	63	23	82	37	-23	218	29	63	23	85	37	-30
219	29	57	21	81	33	-20	220	23	65	35	86	45	-3
221	23	64	25	83	38	-21	222	27	64	15	81	35	-40
223	29	60	19	80	32	-30	224	27	63	26	88	41	-20
225	26	63	49	91	50	43	226	27	64	22	85	36	-30
227	21	69	34	91	46	-13	228	25	67	48	85	60	15
229	21	67	56	88	63	30	230	24	63	47	91	50	39
231	26	66	14	79	33	-40	232	26	69	23	89	43	-25
233	25	68	18	84	38	-33	234	22	63	43	91	49	18

Table A2. Thirty-Year Averages of Climatic Variables (continued).

County Number	Daily Temperature Drop (°F)	Mean Temperature (°F)	Precipitation (in.)	Maximum Relative Humidity (%)	Minimum Relative Humidity (%)	Thornthwaite Moisture Index	County Number	Daily Temperature Drop (°F)	Mean Temperature (°F)	Precipitation (in.)	Maximum Relative Humidity (%)	Minimum Relative Humidity (%)	Thornthwaite Moisture Index
235	19	70	39	96	53	-5	236	20	67	49	85	50	13
237	21	68	42	88	54	10	238	33	65	13	73	30	-40
239	23	68	43	94	46	0	240	26	73	21	90	45	-30
241	21	69	46	90	55	5	242	26	58	23	82	35	-20
243	24	63	30	86	41	-15	244	26	62	29	84	39	-20
245	17	72	27	93	54	-30	246	23	67	35	91	46	-13
247	23	69	30	89	45	-18	248	30	64	13	71	30	-40
249	27	64	37	88	49	-1	250	22	62	43	91	50	35
251	29	59	17	80	32	-30	252	27	64	31	91	51	-15
253	22	74	20	91	45	-40	254	24	71	22	89	43	-30

Table A3. Estimated Volumetric Water Contents for 2 to 4.8 pF Suction Values.

County	Suction (pF)								County	Suction (pF)							
	2.0	2.4	2.8	3.2	3.6	4.0	4.4	4.8		2.0	2.4	2.8	3.2	3.6	4.0	4.4	4.8
1	0.43	0.38	0.32	0.27	0.22	0.17	0.13	0.10	2	0.34	0.28	0.22	0.17	0.12	0.08	0.05	0.04
3	0.30	0.26	0.21	0.17	0.13	0.10	0.07	0.05	4	0.11	0.05	0.02	0.01	0.00	0.00	0.00	0.00
5	0.61	0.38	0.00	0.96	0.37	0.36	0.34	0.30	6	0.30	0.29	0.28	0.26	0.23	0.21	0.18	0.15
7	0.30	0.29	0.28	0.26	0.23	0.21	0.18	0.15	8	0.34	0.29	0.24	0.20	0.16	0.13	0.10	0.08
9	0.30	0.29	0.28	0.26	0.23	0.21	0.18	0.15	10	0.40	0.35	0.29	0.24	0.18	0.13	0.09	0.06
11	0.11	0.05	0.02	0.01	0.00	0.00	0.00	0.00	12	0.27	0.23	0.20	0.17	0.14	0.11	0.08	0.05
13	0.46	0.40	0.34	0.27	0.21	0.16	0.11	0.08	14	0.11	0.05	0.02	0.01	0.00	0.00	0.00	0.00
15	0.30	0.27	0.24	0.21	0.17	0.13	0.09	0.06	16	0.49	0.44	0.39	0.33	0.28	0.24	0.19	0.16
17	0.30	0.29	0.28	0.26	0.23	0.21	0.18	0.15	18	0.48	0.43	0.39	0.34	0.27	0.17	0.10	0.07
19	0.41	0.39	0.36	0.32	0.26	0.20	0.14	0.10	20	0.11	0.05	0.02	0.01	0.00	0.00	0.00	0.00
21	0.11	0.05	0.02	0.01	0.00	0.00	0.00	0.00	22	0.36	0.33	0.30	0.26	0.22	0.17	0.13	0.09
23	0.34	0.32	0.29	0.25	0.21	0.16	0.12	0.09	24	0.45	0.37	0.29	0.22	0.17	0.12	0.09	0.06
25	0.41	0.39	0.36	0.32	0.26	0.20	0.14	0.10	26	0.11	0.05	0.02	0.01	0.00	0.00	0.00	0.00
27	0.41	0.39	0.36	0.32	0.26	0.20	0.14	0.10	28	0.23	0.18	0.15	0.13	0.10	0.08	0.06	0.04
29	0.11	0.05	0.02	0.01	0.00	0.00	0.00	0.00	30	0.41	0.39	0.36	0.32	0.26	0.20	0.14	0.10
31	0.24	0.20	0.18	0.16	0.14	0.12	0.11	0.09	32	0.23	0.19	0.16	0.14	0.11	0.08	0.06	0.04
33	0.23	0.20	0.18	0.16	0.14	0.13	0.11	0.09	34	0.40	0.36	0.32	0.28	0.23	0.19	0.16	0.13
35	0.11	0.05	0.02	0.01	0.00	0.00	0.00	0.00	36	0.11	0.05	0.02	0.01	0.00	0.00	0.00	0.00
37	0.36	0.31	0.25	0.19	0.14	0.10	0.08	0.06	38	0.44	0.40	0.35	0.29	0.23	0.18	0.12	0.08
39	0.40	0.32	0.26	0.20	0.16	0.12	0.09	0.06	40	0.42	0.38	0.33	0.28	0.23	0.19	0.16	0.12
41	0.30	0.29	0.28	0.26	0.23	0.21	0.18	0.15	42	0.11	0.05	0.02	0.01	0.00	0.00	0.00	0.00
43	0.11	0.05	0.02	0.01	0.00	0.00	0.00	0.00	44	0.36	0.32	0.27	0.23	0.19	0.15	0.11	0.09
45	0.34	0.29	0.24	0.20	0.16	0.13	0.10	0.08	46	0.45	0.40	0.35	0.29	0.23	0.18	0.13	0.09
47	0.24	0.21	0.18	0.16	0.12	0.08	0.04	0.02	48	0.11	0.05	0.02	0.01	0.00	0.00	0.00	0.00
49	0.11	0.05	0.02	0.01	0.00	0.00	0.00	0.00	50	0.35	0.31	0.26	0.22	0.18	0.14	0.11	0.09
51	0.39	0.35	0.30	0.26	0.22	0.18	0.14	0.11	52	0.33	0.27	0.21	0.16	0.11	0.08	0.05	0.03
53	0.47	0.43	0.38	0.34	0.27	0.17	0.10	0.06	54	0.30	0.29	0.28	0.26	0.23	0.21	0.18	0.15
55	0.36	0.33	0.30	0.26	0.22	0.17	0.13	0.09	56	0.30	0.29	0.28	0.26	0.23	0.21	0.18	0.15
57	0.11	0.05	0.02	0.01	0.00	0.00	0.00	0.00	58	0.39	0.35	0.30	0.26	0.22	0.18	0.15	0.12
59	0.41	0.39	0.36	0.32	0.26	0.20	0.14	0.10	60	0.11	0.05	0.02	0.01	0.00	0.00	0.00	0.00
61	0.22	0.19	0.17	0.15	0.14	0.12	0.10	0.09	62	0.48	0.43	0.37	0.31	0.25	0.19	0.14	0.10
63	0.36	0.33	0.30	0.26	0.22	0.17	0.13	0.09	64	0.49	0.49	0.49	0.47	0.38	0.19	0.05	0.01
65	0.35	0.30	0.24	0.19	0.14	0.10	0.08	0.05	66	0.45	0.37	0.29	0.22	0.17	0.12	0.09	0.06
67	0.11	0.05	0.02	0.01	0.00	0.00	0.00	0.00	68	0.23	0.20	0.18	0.17	0.15	0.13	0.11	0.10
69	0.36	0.33	0.29	0.25	0.21	0.17	0.13	0.10	70	0.25	0.20	0.16	0.13	0.10	0.08	0.06	0.05
71	0.34	0.27	0.20	0.14	0.09	0.06	0.04	0.02	72	0.11	0.05	0.02	0.01	0.00	0.00	0.00	0.00
73	0.28	0.24	0.21	0.18	0.15	0.11	0.08	0.05	74	0.11	0.05	0.02	0.01	0.00	0.00	0.00	0.00
75	0.11	0.05	0.02	0.01	0.00	0.00	0.00	0.00	76	0.11	0.05	0.02	0.01	0.00	0.00	0.00	0.00
77	0.41	0.39	0.36	0.32	0.26	0.20	0.14	0.10	78	0.49	0.49	0.49	0.47	0.38	0.19	0.05	0.01
79	0.22	0.19	0.17	0.15	0.13	0.12	0.10	0.09	80	0.11	0.05	0.02	0.01	0.00	0.00	0.00	0.00
81	0.40	0.36	0.32	0.28	0.23	0.19	0.16	0.13	82	0.26	0.23	0.20	0.17	0.14	0.10	0.07	0.05
83	0.31	0.28	0.25	0.21	0.18	0.14	0.10	0.06	84	0.54	0.46	0.38	0.30	0.23	0.18	0.13	0.10
85	0.41	0.39	0.36	0.32	0.26	0.20	0.14	0.10	86	0.34	0.31	0.30	0.28	0.23	0.11	0.03	0.01

Table A3. Estimated Volumetric Water Contents for 2 to 4.8 pF Suction Values (continued).

County	Suction (pF)								County	Suction (pF)							
	2.0	2.4	2.8	3.2	3.6	4.0	4.4	4.8		2.0	2.4	2.8	3.2	3.6	4.0	4.4	4.8
87	0.33	0.27	0.22	0.16	0.11	0.07	0.04	0.02	88	0.41	0.39	0.36	0.32	0.26	0.20	0.14	0.10
89	0.46	0.40	0.34	0.27	0.21	0.16	0.11	0.08	90	0.11	0.05	0.02	0.01	0.00	0.00	0.00	0.00
91	0.30	0.29	0.28	0.26	0.23	0.21	0.18	0.15	92	0.27	0.24	0.21	0.18	0.15	0.11	0.08	0.05
93	0.40	0.36	0.32	0.28	0.23	0.19	0.16	0.13	94	0.11	0.05	0.02	0.01	0.00	0.00	0.00	0.00
95	0.27	0.20	0.14	0.08	0.04	0.02	0.01	0.01	96	0.30	0.29	0.28	0.26	0.23	0.21	0.18	0.15
97	0.41	0.39	0.36	0.32	0.26	0.20	0.14	0.10	98	0.48	0.43	0.39	0.34	0.27	0.17	0.10	0.07
99	0.11	0.05	0.02	0.01	0.00	0.00	0.00	0.00	100	0.22	0.19	0.17	0.15	0.13	0.12	0.10	0.09
101	0.42	0.37	0.31	0.25	0.20	0.15	0.12	0.09	102	0.11	0.05	0.02	0.01	0.00	0.00	0.00	0.00
103	0.40	0.36	0.32	0.28	0.23	0.19	0.16	0.13	104	0.39	0.35	0.30	0.26	0.22	0.18	0.15	0.12
105	0.35	0.33	0.30	0.27	0.24	0.20	0.16	0.12	106	0.45	0.40	0.35	0.29	0.23	0.18	0.13	0.09
107	0.24	0.20	0.16	0.13	0.10	0.08	0.06	0.05	108	0.38	0.33	0.27	0.20	0.13	0.09	0.06	0.05
109	0.48	0.43	0.37	0.31	0.25	0.19	0.14	0.10	110	0.11	0.05	0.02	0.01	0.00	0.00	0.00	0.00
111	0.43	0.38	0.33	0.28	0.23	0.19	0.15	0.12	112	0.25	0.20	0.16	0.13	0.10	0.08	0.06	0.05
113	0.28	0.24	0.21	0.18	0.15	0.11	0.08	0.05	114	0.30	0.27	0.24	0.21	0.17	0.13	0.09	0.06
115	0.30	0.29	0.28	0.26	0.23	0.21	0.18	0.15	116	0.36	0.33	0.30	0.26	0.22	0.17	0.13	0.09
117	0.11	0.05	0.02	0.01	0.00	0.00	0.00	0.00	118	0.43	0.36	0.28	0.21	0.16	0.11	0.08	0.05
119	0.40	0.36	0.31	0.26	0.21	0.17	0.14	0.11	120	0.30	0.28	0.26	0.24	0.20	0.10	0.02	0.00
121	0.11	0.05	0.02	0.01	0.00	0.00	0.00	0.00	122	0.42	0.37	0.31	0.25	0.20	0.15	0.12	0.09
123	0.39	0.34	0.29	0.24	0.20	0.16	0.12	0.09	124	0.11	0.05	0.02	0.01	0.00	0.00	0.00	0.00
125	0.36	0.32	0.28	0.23	0.19	0.16	0.12	0.10	126	0.11	0.05	0.02	0.01	0.00	0.00	0.00	0.00
127	0.28	0.24	0.21	0.18	0.15	0.11	0.08	0.05	128	0.30	0.29	0.28	0.26	0.23	0.21	0.18	0.15
129	0.41	0.37	0.32	0.28	0.23	0.19	0.16	0.13	130	0.29	0.25	0.22	0.19	0.16	0.12	0.08	0.06
131	0.47	0.42	0.38	0.33	0.26	0.17	0.10	0.07	132	0.43	0.37	0.32	0.26	0.21	0.16	0.12	0.09
133	0.11	0.05	0.02	0.01	0.00	0.00	0.00	0.00	134	0.34	0.28	0.23	0.18	0.14	0.11	0.08	0.06
135	0.22	0.19	0.17	0.15	0.13	0.12	0.10	0.09	136	0.41	0.39	0.36	0.32	0.26	0.20	0.14	0.10
137	0.11	0.05	0.02	0.01	0.00	0.00	0.00	0.00	138	0.26	0.22	0.19	0.17	0.13	0.10	0.07	0.05
139	0.11	0.05	0.02	0.01	0.00	0.00	0.00	0.00	140	0.43	0.40	0.36	0.30	0.23	0.16	0.10	0.06
141	0.41	0.39	0.36	0.32	0.26	0.20	0.14	0.10	142	0.25	0.21	0.18	0.15	0.12	0.09	0.07	0.04
143	0.34	0.29	0.24	0.20	0.16	0.13	0.10	0.08	144	0.11	0.05	0.02	0.01	0.00	0.00	0.00	0.00
145	0.38	0.32	0.26	0.20	0.16	0.12	0.09	0.06	146	0.27	0.23	0.20	0.18	0.16	0.14	0.12	0.11
147	0.26	0.23	0.20	0.17	0.14	0.10	0.07	0.05	148	0.41	0.39	0.36	0.32	0.26	0.20	0.14	0.10
149	0.41	0.37	0.32	0.28	0.23	0.19	0.16	0.13	150	0.33	0.27	0.22	0.17	0.13	0.09	0.07	0.04
151	0.27	0.22	0.17	0.13	0.10	0.08	0.06	0.04	152	0.30	0.29	0.28	0.26	0.23	0.21	0.18	0.15
153	0.43	0.38	0.33	0.28	0.23	0.19	0.15	0.12	154	0.31	0.28	0.25	0.21	0.18	0.14	0.10	0.06
155	0.40	0.36	0.32	0.28	0.23	0.19	0.16	0.13	156	0.40	0.36	0.31	0.26	0.22	0.17	0.14	0.11
157	0.33	0.27	0.22	0.17	0.13	0.09	0.07	0.04	158	0.11	0.05	0.02	0.01	0.00	0.00	0.00	0.00
159	0.37	0.36	0.34	0.30	0.23	0.15	0.08	0.04	160	0.30	0.24	0.19	0.14	0.10	0.06	0.04	0.02
161	0.11	0.05	0.02	0.01	0.00	0.00	0.00	0.00	162	0.41	0.37	0.32	0.28	0.23	0.19	0.16	0.13
163	0.31	0.28	0.27	0.25	0.20	0.10	0.03	0.00	164	0.33	0.26	0.20	0.16	0.12	0.09	0.07	0.05
165	0.41	0.37	0.32	0.28	0.23	0.19	0.16	0.13	166	0.38	0.32	0.26	0.20	0.16	0.12	0.09	0.06
167	0.48	0.43	0.39	0.34	0.27	0.17	0.10	0.07	168	0.54	0.46	0.38	0.30	0.23	0.18	0.13	0.10
169	0.44	0.39	0.33	0.27	0.21	0.16	0.11	0.08	170	0.54	0.46	0.38	0.30	0.23	0.18	0.13	0.10

Table A3. Estimated Volumetric Water Contents for 2 to 4.8 pF Suction Values (continued).

County	Suction (pF)								County	Suction (pF)							
	2.0	2.4	2.8	3.2	3.6	4.0	4.4	4.8		2.0	2.4	2.8	3.2	3.6	4.0	4.4	4.8
171	0.20	0.16	0.14	0.12	0.11	0.10	0.08	0.07	172	0.40	0.36	0.32	0.28	0.23	0.19	0.16	0.13
173	0.38	0.33	0.27	0.20	0.13	0.09	0.06	0.04	174	0.36	0.32	0.27	0.23	0.18	0.14	0.11	0.09
175	0.26	0.23	0.20	0.17	0.14	0.10	0.07	0.05	176	0.42	0.37	0.31	0.25	0.20	0.15	0.12	0.09
177	0.37	0.33	0.29	0.24	0.20	0.16	0.13	0.10	178	0.11	0.05	0.02	0.01	0.00	0.00	0.00	0.00
179	0.29	0.26	0.23	0.20	0.16	0.12	0.09	0.06	180	0.37	0.34	0.31	0.27	0.23	0.18	0.13	0.09
181	0.42	0.37	0.31	0.25	0.20	0.15	0.12	0.09	182	0.30	0.28	0.26	0.24	0.20	0.10	0.02	0.00
183	0.40	0.35	0.29	0.24	0.20	0.16	0.12	0.09	184	0.20	0.17	0.15	0.14	0.13	0.11	0.10	0.09
185	0.41	0.39	0.36	0.32	0.26	0.20	0.14	0.10	186	0.36	0.31	0.26	0.21	0.16	0.12	0.09	0.06
187	0.44	0.38	0.32	0.26	0.20	0.16	0.12	0.09	188	0.37	0.36	0.34	0.30	0.23	0.15	0.08	0.04
189	0.36	0.33	0.30	0.26	0.22	0.17	0.13	0.09	190	0.31	0.29	0.27	0.25	0.21	0.10	0.03	0.00
191	0.20	0.17	0.14	0.13	0.11	0.10	0.09	0.07	192	0.41	0.39	0.36	0.32	0.26	0.20	0.14	0.10
193	0.25	0.20	0.16	0.13	0.10	0.08	0.06	0.05	194	0.26	0.22	0.19	0.16	0.13	0.10	0.07	0.05
195	0.36	0.33	0.30	0.26	0.22	0.17	0.13	0.09	196	0.11	0.05	0.02	0.01	0.00	0.00	0.00	0.00
197	0.35	0.30	0.24	0.19	0.14	0.10	0.08	0.06	198	0.38	0.32	0.26	0.20	0.16	0.12	0.09	0.06
199	0.11	0.05	0.02	0.01	0.00	0.00	0.00	0.00	200	0.30	0.29	0.28	0.26	0.23	0.21	0.18	0.15
201	0.40	0.36	0.32	0.28	0.23	0.19	0.16	0.13	202	0.40	0.35	0.29	0.24	0.20	0.16	0.12	0.09
203	0.40	0.35	0.29	0.24	0.20	0.16	0.12	0.09	204	0.44	0.38	0.32	0.26	0.20	0.16	0.12	0.09
205	0.11	0.05	0.02	0.01	0.00	0.00	0.00	0.00	206	0.11	0.05	0.02	0.01	0.00	0.00	0.00	0.00
207	0.25	0.20	0.16	0.13	0.11	0.08	0.06	0.05	208	0.30	0.29	0.28	0.26	0.23	0.21	0.18	0.15
209	0.49	0.49	0.49	0.47	0.38	0.19	0.05	0.01	210	0.40	0.35	0.29	0.24	0.20	0.16	0.12	0.09
211	0.30	0.29	0.28	0.26	0.23	0.21	0.18	0.15	212	0.36	0.31	0.25	0.19	0.14	0.10	0.08	0.06
213	0.48	0.43	0.39	0.34	0.27	0.17	0.10	0.07	214	0.48	0.42	0.35	0.28	0.22	0.16	0.12	0.08
215	0.30	0.29	0.28	0.26	0.23	0.21	0.18	0.15	216	0.39	0.35	0.30	0.25	0.21	0.17	0.14	0.11
217	0.22	0.18	0.16	0.14	0.13	0.11	0.10	0.08	218	0.25	0.20	0.16	0.13	0.10	0.08	0.06	0.05
219	0.30	0.29	0.28	0.26	0.23	0.21	0.18	0.15	220	0.36	0.31	0.27	0.23	0.18	0.14	0.10	0.07
221	0.41	0.39	0.36	0.32	0.26	0.20	0.14	0.10	222	0.46	0.40	0.34	0.27	0.22	0.17	0.13	0.09
223	0.52	0.44	0.36	0.28	0.21	0.16	0.11	0.08	224	0.49	0.49	0.49	0.47	0.38	0.19	0.05	0.01
225	0.40	0.36	0.32	0.28	0.23	0.19	0.16	0.13	226	0.33	0.27	0.22	0.16	0.11	0.07	0.04	0.02
227	0.54	0.46	0.38	0.30	0.23	0.18	0.13	0.10	228	0.44	0.38	0.32	0.26	0.20	0.16	0.12	0.09
229	0.42	0.37	0.31	0.25	0.20	0.15	0.12	0.09	230	0.46	0.40	0.34	0.27	0.21	0.16	0.11	0.08
231	0.41	0.39	0.36	0.32	0.26	0.20	0.14	0.10	232	0.31	0.28	0.25	0.21	0.18	0.14	0.10	0.06
233	0.47	0.43	0.38	0.34	0.27	0.17	0.10	0.06	234	0.31	0.29	0.27	0.25	0.21	0.10	0.03	0.00
235	0.11	0.05	0.02	0.01	0.00	0.00	0.00	0.00	236	0.24	0.20	0.17	0.15	0.12	0.09	0.06	0.04
237	0.34	0.29	0.24	0.20	0.16	0.13	0.10	0.08	238	0.33	0.27	0.21	0.16	0.11	0.08	0.05	0.03
239	0.11	0.05	0.02	0.01	0.00	0.00	0.00	0.00	240	0.11	0.05	0.02	0.01	0.00	0.00	0.00	0.00
241	0.11	0.05	0.02	0.01	0.00	0.00	0.00	0.00	242	0.36	0.32	0.28	0.23	0.19	0.16	0.12	0.10
243	0.28	0.25	0.22	0.19	0.15	0.12	0.08	0.06	244	0.22	0.19	0.17	0.15	0.13	0.12	0.10	0.09
245	0.31	0.28	0.27	0.25	0.20	0.10	0.03	0.00	246	0.11	0.05	0.02	0.01	0.00	0.00	0.00	0.00
247	0.45	0.39	0.33	0.27	0.21	0.16	0.11	0.08	248	0.33	0.27	0.21	0.16	0.11	0.08	0.05	0.03
249	0.44	0.38	0.31	0.25	0.20	0.15	0.11	0.08	250	0.40	0.36	0.32	0.28	0.23	0.19	0.16	0.13
251	0.52	0.44	0.36	0.28	0.21	0.16	0.11	0.08	252	0.30	0.29	0.28	0.26	0.23	0.21	0.18	0.15
253	0.11	0.05	0.02	0.01	0.00	0.00	0.00	0.00	254	0.31	0.28	0.25	0.21	0.18	0.14	0.10	0.06

Table A4. Estimated Soil Permeabilities (cm/hr) for 2 to 4.8 pF Suction Values.

County	Suction (pF)								County	Suction (pF)							
	2.0	2.4	2.8	3.2	3.6	4.0	4.4	4.8		2.0	2.4	2.8	3.2	3.6	4.0	4.4	4.8
1	0.05	0.048	0.047	0.047	0.047	0.05	0.047	0.047	2	0.068	0.051	0.049	0.049	0.049	0.068	0.049	0.049
3	0.105	0.049	0.039	0.038	0.037	0.105	0.037	0.037	5	2E-04	9E-05	4E-05	2E-05	6E-06	2E-04	1E-06	5E-07
6	2E-04	9E-05	4E-05	2E-05	6E-06	2E-04	1E-06	5E-07	7	2E-04	9E-05	4E-05	2E-05	6E-06	2E-04	1E-06	5E-07
9	2E-04	9E-05	4E-05	2E-05	6E-06	2E-04	1E-06	5E-07	10	2E-04	9E-05	4E-05	2E-05	6E-06	2E-04	1E-06	5E-07
11	0.052	0.05	0.049	0.049	0.049	0.052	0.049	0.049	12	1E-04	5E-05	2E-05	8E-06	3E-06	1E-04	6E-07	2E-07
13	0.095	0.09	0.089	0.089	0.089	0.095	0.089	0.089	14	2E-07	2E-08	2E-09	2E-10	2E-11	2E-07	3E-13	3E-14
15	1E-04	5E-05	2E-05	1E-05	4E-06	1E-04	7E-07	3E-07	16	0.099	0.094	0.093	0.092	0.092	0.099	0.092	0.092
17	2E-04	9E-05	4E-05	2E-05	6E-06	2E-04	1E-06	5E-07	18	0.11	0.106	0.105	0.105	0.105	0.11	0.105	0.105
19	2E-04	9E-05	4E-05	2E-05	6E-06	2E-04	1E-06	5E-07	20	2E-07	2E-08	2E-09	2E-10	2E-11	2E-07	3E-13	3E-14
21	2E-07	2E-08	2E-09	2E-10	2E-11	2E-07	3E-13	3E-14	23	0.199	0.105	0.082	0.077	0.076	0.199	0.076	0.076
24	0.173	0.149	0.145	0.145	0.144	0.173	0.144	0.144	25	2E-04	9E-05	4E-05	2E-05	6E-06	2E-04	1E-06	5E-07
27	0.099	0.094	0.093	0.092	0.092	0.099	0.092	0.092	28	8E-05	3E-05	1E-05	6E-06	2E-06	8E-05	4E-07	2E-07
29	2E-07	2E-08	2E-09	2E-10	2E-11	2E-07	3E-13	3E-14	30	2E-04	9E-05	4E-05	2E-05	6E-06	2E-04	1E-06	5E-07
31	8E-05	4E-05	1E-05	6E-06	3E-06	8E-05	4E-07	2E-07	32	8E-05	4E-05	1E-05	6E-06	3E-06	8E-05	4E-07	2E-07
33	1E-04	5E-05	2E-05	9E-06	4E-06	1E-04	7E-07	3E-07	35	2E-07	2E-08	2E-09	2E-10	2E-11	2E-07	3E-13	3E-14
36	2E-07	2E-08	2E-09	2E-10	2E-11	2E-07	3E-13	3E-14	38	0.016	8E-04	5E-05	1E-05	4E-06	0.016	7E-07	3E-07
39	0.128	0.121	0.12	0.12	0.119	0.128	0.119	0.119	40	0.097	0.092	0.091	0.091	0.091	0.097	0.091	0.091
41	2E-04	9E-05	4E-05	2E-05	6E-06	2E-04	1E-06	5E-07	42	2E-07	2E-08	2E-09	2E-10	2E-11	2E-07	3E-13	3E-14
43	2E-07	2E-08	2E-09	2E-10	2E-11	2E-07	3E-13	3E-14	44	0.195	0.094	0.073	0.068	0.067	0.195	0.067	0.067
46	0.115	0.112	0.111	0.111	0.111	0.115	0.111	0.111	47	1E-04	4E-05	2E-05	8E-06	3E-06	1E-04	5E-07	2E-07
48	2E-07	2E-08	2E-09	2E-10	2E-11	2E-07	3E-13	3E-14	49	2E-07	2E-08	2E-09	2E-10	2E-11	2E-07	3E-13	3E-14
50	0.089	0.087	0.086	0.086	0.086	0.089	0.086	0.086	51	0.054	0.051	0.051	0.051	0.051	0.054	0.051	0.051
52	0.104	0.051	0.039	0.037	0.036	0.104	0.036	0.036	54	2E-04	9E-05	4E-05	2E-05	6E-06	2E-04	1E-06	5E-07
56	2E-04	9E-05	4E-05	2E-05	6E-06	2E-04	1E-06	5E-07	57	2E-07	2E-08	2E-09	2E-10	2E-11	2E-07	3E-13	3E-14
58	0.097	0.092	0.091	0.091	0.091	0.097	0.091	0.091	59	2E-04	9E-05	4E-05	2E-05	6E-06	2E-04	1E-06	5E-07
61	1E-04	5E-05	2E-05	9E-06	4E-06	1E-04	6E-07	3E-07	62	0.099	0.094	0.093	0.092	0.092	0.099	0.092	0.092
63	0.161	0.085	0.066	0.062	0.061	0.161	0.061	0.061	64	2E-04	9E-05	4E-05	2E-05	6E-06	2E-04	1E-06	5E-07
65	0.15	0.076	0.062	0.06	0.059	0.15	0.059	0.059	68	1E-04	5E-05	2E-05	1E-05	4E-06	1E-04	7E-07	3E-07
69	0.104	0.051	0.039	0.037	0.036	0.104	0.036	0.036	71	0.094	0.057	0.051	0.051	0.05	0.094	0.05	0.05
72	2E-07	2E-08	2E-09	2E-10	2E-11	2E-07	3E-13	3E-14	73	1E-04	5E-05	2E-05	8E-06	3E-06	1E-04	6E-07	2E-07
74	2E-07	2E-08	2E-09	2E-10	2E-11	2E-07	3E-13	3E-14	75	2E-07	2E-08	2E-09	2E-10	2E-11	2E-07	3E-13	3E-14
77	2E-04	9E-05	4E-05	2E-05	6E-06	2E-04	1E-06	5E-07	78	2E-04	9E-05	4E-05	2E-05	6E-06	2E-04	1E-06	5E-07
80	2E-07	2E-08	2E-09	2E-10	2E-11	2E-07	3E-13	3E-14	81	8E-05	4E-05	1E-05	6E-06	3E-06	8E-05	4E-07	2E-07
82	0.128	0.121	0.12	0.12	0.119	0.128	0.119	0.119	83	0.193	0.183	0.181	0.181	0.181	0.193	0.181	0.181
84	0.193	0.183	0.181	0.181	0.181	0.193	0.181	0.181	85	2E-04	9E-05	4E-05	2E-05	6E-06	2E-04	1E-06	5E-07
86	1E-04	5E-05	2E-05	9E-06	4E-06	1E-04	6E-07	3E-07	87	5E-04	5E-04	5E-04	5E-04	5E-04	5E-04	5E-04	5E-04
88	2E-04	9E-05	4E-05	2E-05	6E-06	2E-04	1E-06	5E-07	91	2E-04	9E-05	4E-05	2E-05	6E-06	2E-04	1E-06	5E-07
92	1E-04	5E-05	2E-05	8E-06	3E-06	1E-04	6E-07	2E-07	93	0.097	0.092	0.091	0.091	0.091	0.097	0.091	0.091
94	2E-07	2E-08	2E-09	2E-10	2E-11	2E-07	3E-13	3E-14	95	0.135	0.086	0.078	0.077	0.076	0.135	0.076	0.076
96	2E-04	9E-05	4E-05	2E-05	6E-06	2E-04	1E-06	5E-07	97	2E-04	9E-05	4E-05	2E-05	6E-06	2E-04	1E-06	5E-07
99	2E-07	2E-08	2E-09	2E-10	2E-11	2E-07	3E-13	3E-14	100	1E-04	5E-05	2E-05	8E-06	4E-06	1E-04	6E-07	3E-07
102	2E-07	2E-08	2E-09	2E-10	2E-11	2E-07	3E-13	3E-14	103	0.081	0.077	0.076	0.076	0.076	0.081	0.076	0.076
104	0.097	0.092	0.091	0.091	0.091	0.097	0.091	0.091	105	0.039	0.03	0.029	0.029	0.029	0.039	0.029	0.029
106	0.115	0.112	0.111	0.111	0.111	0.115	0.111	0.111	107	0.006	3E-04	1E-05	4E-07	2E-08	0.006	3E-11	1E-12
108	0.09	0.065	0.062	0.061	0.061	0.09	0.061	0.061	109	0.097	0.092	0.091	0.091	0.091	0.097	0.091	0.091

Table A4. Estimated Soil Permeabilities (cm/hr) for 2 to 4.8 pF Suction Values (continued).

County	Suction (pF)								County	Suction (pF)							
	2.0	2.4	2.8	3.2	3.6	4.0	4.4	4.8		2.0	2.4	2.8	3.2	3.6	4.0	4.4	4.8
110	2E-07	2E-08	2E-09	2E-10	2E-11	2E-07	3E-13	3E-14	111	0.104	0.099	0.098	0.098	0.098	0.104	0.098	0.098
112	0.059	0.059	0.059	0.059	0.059	0.059	0.059	0.059	113	1E-04	5E-05	2E-05	8E-06	3E-06	1E-04	6E-07	2E-07
114	1E-04	5E-05	2E-05	1E-05	4E-06	1E-04	7E-07	3E-07	115	2E-04	9E-05	4E-05	2E-05	6E-06	2E-04	1E-06	5E-07
117	2E-07	2E-08	2E-09	2E-10	2E-11	2E-07	3E-13	3E-14	118	0.113	0.089	0.086	0.085	0.085	0.113	0.085	0.085
119	0.115	0.109	0.108	0.108	0.108	0.115	0.108	0.108	121	2E-07	2E-08	2E-09	2E-10	2E-11	2E-07	3E-13	3E-14
122	0.094	0.065	0.064	0.063	0.063	0.094	0.063	0.063	123	0.119	0.118	0.118	0.118	0.118	0.119	0.118	0.118
124	2E-07	2E-08	2E-09	2E-10	2E-11	2E-07	3E-13	3E-14	125	0.014	6E-04	2E-05	9E-07	4E-08	0.014	6E-11	2E-12
126	2E-07	2E-08	2E-09	2E-10	2E-11	2E-07	3E-13	3E-14	127	1E-04	5E-05	2E-05	8E-06	3E-06	1E-04	6E-07	2E-07
128	2E-04	9E-05	4E-05	2E-05	6E-06	2E-04	1E-06	5E-07	129	0.089	0.084	0.083	0.083	0.083	0.089	0.083	0.083
130	1E-04	5E-05	2E-05	9E-06	4E-06	1E-04	6E-07	3E-07	131	0.109	0.106	0.105	0.105	0.105	0.109	0.105	0.105
132	0.041	0.002	8E-05	4E-06	2E-07	0.041	3E-10	1E-11	133	2E-07	2E-08	2E-09	2E-10	2E-11	2E-07	3E-13	3E-14
134	0.103	0.1	0.099	0.099	0.099	0.103	0.099	0.099	136	2E-04	9E-05	4E-05	2E-05	6E-06	2E-04	1E-06	5E-07
138	1E-04	4E-05	2E-05	8E-06	3E-06	1E-04	5E-07	2E-07	139	2E-07	2E-08	2E-09	2E-10	2E-11	2E-07	3E-13	3E-14
140	0.072	0.068	0.067	0.067	0.067	0.072	0.067	0.067	141	2E-04	9E-05	4E-05	2E-05	6E-06	2E-04	1E-06	5E-07
142	9E-05	4E-05	2E-05	7E-06	3E-06	9E-05	5E-07	2E-07	143	0.054	0.051	0.051	0.051	0.051	0.054	0.051	0.051
145	0.094	0.066	0.062	0.062	0.062	0.094	0.062	0.062	146	2E-07	2E-08	2E-09	2E-10	2E-11	2E-07	3E-13	3E-14
147	1E-04	4E-05	2E-05	8E-06	3E-06	1E-04	6E-07	2E-07	148	2E-04	9E-05	4E-05	2E-05	6E-06	2E-04	1E-06	5E-07
150	0.058	0.046	0.044	0.044	0.044	0.058	0.044	0.044	151	0.057	0.026	0.023	0.022	0.022	0.057	0.022	0.022
152	2E-04	9E-05	4E-05	2E-05	6E-06	2E-04	1E-06	5E-07	160	4E-04	4E-04	4E-04	4E-04	4E-04	4E-04	4E-04	4E-04
161	2E-07	2E-08	2E-09	2E-10	2E-11	2E-07	3E-13	3E-14	154	1E-04	6E-05	2E-05	1E-05	4E-06	1E-04	7E-07	3E-07
156	0.062	0.059	0.058	0.058	0.058	0.062	0.058	0.058	158	2E-07	2E-08	2E-09	2E-10	2E-11	2E-07	3E-13	3E-14
159	2E-04	9E-05	4E-05	2E-05	6E-06	2E-04	1E-06	5E-07	163	1E-04	5E-05	2E-05	8E-06	3E-06	1E-04	6E-07	2E-07
164	0.097	0.092	0.091	0.091	0.091	0.097	0.091	0.091	165	0.089	0.084	0.083	0.083	0.083	0.089	0.083	0.083
167	2E-04	9E-05	4E-05	2E-05	6E-06	2E-04	1E-06	5E-07	168	0.193	0.183	0.181	0.181	0.181	0.193	0.181	0.181
169	0.079	0.075	0.074	0.074	0.074	0.079	0.074	0.074	170	0.193	0.183	0.181	0.181	0.181	0.193	0.181	0.181
171	9E-05	4E-05	2E-05	7E-06	3E-06	9E-05	5E-07	2E-07	172	8E-05	4E-05	1E-05	6E-06	3E-06	8E-05	4E-07	2E-07
173	0.161	0.108	0.096	0.093	0.093	0.161	0.093	0.093	174	3E-04	3E-04	3E-04	3E-04	3E-04	3E-04	3E-04	3E-04
175	1E-04	4E-05	2E-05	8E-06	3E-06	1E-04	6E-07	2E-07	176	0.094	0.065	0.064	0.063	0.063	0.094	0.063	0.063
177	0.081	0.076	0.075	0.075	0.075	0.081	0.075	0.075	178	2E-07	2E-08	2E-09	2E-10	2E-11	2E-07	3E-13	3E-14
179	1E-04	5E-05	2E-05	9E-06	4E-06	1E-04	7E-07	3E-07	180	0.129	0.068	0.053	0.05	0.049	0.129	0.049	0.049
182	1E-04	4E-05	2E-05	8E-06	3E-06	1E-04	6E-07	2E-07	183	0.041	0.034	0.033	0.033	0.033	0.041	0.033	0.033
184	1E-04	5E-05	2E-05	1E-05	4E-06	1E-04	7E-07	3E-07	185	2E-04	9E-05	4E-05	2E-05	6E-06	2E-04	1E-06	5E-07
186	0.1	0.088	0.086	0.086	0.086	0.1	0.086	0.086	187	0.101	0.073	0.071	0.071	0.071	0.101	0.071	0.071
188	2E-04	9E-05	4E-05	2E-05	6E-06	2E-04	1E-06	5E-07	190	1E-04	5E-05	2E-05	8E-06	3E-06	1E-04	6E-07	2E-07
191	1E-04	4E-05	2E-05	7E-06	3E-06	1E-04	5E-07	2E-07	194	1E-04	4E-05	2E-05	7E-06	3E-06	1E-04	5E-07	2E-07
195	0.158	0.083	0.065	0.061	0.06	0.158	0.06	0.06	196	2E-07	2E-08	2E-09	2E-10	2E-11	2E-07	3E-13	3E-14
197	0.149	0.076	0.062	0.059	0.059	0.149	0.059	0.059	199	1E-04	5E-05	2E-05	9E-06	4E-06	1E-04	6E-07	3E-07
200	2E-04	9E-05	4E-05	2E-05	6E-06	2E-04	1E-06	5E-07	201	0.081	0.077	0.076	0.076	0.076	0.081	0.076	0.076
204	0.101	0.073	0.071	0.071	0.071	0.101	0.071	0.071	205	2E-07	2E-08	2E-09	2E-10	2E-11	2E-07	3E-13	3E-14
206	2E-07	2E-08	2E-09	2E-10	2E-11	2E-07	3E-13	3E-14	207	0.062	0.062	0.062	0.062	0.062	0.062	0.062	0.062
208	2E-04	9E-05	4E-05	2E-05	6E-06	2E-04	1E-06	5E-07	209	2E-04	9E-05	4E-05	2E-05	6E-06	2E-04	1E-06	5E-07
211	2E-04	9E-05	4E-05	2E-05	6E-06	2E-04	1E-06	5E-07	212	0.081	0.062	0.059	0.059	0.059	0.081	0.059	0.059
214	0.122	0.116	0.114	0.114	0.114	0.122	0.114	0.114	215	2E-04	9E-05	4E-05	2E-05	6E-06	2E-04	1E-06	5E-07
216	0.106	0.1	0.099	0.099	0.099	0.106	0.099	0.099	217	1E-04	5E-05	2E-05	8E-06	3E-06	1E-04	6E-07	2E-07

Table A4. Estimated Soil Permeabilities (cm/hr) for 2 to 4.8 pF Suction Values (continued).

County	Suction (pF)								County	Suction (pF)							
	2.0	2.4	2.8	3.2	3.6	4.0	4.4	4.8		2.0	2.4	2.8	3.2	3.6	4.0	4.4	4.8
218	0.059	0.059	0.059	0.059	0.059	0.059	0.059	0.059	219	2E-04	9E-05	4E-05	2E-05	6E-06	2E-04	1E-06	5E-07
220	0.048	0.046	0.045	0.045	0.045	0.048	0.045	0.045	221	2E-04	9E-05	4E-05	2E-05	6E-06	2E-04	1E-06	5E-07
222	0.156	0.151	0.15	0.15	0.15	0.156	0.15	0.15	223	0.118	0.107	0.105	0.105	0.105	0.118	0.105	0.105
225	8E-05	4E-05	1E-05	6E-06	3E-06	8E-05	4E-07	2E-07	226	5E-04	5E-04	5E-04	5E-04	5E-04	5E-04	5E-04	5E-04
227	0.193	0.183	0.181	0.181	0.181	0.193	0.181	0.181	230	0.097	0.092	0.091	0.091	0.091	0.097	0.091	0.091
232	1E-04	6E-05	2E-05	1E-05	4E-06	1E-04	7E-07	3E-07	233	0.103	0.1	0.099	0.099	0.099	0.103	0.099	0.099
234	1E-04	5E-05	2E-05	8E-06	3E-06	1E-04	6E-07	2E-07	235	2E-07	2E-08	2E-09	2E-10	2E-11	2E-07	3E-13	3E-14
236	9E-05	4E-05	2E-05	7E-06	3E-06	9E-05	5E-07	2E-07	238	0.008	3E-04	1E-05	5E-07	2E-08	0.008	3E-11	1E-12
239	2E-07	2E-08	2E-09	2E-10	2E-11	2E-07	3E-13	3E-14	240	2E-07	2E-08	2E-09	2E-10	2E-11	2E-07	3E-13	3E-14
242	0.041	0.002	8E-05	4E-06	2E-07	0.041	3E-10	1E-11	243	1E-04	5E-05	2E-05	9E-06	4E-06	1E-04	6E-07	3E-07
245	1E-04	5E-05	2E-05	8E-06	3E-06	1E-04	6E-07	2E-07	246	2E-07	2E-08	2E-09	2E-10	2E-11	2E-07	3E-13	3E-14
247	0.085	0.081	0.08	0.08	0.08	0.085	0.08	0.08	249	0.097	0.069	0.067	0.067	0.067	0.097	0.067	0.067
250	0.081	0.077	0.076	0.076	0.076	0.081	0.076	0.076	254	2E-04	9E-05	4E-05	2E-05	6E-06	2E-04	1E-06	5E-07